STUDY OF THE BIOSYNTHETIC PATHWAY AND THE ROLE OF HEPARAN SULFATE IN BIOLOGICAL SYSTEMS

by

Leyla Gasimli Ehtibar qizi

A Thesis Submitted to the Graduate
Faculty of Rensselaer Polytechnic Institute
in Partial Fulfillment of the
Requirements for the degree of
DOCTOR OF PHILOSOPHY
Major Subject: BIOLOGY

Approved by the
Examining Committee:

_____
Robert J. Linhardt, Thesis Adviser

_____
Jonathan S. Dordick, Member

_____
Blanca Barquera, Member

_____
Susan T. Sharfstein, Member

Rensselaer Polytechnic Institute
Troy, New York

April 2013
(For Graduation May 2013)

CONTENTS

LIST OF TABLES

LIST OF FIGURES

LIST OF ABBREVIATIONS

AFP	alpha-fetoprotein
ATIII	antithrombin III
BCA assay	bicinchoninic acid assay
BEH	ethylene bridged hybrid
BM	basement membrane
BMP	bone morphogenic protein
cDNA	complementary deoxyribonucleic acid
CHAPS	3-[(3-cholamidopropyl)dimethylammonio]-1-propanesulfonate
CHO	chinese hamster ovary
CS	chondroitin sulfate
DS	dermatan sulfate
ECM	extracellular matrix
EGF	epidermal growth factor
ESC	embryonic stem cell
ESI	electrospray ionization
Ext	exostosin
Extl3	glucosaminyltransferase
FGF	fibroblast growth factor
FGFR	fibroblast growth factor receptor
FOXA2	hepatic nuclear factor 3-beta
GAG	glycosaminoglycan
GalNAc	*N*-acetylgalactosamine
GalNAcT	*N*-acetylgalactosamine transferase
GFAP	glial fibrillary acidic protein
GlcA	glucuronic acid
Glce	glucuronyl C5-epimerase
GlcNAc	*N*-acetylglucosamine
GlcNS	*N*-sulfoglucosamine

GPI	glycosyl-phosphatidylinositol
h	human
HA	hyaluronic acid
HGF	hepatocyte growth factor
HNF	hepatic nuclear factor
HNK	human natural killer
HP	heparin
HRP	horseradish peroxidase
HS	heparan sulfate
Hs2st	heparan sulfate 2-*O*-sulfotransferase
Hs3st	heparan sulfate 3-*O*-sulfotransferase
Hs6st	heparan sulfate 6-*O*-sulfotransferase
HSC	hematopoietic stem cell
HXA	hexylamine
IdoA	L-iduronic acid
KRTAP3-2	keratin associated protein 3-2
KS	keratan sulfate
LeX	Lewis X antigen
LIF	leukemia inhibitory factor
miRNA	micro RNA
MS	mass spectrometry
Ndst	*N*-deacetylase/*N*-sulfotransferase
NSC	neural stem cell
PBS	phosphate buffered saline
PDGF	platelet-derived growth factor
PG	proteoglycan
PIP_2	phosphatidyl inositol biphosphate
PK	protein kinase
qRT-PCR	quantitative reverse transcription-polymerase chain reaction
RA	retinoic acid
RNA	ribonucleic acid

RPIP	reverse-phase ion-pairing
RPS18	ribosomal protein S18
SC	stem cell
SLRP	small leucine-rich proteoglycans
SSEA	stage specific embryonic antigen
TGF	transforming growth factor
TrBA	tributylamine
UPLC	ultra-performance liquid chromatography
VEGF	vascular endothelial growth factor
WNT	wingless-int

ACKNOWLEDGMENT

I would like to thank my advisor, Professor Robert J. Linhardt, for giving me an opportunity to work in such a diverse research group containing chemists, chemical engineers, molecular biologists, microbiologists, and nanoscientists. This environment afforded me the opportunity to appreciate the interdisciplinary aspect of modern science and gave me a chance to contribute my skills in those multidisciplinary projects as well as improve them. I truly appreciate his direction and continuous support through the arduous yet rewarding journey that is a Ph.D. project.

Next, I would like to thank my co-advisor and member of my thesis committee, Dr. Susan T. Sharfstein, who has provided invaluable advice and guidance. Dr. Sharfstein helped make my projects considerably easier and more enjoyable. Her expertise in the area of metabolic engineering was key for my gaining a deeper understanding of the projects and in that way facilitated progress in them.

I would also like to thank the remaining members of my thesis committee, Dr. Jonathan S. Dordick and Dr. Blanca Barquera for lending their expertise to my research. I am grateful to Dr. Janet L. Paluh, who contributed her knowledge in the area of stem cells and provided vital advice to our stem cell team in the initial stages of the research.

I also would like to thank our collaborators, the labs of Dr. Stephen Dalton and Dr. Kelly W. Moremen at the University of Georgia at Athens. In particular, Dr. Alison V. Nairn from Moremen's group and Dr. Michael Kulik from Dalton's group had a positive influence on various aspects of our projects.

I also thank all the past and present members of the Linhardt and Sharfstein labs for their help and advice and for creating a friendly and warm research atmosphere that made graduate life more pleasant.

I would like to give special thanks to my family in Baku, Azerbaijan for unceasing support and compassion throughout the years for my love of research. I am also grateful to my husband, Eric R. Gamache, for his help and encouragement, as well as his honest criticisms during most of the course of my Ph.D. studies. Without them it would be a far greater challenge to achieve what I have.

ABSTRACT

Heparan sulfate (HS) is a linear, highly charged acidic glycosaminoglycan (GAG) that interacts with multiple signaling molecules. These interactions have the ability to modulate signaling pathways that determine cell fate at various stages of development. HS is a polymeric carbohydrate with repeating disaccharide units consisting of *N*-acetylglucosamine / *N*-sulfoglucosamine and uronic acid. HS is attached to core proteins and localizes to the extracellular environment, associating with either the cell-surface or the extracellular matrix. A veritable orchestra of HS chain initiation, polymerization, and chain modification enzymes works together to biosynthesize HS chains with varying length and structure, which account for the prodigious heterogeneity of HS. Some of these enzymes have isozyme forms that possess unique spatial and temporal distribution.

Although the HS biosynthetic pathway has been analyzed previously, many aspects of it remain unresolved. For example, the factors that determine which isozyme is active and how that activity affects the final structure of HS is unknown. Another subject of interest is how heterogeneity of the HS chain affects its interaction with diverse biologically active molecules at different stages of development.

Chinese hamster ovary (CHO) cells have been used as a model to examine the effect that HS pathway modification has upon HS structure. We bioengineered CHO cell clones with the aim of producing heparin (HP), the oversulfated anticoagulant version of HS. We introduced human *N*-deacetylase/*N*-sulfotransferase (NDST2) (responsible for *N*-sulfonation) and mouse heparan sulfate 3-*O*-sulfotransferase 1 (Hs3st1) (responsible for 3-*O*-sulfonation) enzymes into CHO cells. Although we have observed increased *N*-sulfonation of the HS chain in our clones, we detect only a modest increase in 3-*O*-sulfonation, which is important for anticoagulation activity.

We used murine mastocytoma cells (MST), natural producers of HP, to establish expression levels and localization of HS biosynthetic enzymes, and also to investigate expression levels of core proteins required to produce HS chains similar in structure to HP. Our aim is to apply knowledge gained from these experiments to our CHO cell system in order to produce HP. Although MST cells express non-anticoagulant HP, its structure is similar to the clinically relevant form of HP. When we compared MST cells

to Dual-29 cells (a clonal line of NDST2 and Hs3st1 bioengineered CHO cells), we observed that all HS biosynthetic enzymes transcripts were expressed in both cell lines, but the protein levels of these enzymes were reduced less in MST cells than in Dual-29 cells. Ext2, Hs3st1 and Hs6st1 were not detected in MST cells, whereas they were observed in Dual-29 cells. MST cells expressed only glypican-1 and syndecan-1 proteoglycans core proteins, whereas Dual-29 expressed syndecan-1 and -3 and glypican-1, -2, -3, -5 and -6. When we compared MST-10H cells (HS3ST1 transfected) with Dual-29 cells, we also observed reduced enzyme expression in MST-10H cells compared to Dual-29 cells. However the expression pattern of core proteins was the same for both MST-10H and Dual-29 cells except for glypican-6, which was detected only in Dual-29 cells. Nevertheless, not only were trisulfated disaccharide levels increased, but in MST-10H cells we also detected 3-*O*-sulfo group-containing structures, which are required for anticoagulation activity. The reason why we observe all biosynthetic enzymes including Hs3st1 being expressed in Dual-29 cells despite producing less sulfated HS compared to MST and MST-10H cells and how transfection of Hs3st1 affects trisulfation of the HS structure, are questions that remain to be answered.

We used the teratocarcinoma line NCCIT and human embryonic stem cells as models to study changes in the cellular proteoglycan composition along differentiation towards various cell lineages. Our analysis revealed retinoic acid-induced changes in the abundance of transcripts for genes encoding core proteins, enzymes that are responsible for early and late linkage region biosynthesis, as well as enzymes for GAG chain extension and modification in NCCIT cells. Disaccharide analysis of the glycans in HS/HP and chondroitin/dermatan sulfate revealed RA-induced changes restricted to chondroitin/dermatan sulfate glycans.

Human embryonic stem cell line WA09 (H9) was differentiated into Isl-1 and early hepatic cells and glycomic changes accompanying these transitions were studied. Pluripotent H9 cells use the non-glycosylated form of lumican whereas Isl-1 cells use the glycosylated form. The most dramatic difference among HS biosynthetic enzymes was observed in expression of Hs3st2, which was reduced ~29-fold in Isl-1 cells. H9 cells use simple primarily non-sulfated HS chains whereas upon differentiation towards both

Isl-1 and hepatic lineages *N*-sulfonation increases, with the greatest change being observed in the structure of HS from early hepatic cells.

The HS biosynthetic pathway is a complex yet elegant system where the cooperative effort of various components results in HS chains of various structures important for interaction with different molecules. Understanding the details of this pathway will enable us to gain better control over it with the aim to produce HS chains of the desired structure, including the one with anticoagulant activity. This knowledge will provide us with powerful tools to control and direct stem cell differentiation.

1. INTRODUCTION

1.1 Proteoglycans

A proteoglycan is a core protein having one or more glycosaminoglycan (GAG) chains, which are covalently attached through serine residues. They are primarily located in the ECM and on the cell surface, but are also found intracellularly (**Figure 1.1**).

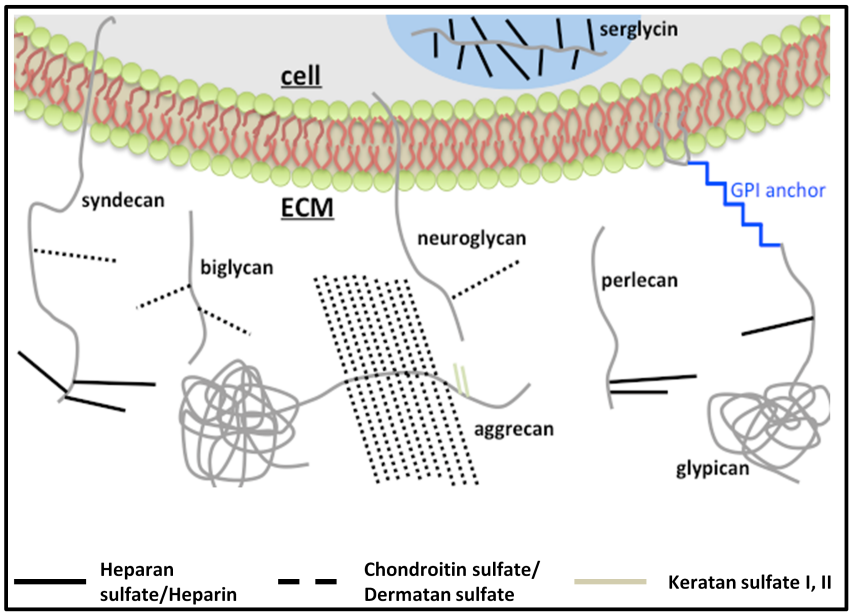

Figure 1.1. Distribution of cellular proteoglycans. Proteoglycans are widely distributed on the cell surface, where they can associate via a transmembrane domain or glycosyl-phosphatidylinositol (GPI) anchoring, and inside of secretory granules. They are also abundant in the extracellular matrix. Intracellular proteoglycans primarily have storage functions whereas extracellular and membrane-associated proteoglycans are involved in cell adhesion and migration processes as well as transduction of signals generated by growth factors, morphogens, and cytokines. Adapted from (Ly, Laremore, and Linhardt 2010).

PGs play important roles in cell migration and adhesion, and also bind to various morphogens, cytokines, chemokines, and growth factors (Lander and Selleck 2000; Kjellen and Lindahl 1991; Bernfield et al. 1999; Yoneda and Couchman 2003; Linhardt

---

This chapter previously appeared as: Gasimli, L., R. J. Linhardt, and J. S. Dordick. 2012. Proteoglycans in stem cells. *Biotechnol. Appl. Biochem.* 59 (2):65-76.

and Toida 2004). They stabilize or modulate receptors required for cell viability, development and morphogenesis (Esko, Kimata, and Lindahl 2009). GAGs are linear, highly charged, acidic carbohydrates with a repeating disaccharide unit. Based on the structure of the repeating disaccharide, GAGs can be divided into four classes: heparan sulfate/heparin (HS/HP), chondroitin sulfate/dermatan sulfate (CS/DS), keratan sulfate (KS) and hyaluronic acid (HA) (Ly, Laremore, and Linhardt 2010).

1.1.1 Structure and biosynthesis of heparan sulfate/heparin and chondroitin sulfate/dermatan sulfate glycosaminoglycans

CS and DS glycosaminoglycans consist of *N*-acetylgalactosamine (GalNAc) and glucoronic acid (GlcA), or iduronic acid (IdoA). This basic structure can be modified through the additions of sulfo groups at positions C4 and C6 of GalNAc and C2 of GlcA/IdoA. HS/HP chains are composed of repeating dissacharide units of *N*-acetylglucosamine (GlcNAc)/*N*-sulfoglucosamine (GlcNS) and GlcA/IdoA. This structure can be modified through the addition of sulfo groups at C6 and C3 of the GlcNAc or GlcNS residue and C2 of the GlcA/IdoA residue (**Figure 1.2**).

CS/DS and HS/HP proteoglycans share the initial steps of biosynthesis, which start in the endoplasmic reticulum where xylose is covalently attached to the serine residue of a core protein. Next two galactoses are added to the xylose, followed by glucoronic acid addition. At this point, the biosynthetic pathways diverge. The exostose-like-3 enzyme directs biosynthesis towards HS/HP, by adding GlcNAc to the chain, whereas GalNAc-transferase (GalNAcT) drives biosynthesis towards CS/DS by transfering GalNAc onto the chain. HS/HP chain polymerization is catalyzed by exostose-1 and -2 (EXT-1 and EXT-2), which add GlcNAc and GlcA, respectively. The growing chain receives further modification through the introduction of sulfo groups in various positions and epimerization of GlcA into IdoA. Those processes are mediated by sulfotranferases (*N*-deacetylase/*N*-sulfotransferase, 2-*O*-sulfotransferase, 6-*O*-sulfotransferase and 3-*O*-sulfotransferase) and the GlcA C5-epimerase, which converts GlcA to IdoA. The HS chain is highly heterogeneous, due to the fact that these modifications are not always completed and result in highly modified sections of HS alternating with less highly modified sections, which creates domains within the chain. Heparin is a more highly

sulfated version of the HS chain consisting primarily of IdoA. HS/HP biosynthetic enzymes have various isozymes, which have distinct temporal and spatial distribution. Chain elongation and modification of CS/DS is regulated by β3GlcA transferase and β4GalNac transferase, GlcA C5-epimerase, 4-*O*-sulfotransferase, 6-*O*-sulfotransferase and 2-*O*-sulfotransferase. GlcA C5-epimerase, a distinct enzyme from the HS/HP biosynthetic pathway epimerase, is required for DS synthesis (Esko, Kimata, and Lindahl 2009).

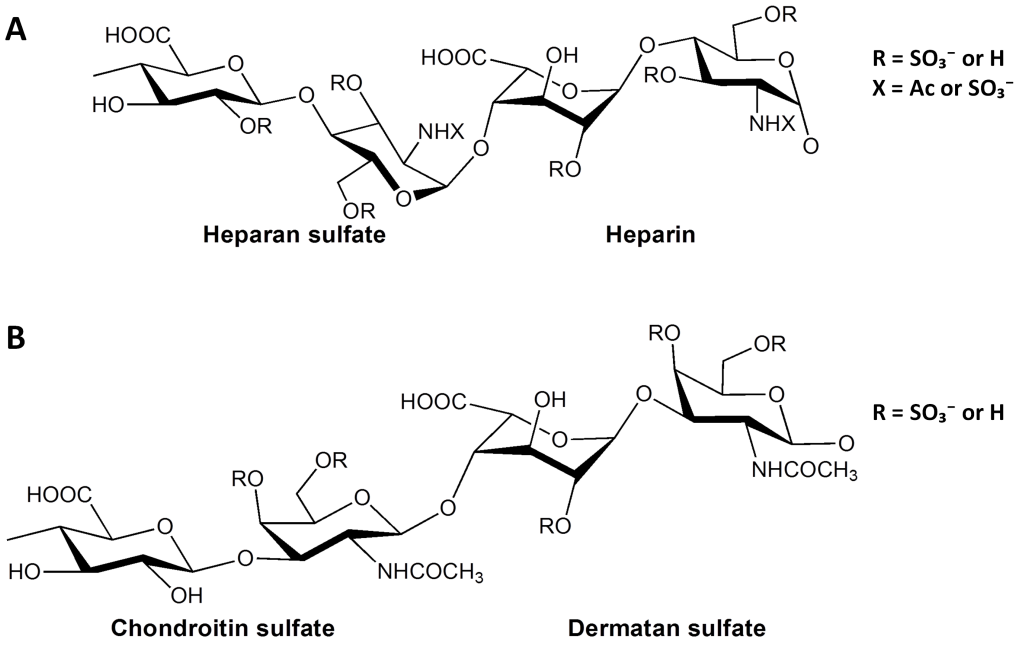

Figure 1.2. Disaccharide composition of the GAG chain of heparan sulfate/heparin and chondrotin sulfate/dermatan sulfate proteoglycans. (A) Heparan sulfate/heparin disaccharide composition. HP chains largely consist of fully sulfated repeating disaccharides of *N*-sulfoglucosamine and iduronic acid. HS disaccharide primarily contains low sulfated *N*-acetylglucosamine and glucoronic acid. **(B)** Chondroitin sulfate/dermatan sulfate disaccharide composition. CS/DS chains are constructed of disaccharides of galactosamine and glucoronic acid, whereas DS consists of galactosamine and iduronic acid. Adapted from (Gasimli, Linhardt, and Dordick 2012).

1.1.2 Proteoglycan classes

Based on their distribution, PGs can be classified into extracellular matrix, membrane-bound and intracellular PGs (**Table 1.1**). ECM PGs can be separated into small leucine-rich proteoglycans (SLRPs), aggrecan (hyalectin) family PGs, and basement membrane PGs. SLRPs, which include decorin, biglycan, lumican and fibromodulin, have leucine-rich repeats and cysteine clusters on *N*-termini, and can carry CS, DS and KS chains. They are known to be involved in multiple signaling pathways driven by transforming growth factor (TGF)-β, BMP, Toll-like-receptors, receptor tyrosine kinases, and insulin-like growth factor-like receptors (Schaefer and Iozzo 2008). The aggrecan family includes four members: aggrecan, neurocan, versican and brevican. All four can bind HA, carry CS chains, and can sometimes carry KS chains. Aggrecan, a relatively large PG with many GAG chains, represents the major cartilage PG. Neurocan, versican and brevican affect different aspects of neuronal morphogenesis (Esko, Kimata, and Lindahl 2009). Basement membrane (BM) PGs, along with various proteins and glycoproteins, make up the complex layer of the ECM that separates the epithelium and endothelium from underlying connective tissue. Major BM PGs are collagen XVIII, perlecan, agrin and leprecan (Esko, Kimata, and Lindahl 2009; Iozzo 2005). Perlecan, one of the largest single chain polypeptides in the cell with molecular weight of ~ 400 kDa, is a modular protein, wherein the modules interact with different growth factors and proteins involved in lipid metabolism and adhesion (Iozzo 1998) (**Table 1.1**). Perlecan and collagen XVIII, a member of the multiplexin family (Oh et al. 1994), modulate the activity of numerous growth factors and the angiogenic processes (Iozzo 2005), in addition to contributing to cellular homeostasis (Iozzo and San Antonio 2001). Agrin plays a role in neuromuscular junction activity by aggregating acetylcholine receptors (Bezakova and Ruegg 2003) and has also been proposed to be important in renal ultrafiltration (Groffen et al. 1998). Leprecan has been shown to be involved in notochord development in tunicate *Ciona intestinalis* (Dunn and Di Gregorio 2009).

Membrane-bound PGs can be transmembrane (syndecans, betaglycan, NG2 CSPG, neurophilin-1, CD44 and phosphacan) or glycosyl-phosphatidylinositol (GPI)-anchored (glypicans). Transmembrane PGs are type I proteins, which have a small cytoplasmic, single-span transmembrane domain in addition to extracellular domains

with HS and/or CS chains attached (Tkachenko, Rhodes, and Simons 2005). Although the primary function of transmembrane PGs is associated with their GAG chains, some transmembrane PGs have functions independent of their GAG chains (Tkachenko, Rhodes, and Simons 2005; Schwarz and Ruhrberg 2010). The primary function of transmembrane PGs is linked to cell adhesion and migration processes (Couchman 2010) as well as mediating the function of metalloproteases (Munesue et al. 2007). They can be "full-time PGs", such as syndecans and NG2, with GAG chains continuously attached, or "part-time PGs", such as betaglycan, neurophilin-1 and CD44 (Couchman 2010), which can function without the GAG chain. Phosphacan is found in three alternatively spliced forms, one of which is present in the ECM, the other two of which are of the protein-tyrosine phosphatase type of transmembrane receptor (Esko, Kimata, and Lindahl 2009). Betaglycan is referred to as a "TGF-β type III receptor", as it binds various members of the TGF-β family and associates with TGF-β type I and type II receptors (Bernabeu, Lopez-Novoa, and Quintanilla 2009). CD44 is a vertebrate receptor for hyaluronic acid and coreceptor for epidermal growth factor (EGF) and hepatocyte growth factor (HGF) (Ponta, Sherman, and Herrlich 2003). NG2 CSPG carries one CS chain and is expressed in vascular mural cells and pericytes, and is a marker for oligondendrocyte progenitors. It interacts with type V and VI collagen, fibroblast growth factor (FGF) 2 and platelet-derived growth factor (PDGF)-AA (Stallcup and Huang 2008).

Each member of the syndecan (1-4) family has a distinct temporal and spatial distribution. They have been implicated in the same pathways as different growth factors such as FGF, vascular endothelial growth factor (VEGF), TGF-β and PDGF (Tkachenko, Rhodes, and Simons 2005). The extracellular domains of syndecan-1 and -3 carry HS and CS chains, whereas syndecan-2 and -4 carry only HS chains. In addition to the extracellular domain, the cytoplasmic tail of syndecans plays an important role in interactions affecting cell migration and adhesion. The cytoplasmic domain consists of three regions, each of which possess unique functionality, such as interaction with cytoskeletal proteins, activation of protein kinase Cα (PKCα) or interaction with PDZ proteins involved in intracellular targeting and trafficking. The transmembrane domain is engaged in dimerization of syndecans (Dews and Mackenzie 2007). It has been

shown that syndecan-4 activation of PKCα requires phosphatidylinositol-4,5-bisphosphate (PIP_2) interaction with a specific region of the cytoplasmic tail (Horowitz et al. 1999; Oh et al. 1998). Cell adhesion and stress fiber formation and spreading are processes affected by this signaling. Syndecans are closely associated with metalloproteases and can act as their substrates prior to shedding (Ryu et al. 2009), and can also mediate their activity (Yu et al. 2000). Shed syndecans can compete with ligand binding to the cell surface PGs (Tkachenko, Rhodes, and Simons 2005).

Glypicans are HSPGs that are located on the cell surface and are connected to the external side of the membrane through the GPI-anchor. There are six members in this family in mammals. Unlike syndecans, with HS chains at the distal end of the protein, glypicans have HS chains, which are attached to the end of the protein that is proximal to the membrane. Glypican activity has been linked to important processes in development and morphogenesis such as the regulation of FGF, Hedgehog, Wingless –Int (Wnt) and bone morphogenic protein (BMP) signaling (Filmus, Capurro, and Rast 2008). Glypican-3 has a galvanizing effect on Wnt signaling by facilitating and stabilizing the ligand-receptor interaction (Capurro, Xiang, et al. 2005). The same mechanism is proposed for its effect in FGF signaling (Song, Shi, and Filmus 1997). In Hedgehog signaling, glypicans have an inhibitory effect by binding to the Hedgehog protein and competing with the Patched receptor (Capurro et al. 2008). Glypicans have also been linked to the uptake of polyamines (Fransson 2003). Like syndecans, glypicans can be shed into the extracellular environment.

Serglycin is the major PG present in secretory granules of mast cells, which carry HP and oversulfated CS chains (Pejler, Abrink, and Wernersson 2009; Thompson, Schulman, and Metcalfe 1988). Serglycin functions in granules as a storage unit for basic molecules such as proteases (Humphries et al. 1999) through the interaction with serglycin's negatively charged HP chains. After release from the granules, PG partners can detach from the PG or remain associated (Kolset, Prydz, and Pejler 2004). In the latter case, the PG can present the bound partner to the HP-binding molecules (Tchougounova and Pejler 2001) or can modulate the activity of bound components. This is exemplified in the interaction of HP with the antithrombin serine protease, enabling that complex to have a higher affinity to thrombin (Danielsson et al. 1986),

which is required for the anticoagulation process. It has also been suggested that PGs might play a role in trafficking of the PG/partner complex as well as protecting partners from inhibitors (Kolset, Prydz, and Pejler 2004).

Table 1.1. Distribution and properties of common proteoglycans (Esko, Kimata, and Lindahl 2009).

Proteoglycan localization	Proteoglycan class	Proteoglycan name	Number and type of GAG chain attached	Core protein size (kDa)
Extracellular matrix	Small leucine rich PGs	Decorin	1 CS	36
		Biglycan	1-2 CS	38
	Aggrecan family	Aggrecan	~100 CS	208-220
		Versican	12-15 CS	265
		Neurocan	1-2 CS	145
		Brevican	0-4 CS	96
	Basement membrane	Leprecan	1-2 CS	82
		Perlecan	1-3 HS	400
		Agrin	1-3 HS	200
		Collagen type XVIII	2-3 HS	147
Membrane-bound	Transmembrane	NG2	2-3 CS	251
		CD44	1-4 CS	37
		Betaglycan	1 CS/1 HS	110
		Syndecans 1-4	1-3 CS/1-2 HS	31-45
	GPI-anchored	Glypicans 1-6	1-3 HS	~ 60
Intracellular		Serglycin	10-15 HP/CS	10-19

1.2 Stem cells

Stem cells (SCs) are a powerful tool in regenerative medicine. Their ability to give rise to many cell types can be harnessed to regenerate tissues that have been injured or lost in devastating diseases including Parkinson's, diabetes, multiple sclerosis and numerous others. Currently SCs are isolated from embryos, as well as fetal and adult tissues, and can be differentiated into a multitude of cell types including cardiomyocytes, neurons, hepatocytes, and insulin-producing cells (Schuldiner et al. 2001; Kehat et al. 2001; Hay et al. 2008).

Stem cells are also invaluable in research areas such as drug discovery and developmental biology. Cells derived from SCs can serve as models to develop drugs against specific targets in tissues of interest. Their use offers advantages over primary tissues, immortalized tumor cells, or genetically transformed cells because they can give rise to an unlimited number of uniform and genetically natural cells that can be used for drug target identification (Amit et al. 2000). Embryonic stem cells (ESCs) can be used to study the role of various developmental genes. As an example, genes of interest can be modified in the ESCs, and development can be monitored in knockout mice (Rathjen et al. 1998; Jones and Thomson 2000). Various effective methods for modification of the human ESC genome have been proposed, and are in fact well-suited for these purposes (Rathjen et al. 1998).

A stem cell can give rise to different cell types and can self-proliferate (**Figure 1.3**). SCs can be embryonic, fetal or adult. Embryonic stem cells are isolated from the inner cell mass of preimplanted embryo and represent a pluripotent cell type that can give rise to cells from all three germ layers of the body. Embryonic germ SCs are also pluripotent and are isolated from primordial germ cells of the gonadal ridge and beget the gonads. Adult and fetal SCs are unspecialized cells located within specialized tissues and give rise to the cells of that particular tissue. They are limited in regards to the cell types to which they have the capability to differentiate into, and hence are defined as possessing multipotency. Certain adult SCs can give rise to relatively few or only one cell type of a specific tissue and are considered oligopotent and unipotent, respectively. Recently it was shown that adult SCs from one tissue can give rise to cell types from another tissue, which can be generated from the same or a different germ layer. This property is known

as plasticity (Poulsom et al. 2002). Examples include hematopoietic stem cells (HSCs), which can give rise to all blood cell types in addition to liver cells (Theise et al. 2000; Lagasse et al. 2000), which are also of mesodermal origin. HSCs also can give rise to neurons (Mezey et al. 2000), which are ectodermal in origin. Adult tissue SCs can proliferate throughout the life of the organism. They usually give rise to progenitor cells, which are non-differentiated cells within a given tissue. Progenitor cells are "committed" and ultimately yield terminally differentiated (primary) cells. During division, progenitor cells can produce only two progenitor cells or two specialized cells. Stem cells, on the other hand, can divide with potential to yield one stem cell along with one progenitor cell (Fuchs, Tumbar, and Guasch 2004) (**Figure 1.3**).

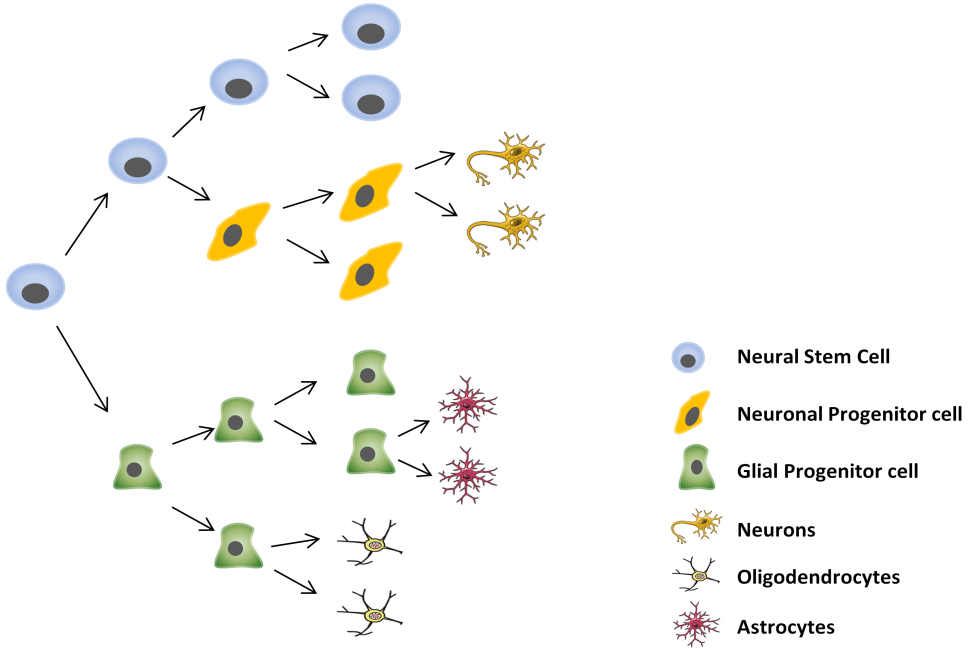

Figure 1.3. Self-renewal and differentiation potential of stem cells. Stem cells are capable of symmetric (production of two stem cells) as well as asymmetric (production of a stem cell and a progenitor cell) division. In contrast, tissue stem cells primarily differentiate through progenitor cells, which cannot undergo asymmetric division. Adapted from (Gasimli, Linhardt, and Dordick 2012).

Tissue replenishment occurs primarily through progenitor cells, as tissue SCs are normally slow proliferative in the absence of additional stimulating signals. Known sources of adult stem cells are bone marrow, blood, brain, skin, lining of the

gastrointestinal tract, pancreas, skeletal muscle, liver, cornea and retina (Korbling and Estrov 2003).

1.3 Mechanisms Controlling Stem Cell State

Stem cells possess the extraordinary potential to self-renew or differentiate into other cell types. The state of SCs (non-differentiated *versus* differentiated) is determined by the intricate orchestration of cell-intrinsic and cell-extrinsic signals filtered through a large number of signaling pathways (**Figure 1.4**).

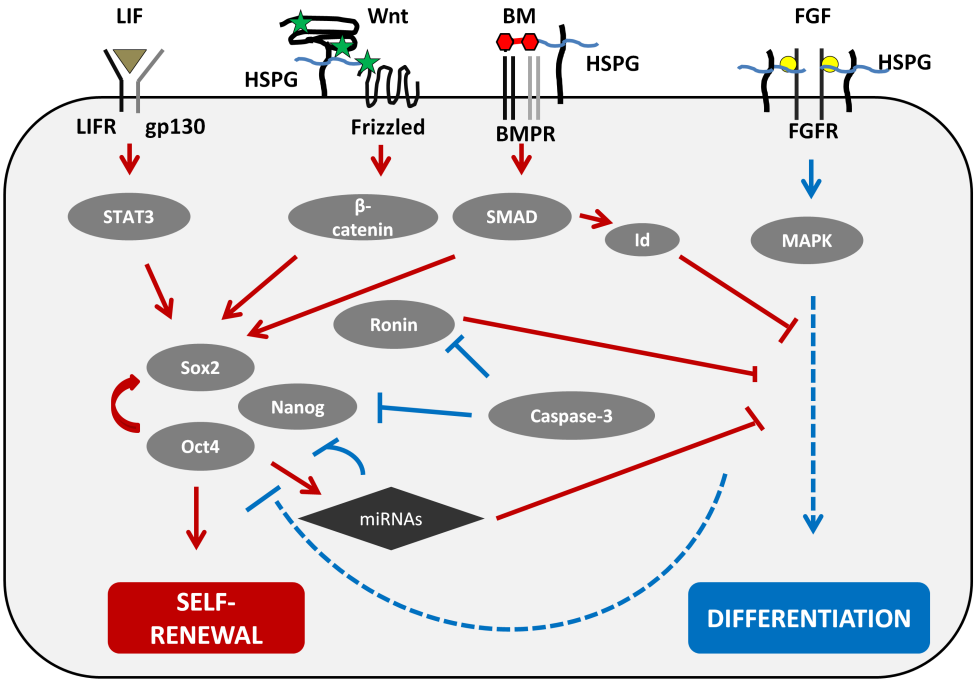

Figure 1.4. Signaling pathways involved in regulation of mouse embryonic stem cells pluripotency. Stem cell fate, influenced by a complex interplay of intrinsic and extrinsic signals, is transduced through multiple interconnected pathways. LIF, Wnt, BMP and FGF are of primary importance for mouse embryonic stem cell fate coordination. LIF, Wnt and BMP signaling support pluripotency, whereas FGF signaling works in opposition. Wnt, BMP and FGF signaling are mediated by heparan sulfate proteoglycans. Adapted from (Gasimli, Linhardt, and Dordick 2012).

The primary mechanisms to control SC state have been studied in non-human organisms such as *Caenorhabditis elegans, Drosophila melanogaster* and *Mus musculus,* with growing attention focused on human cell-based research.

1.3.1 Cell intrinsic regulation of stem cell fate

Stem cell state is directed on several levels including regulation by transcription factors (Boyer et al. 2005; Kim et al. 2008; Chen et al. 2008), their cofactors (Chen et al. 2008; Alarcon et al. 2009; Fryer, White, and Jones 2004; Taatjes 2010; Kagey et al. 2010; Xiong and Gerton 2010), chromatin structure regulators (Pasini et al. 2010; Shen et al. 2009; Landeira et al. 2010; Loh et al. 2007) and noncoding RNAs (Marson et al. 2008; He et al. 2005; Wang et al. 2008; Lichner et al. 2011; Tay et al. 2008; Melton, Judson, and Blelloch 2010). Several transcription factors have been established as key players in controlling the self-renewal of pluripotent ESCs, which comprise the "core regulatory circuitry". Oct4, Nanog and Sox2 (Boyer et al. 2005) regulate the expression of many genes required for self-renewal, as well as suppression of genes that are required for fate commitment (**Figure 1.5**). They function together to modulate their own expression in addition to the transcription of many protein-coding (Kim et al. 2008; Chen et al. 2008; Boyer et al. 2005) and non-coding RNAs (Marson et al. 2008) involved in maintaining the pluripotency of ESCs. Oct4 has been given special attention because of the broad range of genes it oversees. For example, Oct4 positively regulates expression of histone modifying enzymes such as Jmjd1a and Jmjd2c (histone 3 lysine 9 demethylases), and this regulation provides a mechanism to de-repress genes required for pluripotency (Loh et al. 2007). Oct4 can also upregulate the chromatin modifier Polycomb Repressive Complex 2 to suppress the activity of fate commitment genes (Pasini et al. 2010; Shen et al. 2009; Landeira et al. 2010).

Core regulatory circuitry cooperates with other transcription factors such as Sall4, Tcf3, Smad1, Stat3, Esrrb, Klf4, Klf2, Klf5, E2f1, n-myc, Zfx and Ronin to maintain ESC self-renewal (Ng and Surani 2011; Cole et al. 2008; Zhang et al. 2006; Dejosez et al. 2010; Young 2011). One of the primary transcription factors that work in concert with Oct4 is the proto-oncogene c-myc (Cartwright et al. 2005). The c-myc protein

binds to promoter sequence and facilitates RNA elongation by stimulation of the transcriptional pause release (Cartwright et al. 2005; Rahl et al. 2010), thereby promoting transcription of genes activated by the core regulatory circuitry.

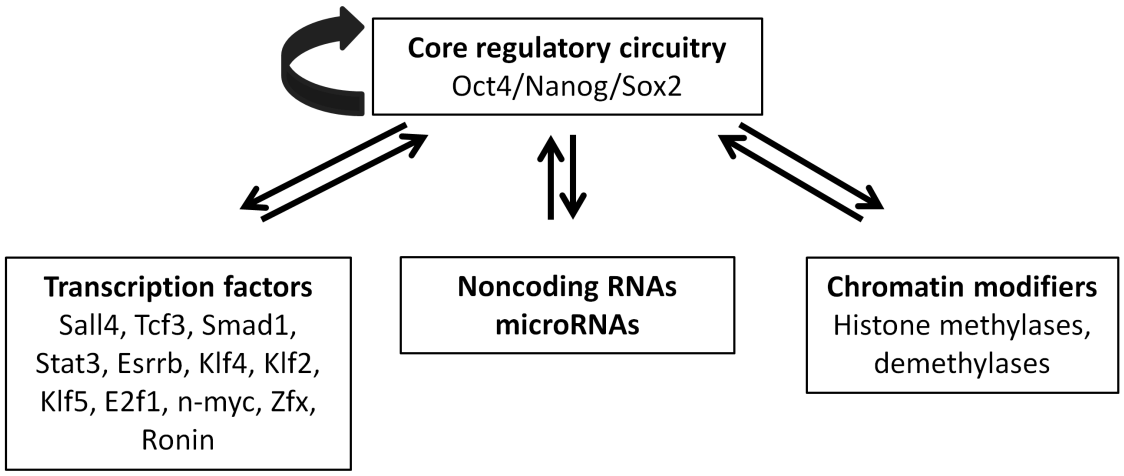

Figure 1.5. Mechanisms of controlling stem cell state by core regulatory circuitry. Core regulatory circuitry, consisting of the Oct4/Nanog/Sox2 transcription factors, maintains stem cell pluripotency by activating self-renewal genes and suppressing lineage-specific genes. In addition to regulating its own expression, regulatory circuitry also exploits the noncoding RNA network and chromatin modifiers to fine-tune expression of pluripotency genes. Adapted from (Gasimli, Linhardt, and Dordick 2012).

Many actively transcribed genes in SCs are populated with transcription cofactors, which contribute to gene expression regulation by bridging the interaction between required transcription factors without actually binding to DNA themselves (Young 2011). ESCs are sensitive to reduced levels of cofactors such as p300 (Chen et al. 2008) and mediator (Alarcon et al. 2009; Fryer, White, and Jones 2004; Taatjes 2010). Cohesin, in concert with mediator, physically brings together the enhancer and promoter sites of genes, a requirement for transcriptional initiation (Kagey et al. 2010; Xiong and Gerton 2010). DNA modifications, such as methylation, have also been shown to be important to stem cell state. SCs lacking DNA methylases would undoubtedly be deficient in differentiation due to an inability to suppress pluripotency genes (Feldman et al. 2006; Jackson et al. 2004).

The micro RNA (miRNA) network assumes an active role in maintenance of the SC state. Oct4/Nanog/Sox2 facilitates self-renewal of SCs through miRNA in various ways. They activate genes coding for miRNAs, which in turn are involved in "fine-tuning" of self-renewal genes and clearing the transcripts of fate commitment genes (Marson et al. 2008; He et al. 2005; Wang et al. 2008; Lichner et al. 2011). Oct4/Nanog/Sox2 suppress the miRNAs involved in expression of lineage-specific genes, while simultaneously suppressing miRNA, which inhibit pluripotency genes (Marson et al. 2008; Tay et al. 2008; Melton, Judson, and Blelloch 2010). Longer chain noncoding RNAs have been shown to recruit and stabilize the Polycomb Repressive Complexes required to quench expression of fate-commitment genes (Yap et al. 2010; Zhao et al. 2010; Kanhere et al. 2010).

Adult stem cell fate regulatory mechanisms are essentially the same as in pluripotent SCs. Transcriptional regulatory networks and epigenetic control ensure proper SC state. Expression of lineage specific genes is inhibited at the transcriptional or translational level by transcription factors, RNA-binding proteins and chromatin methylation. In *Caenorhabditis elegans* germ-line stem cells, Fbf-1 and Fbf-2 RNA binding proteins repress translation of factors responsible for entry into the meiotic cycle (Kimble and Crittenden 2007). In mammalian systems, the ATF5 transcription factor (Angelastro et al. 2005; Angelastro et al. 2003), SoxB1 family proteins (Avilion et al. 2003; Graham et al. 2003), the nuclear receptor Tailless and the nuclear co-receptor N-coR (Shi et al. 2004; Hermanson, Jepsen, and Rosenfeld 2002) are important in maintaining self-renewal of neural stem cells by attenuating the expression of lineage-specific genes. Differentiation towards astrocytes is also suppressed by DNA methylation of astrocyte-specific genes, such as *Gfap* (Takizawa et al. 2001). In HSC lineages, specific genes can influence alternative fates. It has been proposed that mutual inhibition of these genes might be one way to prevent differentiation (Ye et al. 2003; Orkin and Zon 2008).

1.3.2 Cell extrinsic regulation of stem cell fate

Stem cells sense changes in the environment and react to it by altering their state. Most SCs reside within specialized microenvironments called niches (Morrison and Spradling 2008). The niche contains cells and molecules that facilitate SC maintenance and function, and is involved in delivering the local and long-range signals that regulate SC state and cell cycle status (He, Nakada, and Morrison 2009). In SCs, signals are transduced to the genome through the relevant signaling pathways. The niche also provides physical anchorage for SCs. As observed in *Caenorhabditis elegans,* (He, Nakada, and Morrison 2009; Kimble and Crittenden 2007) and *Drosophila melanogaster* (Kiger et al. 2001; Fuller and Spradling 2007; Tulina and Matunis 2001), displacement of SCs from the niche environment often leads to their differentiation as they no longer receive self-renewal signals from the niche.

In mouse embryonic stem cells, leukemia inhibitory factor (LIF), Wnt and TGF-β/BMP signaling pathways have been shown to be important for maintenance of pluripotency (Okita and Yamanaka 2006; Sato et al. 2004; Smith et al. 1988; Williams et al. 1988; Ying et al. 2003) (**Figure 1.5**). Transcription factors associated with those pathways (Stat3, Tcf3 and Smad1) have been shown to contact the core regulatory circuitry directly, and in this way transduce signals into cells (Chen et al. 2008; Chen, Vega, and Ng 2008; Cole et al. 2008; Tam et al. 2008; Wu et al. 2006). BMP4 has also been proposed to suppress differentiation through induction of *Id* gene expression (Ying et al. 2003). FGF signaling is associated with differentiation in mouse ESCs (Kunath et al. 2007).

Human ESCs require FGF2 and the Activin/Nodal signaling pathways for self-renewal (Xu et al. 2005; Beattie et al. 2005; James et al. 2005; Brown et al. 2011). It has been shown that activin mediated SMAD2/3 directly activates *NANOG* in human ESCs (hESC) to maintain the pluripotent state (Vallier et al. 2009; Xu et al. 2008). In mammalian HSCs, the chemokine CXCL12 and glycoprotein angiopoietin-1 are required factors to maintain self-renewal (Kollet et al. 2006; Sacchetti et al. 2007; Sugiyama et al. 2006) and quiescence (Arai et al. 2004), respectively. It has been proposed that the niche for HSC is created by bone-lining endosteal cells and/or perivascular cells in bone marrow. Regulator molecule release has also been associated

with some of those cells, but the precise mechanism governing the way those cells regulate HSC state remains undefined (Kiel and Morrison 2008).

To summarize, the extracellular environment, in collaboration with intracellular events, regulate SC fate. Proteoglycans, which primarily reside on the cell surface and in the ECM, interact with various growth factors, and these factors establish PGs as ideal candidates for SC niche creation and signal transduction events (**Figure 1.6**).

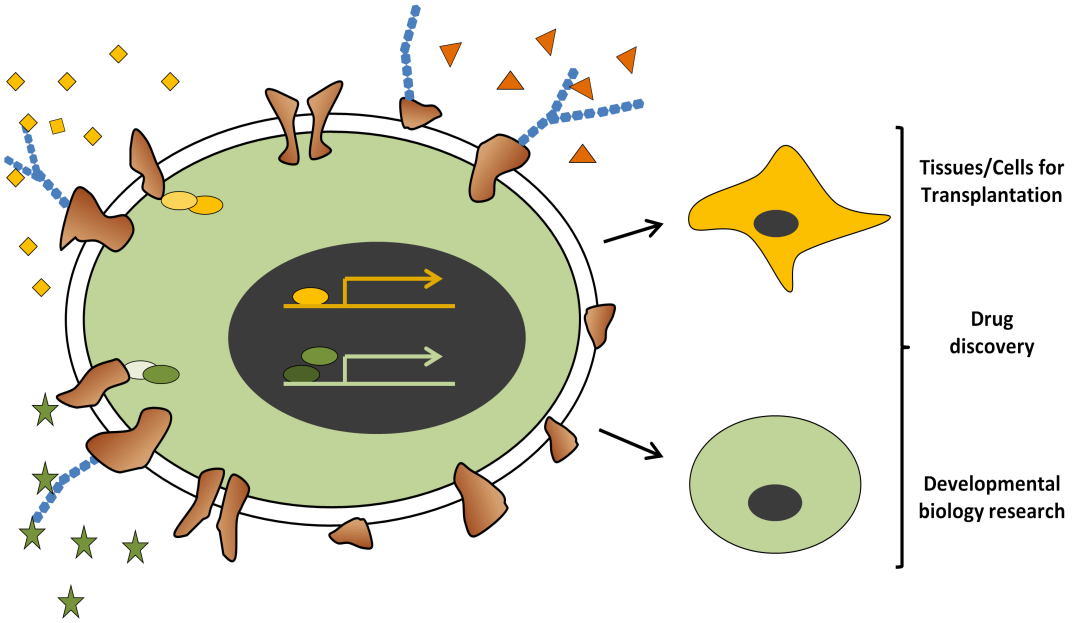

Figure 1.6. Proteoglycans play an important role in stem cell communication. Growth factors (orange triangles, green stars and yellow squares) in extracellular environment interact with proteoglycans (blue hexagons) to signal stem cell self-renewal or differentiation.

1.4 Proteoglycans in Stem Cells

Proteoglycans function in signal transduction and reside in prominent locations in the ECM and at the cell surface. Some SCs are anchorage-dependent and their fate depends on extrinsic signals. Thus, it is easy to conclude that PGs are important in determining SC fate.

1.4.1 Chondroitin sulfate and dermatan sulfate proteoglycans in stem cells

Chondroitin sulfate and dermatan sulfate proteoglycans have been found in several tissue stem cell types including neural stem cells and skeletal muscle stem cells, where they interact with various mitogens and morphogens and play an important role in SC niche creation and signal transduction. Many CSPGs have been identified in neural stem cells (NSC) and neural progenitor cells. Neurocan, phosphacan, and neuroglycan C have been found in the rat ventricular zone of the telencephalon, with additional tenascin, aggrecan (Kabos et al. 2004), and NG2 (Ida et al. 2006) in experiments with neurospheres that consist of NSC and neural progenitor cells.

Tenascin C is expressed in the mammalian embryonic central nervous system, and is important in regulating the sequential transitions of neurogenesis. NSCs deficient in tenascin C delay in transition to an EGF-responsive state. The proposed mechanism suggests that tenascin C mediates stimulatory FGF-signaling and inhibitory BMP4-signaling; requirements for transitioning NSCs to the EGF responsive state that is a prerequisite for proper neurogenesis and gliogenesis. Cells deficient in tenascin C are primarily differentiated into a neuronal fate rather than glial (Garcion et al. 2004). Tenascin C was also shown to be important in proper haematopoiesis (Klein, Beck, and Muller 1993). The versican-like PG, designated DSD-1-PG, was isolated from postnatal mouse brain. It is expressed in early astrocytes and oligodendrocytes and carries CS/DS chains. It promotes neurite outgrowth on neurons at different stages of neurogenesis in rats (Faissner et al. 1994).

NG2 CSPGs have been linked with progenitor cells in several tissues, such as oligodendrocyte progenitors in the central nervous system (Nishiyama, Yang, and Butt 2005), as well as chondroblasts and osteoblasts in skeletal tissue (Nishiyama, Dahlin, and Stallcup 1991). In the mature central nervous system, NG2-expressing glial cells can give rise to oligondendrocytes (Nishiyama, Yang, and Butt 2005). Some NG2-expressing cells have the ability to give rise to both neurons and oligodendrocytes, and thus are considered to be multipotent NSCs (Belachew et al. 2003). This property was confirmed experimentally when NG2 was observed in neurospheres obtained from rat telencephalon (Ida et al. 2006). NG2-positive cells from postnatal hippocampus can differentiate into neurons capable of propagating action potential (Belachew et al. 2003).

NG2 positive cells from the postnatal subventricular zone possess migratory ability and can differentiate into both glial cells and neurons in the olfactory bulb, hippocampus and striatum. NG2-positive cells from the cortex, cerebellum and olfactory bulb have limited migratory ability and give rise to glia only in striatum and subcortical white matter (Aguirre and Gallo 2004). Taken together, these data suggest the existence of distinct populations of NG2-expressing cells within the central nervous system with varying differentiational capacities. One possible mechanism of NG2 functionality might be through FGF2 and PDGF-AA signaling, as the NG2 core protein has been demonstrated to have high affinity for those growth factors (Goretzki et al. 1999). The Olig2 transcription factor is involved in the regulation of NG2 expression, as it has been shown that mice deficient in Olig2 fail to produce NG2 positive cells at the embryonic and perinatal stages (Ligon et al. 2006).

NG2 PGs have also been associated with epithelial and hair follicle SCs. NG2 PGs have marked chronological and spatial allotment during skin development. In the early stages of development, NG2 expression has been detected in all layers of the skin such as subcutis (adipose), dermis, the outer root sheath of hair follicles and basal keratinocytes of the epidermis. Later in development, depending on the hair growth cycle, NG2 is mainly expressed in the bulge region of the hair follicle, dermal papillae or the outer root sheath. The NG2 null mouse has a thinner epidermis and subcutis compared to wild type, which is explained by the observed reduction in keratinocyte and adipocyte proliferation (Kadoya et al. 2008).

CSPGs have also been associated with stage specific embryonic antigen-1 (SSEA-1), which is also called Lewis X (LeX) because the antigenic epitope contains a disaccharide fucose *N*-acetyl lactosamine structure (Kabos et al. 2004). In the nervous system, SSEA-1 can use different molecules as carriers including CSPGs (Yanagisawa et al. 2005). This association is affiliated with non-differentiated and progenitor cells, such as embryonic cells and adult neural stem cells and neural progenitor cells (Capela and Temple 2006). However, its expression has also been reported in other mature cells such as primary sensor neurons in quail (Sieber-Blum 1989). SSEA-1 function is associated with cell adhesion and compaction of the embryo at the morula stage. SSEA-1 may also be involved in Wnt and FGF8 signaling, as its expression is observed in

proliferative-dense regions of the brain, which requires functionality in these signaling pathways. In the later stages of mouse cell neurogenesis, SSEA-1 is expressed in the fraction of cells that will have glial progeny (Capela and Temple 2006). In humans, SSEA-3 and SSEA-4, which have a different oligosaccharide structure from SSEA-1, are expressed (Muramatsu and Muramatsu 2004), although little is known about their function or respective carrier molecules. Another CSPG-carried molecule in the nervous system is the human natural killer-1 (HNK-1) antigen, also known as CD57 (Domowicz et al. 1995). It is expressed in avian (Bronner-Fraser 1987) and rodent (Nagase et al. 2003) neural crest cells, which migrate from the neural fold to different locations during embryonic development (Anderson 1997) and can give rise to various cell types including sensory neurons, autonomic neurons, Schwann cells and smooth muscle cells (Shah, Groves, and Anderson 1996; Shah et al. 1994). HNK-1 antigen can be carried by different molecules, including aggrecan. Despite being products of the same gene locus (Domowicz et al. 1995), this aggrecan form is different from cartilage aggrecan in that it lacks keratan sulfate chains. Experiments with mice deficient in HNK-1 antigen display defective spatial memory formation, suggesting its importance in synaptic plasticity of the hippocampus (Yamamoto et al. 2002).

Certain SLRPs have also been shown to be important in myogenesis. Adult muscle regeneration happens as a result of the activity of satellite cells residing at the surface of the basal lamina of muscle fibers. Satellite cells are committed muscle cell progenitors. Under normal conditions they are quiescent, but when muscle tissue is injured they are activated and differentiate into myocytes to repair or revitalize muscle tissue. There are several signaling pathways, such as FGF2, TGB-β and HGF, involved in the maintenance of satellite cell homeostasis (Brunetti and Goldfine 1990; Cornelison et al. 2004). Decorin and biglycan, along with betaglycan, modulate this signaling by competing with TGF-β receptors for TGF-β (Droguett et al. 2006). Decorin and biglycan exploit the same mechanism to regulate proliferation and survival of bone marrow stromal cells, which are mesenchymal stem cells. Bone marrow stromal cells can give rise to different cell types including osteoblasts, chondrocytes and adipocytes (Bi et al. 2005).

1.4.2 Heparan sulfate proteoglycans in stem cells

The primary effect of HSPGs stems comes from their requirement as cofactors and mediators for many mitokines and morphogens, including FGF, VEGF, PDGF, and BMP. One of the best characterized is the interaction of HS with FGF and FGF receptor (FGFR). It is proposed that HS mediates interaction of FGF with FGFR and the stoichiometry of this interaction is 2:2:2 (Ibrahimi et al. 2004) (**Figure 1.7**). HSPGs have been primarily associated with neurogenesis and myogenesis. Perlecan, glypican-4, and syndecan-1, -3 and -4 are among those that have been identified associated with SCs.

Glypican-4 and syndecan-1 are highly expressed in the developing mouse brain and localize to the ventricular regions where neural precursor cells reside. When HS synthesis is restricted, FGF2-mediated proliferation is inhibited, confirming the role of HSPG in FGF2 signaling (Ford-Perriss et al. 2003). Glypican-4 has also been shown to be upregulated in rat neural precursor cells, but downregulated in more mature and terminally differentiated neurons (Hagihara et al. 2000).

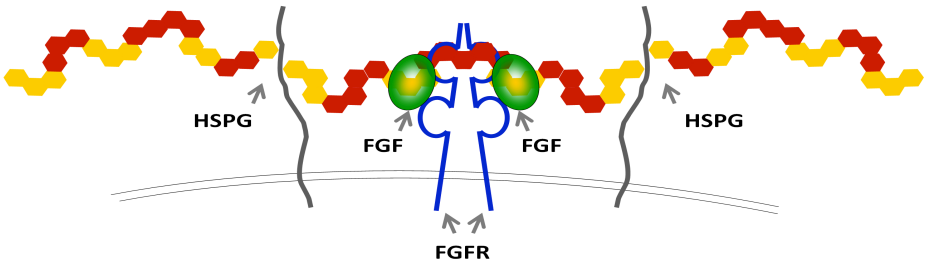

Figure 1.7. Heparan sulfate mediated FGF signaling. HS is involved in many developmental processes via FGF signaling, where it mediates the interaction of the FGF receptor with its ligand. A model of FGF signaling, which requires 2 FGF molecules, 2 FGF receptors and 2 heparan sulfate molecules (2:2:2) for proper signaling, is presented here. Adapted from (Ibrahimi et al. 2004).

Syndecan-3 is another HSPG important for brain development, and of particular importance is its HS chain. Ext1-null mice, which are deficient in HS, do not undergo proper brain morphogenesis, which is in turn linked to FGF8 signaling. Neuronal proliferation is reduced, and as a result the cerebral cortex is thinner than in wild-type mice. Although migration of neurons is not affected, axonal guidance is altered (Inatani

et al. 2003). Syndecan-3 is also involved in regulation of skeletal muscle SC differentiation. It has been shown that syndecan-3 inhibition results in aberration of myoblast fusion and altered fiber structure, although proliferation of myocytes was only slightly affected. Syndecan-3 null mice mislocalize the MyoD transcription factor, which is important for proper muscle cell differentiation. As a result, altered differentiation of myoblasts is observed (Cornelison et al. 2004). Syndecan-3 was later linked to the Notch signaling pathway and was subsequently proposed to be required for proper Notch processing. Both syndecan-3 and Notch are required to maintain satellite cell self-renewal. It has also been shown that HS chains, as well as the core protein portion of syndecan-3, are important in Notch interaction (Pisconti et al. 2010). Syndecan-3 also mediates Hedgehog regulation of chondrocyte proliferation (Shimo et al. 2004).

Syndecan-4 has been shown to be important in neural induction in the *Xenopus laevis* embryo. Inhibition of BMP signaling is insufficient for directing ectodermal cells toward a neuronal fate. Syndecan-4 can modulate this process through two signaling pathways: FGF/ERK and PKCα. Syndecan-4 modulates FGF signaling through GAGs attached to its external domain, whereas its intracellular domain is involved in PKCα signaling (Kuriyama and Mayor 2009).

In addition to ECM maintenance, basement membrane PGs play an important role in cell survival, motility and tissue morphogenesis through their interaction with growth factors and surface receptors (Iozzo 2005). Perlecan has five modules, which are involved in binding to growth factors such as FGF2, VEGF and PDGF (Knox et al. 2002; Gohring et al. 1998). Since signaling pathways involving those growth factors are important for embryonic development and tissue morphogenesis, it was hypothesized that perlecan should play a role in those processes (Iozzo 2005). Indeed one of the phenotypes of *Hspg2* (the mammalian gene coding for perlecan) mutant mice is an altered pattern of chondrocyte proliferation during cartilage development. This might be a result of an abolished interaction between perlecan and FGFs, which is required to control the amount of available FGF to interact with FGFR (Iozzo 2005). Mutations in the *trol* gene, which codes for perlecan and interacts with Hedgehog in *Drosophila melanogaster*, cause cell-cycle arrest in the larval brain, and the addition of FGF2

rescues this phenotype (Park et al. 2003; Voigt et al. 2002). Taken together, these interactions highlight the importance of perlecan in SC proliferation and differentiation, and one mechanism is the mediation of FGF signaling.

Endostatin is an endogenous antiangiogenic protein that is formed from another basement membrane PG, collagen XVIII, as a result of proteolytic cleavage of the NC1 fragment (Iozzo 2005). Endostatin inhibits endothelial cell migration and proliferation (Iozzo 2005), and has been shown to affect the expression of STAT1 and STAT3 (Abdollahi et al. 2004), which are important regulators of core regulatory circuitry in the SC state (Niwa et al. 1998). Endostatin, in a time- and dosage-dependent manner, suppresses expression of proteins Id1 and Id3 (Abdollahi et al. 2004), which play important roles in SC self-renewal by inhibiting differentiation (Ying et al. 2003).

Serglycin has historically been associated with hematopoietic cells, but its expression was detected in Tal-1 null mouse ESCs and embryoid bodies, which could not produce blood cells. Treatment with retinoic acid, a neurogenesis-directing morphogen (Damjanov, Horvat, and Gibas 1993), elevates expression of serglycin. Interestingly, the core protein of serglycin was modified upon retinoic acid treatment. Taken together, these data suggest that the serglycin core protein might not be involved in hematopoiesis (Schick et al. 2003), but rather in neurogenesis.

1.4.3 Role of the structure of the GAG chain on stem cells

The majority of work shows that PGs primarily affect stem cells through their GAG chains with their core protein having only a secondary impact. The HS chain is required for SCs to exit self-renewal and commit to certain lineages; one of them was shown to be neurogenesis (Johnson et al. 2007). Null *Ext1* ESCs fail to differentiate. This effect is linked to alterations in HS-mediated FGF signaling, which in turn has a negative effect on *Nanog* (Kraushaar, Yamaguchi, and Wang 2010). Oct4 and Sox2, in addition to Nanog, are vital factors in maintaining the SC undifferentiated state (Boyer et al. 2005).

The importance of the GAG chain in fact goes beyond its essential requirement. Its composition and sulfation pattern have also been shown to be indispensible for proper regulation of many signaling pathways leading to SC fate determination. ESCs express

simple, *N*-sulfo HS (Johnson et al. 2007). Upon differentiation toward embryoid bodies, the total amounts of HS and CS increase in tandem with an elevated level of 6-*O*-sulfo groups (Nairn et al. 2007). Augmented levels of *N*-, 2-*O*- and 6-*O*-sulfo groups accompany differentiation toward a neuronal fate (Johnson et al. 2007). The presence of 3-*O*-sulfo groups in the HS chain have been shown to be important in differentiation towards hemangioblasts, which are precursors for hematopoietic and endothelial cells (Baldwin et al. 2008; Tam and Behringer 1997). Verifying the expression level of the HS biosynthetic enzymes began the progression towards establishing the change in the level of sulfation of the HS chain (Johnson et al. 2007; Nairn et al. 2007). A striking observation is that the increased level of *N*-sulfo groups does not drastically affect the distribution of domains along the HS chain, but rather it escalates sulfation within previously sulfated domains and transition zones (Johnson et al. 2007). Taken together, these results suggest that modification of HS domains during development might be a viable mechanism for the cell to interact with various growth factors and morphogens at different stages of development. Another intriguing result is that certain configurations of HS interact with certain receptors, as was demonstrated in the case of FGF receptors. HS expressed in neural precursor cells do not interact with FGFR3, whereas it does interact with FGFR1 (Brickman et al. 1995).

Unlike HS, there are relatively few studies linking the structure of chondroitin sulfate and dermatan sulfate to stem cell fate. It has been shown that the sulfation pattern of CS did not affect the transduction of extrinsic signals required for pluripotency in mouse ESCs (Nishihara 2011). Although expression of CS is important for FGF2-mediated neural progenitor cell proliferation, the overall structure of the CS chain does not affect proliferation (Ida et al. 2006). Levels of 2-*O*-sulfo groups and 4-*O*-sulfo groups in the CS chain increase upon differentiation of mESCs towards embryoid bodies (Nairn et al. 2007).

Analyses of PGs upon SC differentiation have been performed along a limited number of lineages, such as neurogenesis, myogenesis and haematopoiesis. One of the growth factors mediated by PGs is hepatocyte growth factor, which requires GAG to signal through its c-Met receptor (Deakin and Lyon 1999). HGF is also required for

differentiation of SCs towards hepatocytes (Hay et al. 2008), which suggests a role for PGs in directing SCs to the hepatic lineage, but there is no direct evidence for this.

1.5 Conclusions

GAG biosynthetic pathways are complex systems, where interplay of the biosynthetic enzymes results in synthesis of GAG with different structures. Although numerous enzymes involved in these pathways are defined, many aspects of these pathways remain unclear. PGs are primarily found on the cell surface and in the ECM. PGs are known to interact with various growth factors and are critically involved in diverse signaling pathways and it is through these pathways that they are thought to exert control over and direct developmental processes. The stem cell state (non-differentiated *versus* differentiated) is controlled on multiple levels including genomic, proteomic, transcriptomic and epigenomic. While all of these levels have been studied in growing detail, cellular glycomics, a subdivision of epigenomics, has received considerably less attention. Glycomics is the study of glycoconjugates, including proteoglycans, glycoproteins and glycolipids.

In the following chapters we will discuss how Chinese hamster ovary cells and murine mastocytoma cells have been used as models to study details of the HS/HP biosynthetic pathway. These studies establish a correlation between the level of expression of GAG biosynthetic enzymes and GAG structure, intracellular localization of enzymes, and the choice of core proteins to carry GAG chains. The teratocarcinoma cell line NCCIT and human embryonic stem cells were exploited to demonstrate how the structure of HS/HP and CS/DS glycans changes upon differentiation towards neural, hepatic and pancreatic lineages. Understanding the details of the HS/HP biosynthetic pathway will allow us to modify the pathway with the goal to produce GAG chains of desired structure, including the one that possesses anticoagulant activity. Understanding of PGs in stem cells has many potential applications, some as simple as establishing markers for SC derivatives, and others as expansive as regulating and directing SC fate.

2. CHINESE HAMSTER OVARY CELLS AS A MODEL SYSTEM TO PRODUCE HEPARIN, OVERSULFATED HEPARAN SULFATE

2.1 Introduction

Heparin (HP) is a highly sulfated, linear glycosaminoglycan (GAG), which consists of repeated disaccharides, L-iduronic acid (IdoA) or D-glucuronic acid (GlcA) and *N*-acetyl-D-glucosamine (GlcNAc). Heparin chains are polydisperse (molecular weight: 5,000 – 40,000) and contain significant sequence heterogeneity (Ahsan et al. 1995). Fully sulfated HP chains are composed of uniform, repeating sequences of trisulfated disaccharides whereas HP chains having intermediate level of sulfation (2.5 sulfo groups per disaccharide) are composed of long segments of fully sulfated sequences with intervening undersulfated domains (**Figure 2.1**). Heparin is widely used clinically as an anticoagulant, particularly for surgery and kidney dialysis. However, in early 2008, there was a marked increase in serious adverse events associated with HP therapy, with thousands of patients who showed severe symptoms such as rash, angioedema, hypotension, and tachycardia, and nearly 100 associated deaths in the United States alone. After a thorough investigation, it was discovered that the HP injected into patients had been adulterated with oversulfated chondroitin sulfate (Guerrini et al. 2008; Pan et al. 2010), highlighting the potential risks of contamination from the current methods of HP production.

Currently, HP is extracted from animal tissues such as porcine intestines or bovine lungs. In addition to possible contamination, lot-to-lot variation is also a limitation in HP extraction because factors such as animal-care conditions affect HP quality and composition. In addition, the supply of animal tissues is limited, while the demand for HP is increasing. Moreover, there is a risk of the presence of infectious agents (e.g. prions or viruses) in HP prepared from animal tissues. Therefore, it would be preferable to produce HP under conditions where the quality and quantity of HP could be

---

Portions of this chapter previously appeared as: Baik, J. Y., L. Gasimli, B. Yang, P. Datta, F. Zhang, C. A. Glass, J. D. Esko, R. J. Linhardt, and S. T. Sharfstein. 2012. Metabolic engineering of Chinese hamster ovary cells: towards a bioengineered heparin. *Metab. Eng.* 14 (2):81-90.

controlled. Thus, the situation for HP production today is akin to the production of biological proteins and peptides such as insulin before the advent of recombinant DNA technology.

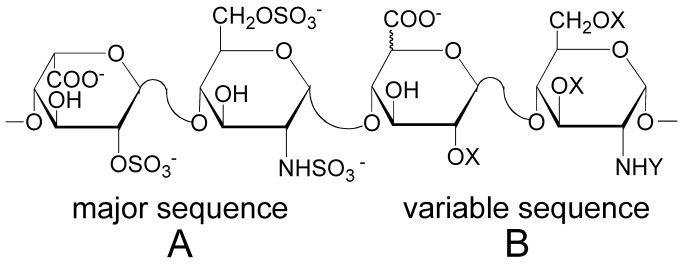

Figure 2.1. Structure of the major (A) and variable (B) repeating disaccharides comprising heparin, where X = SO_3^- or H and Y = SO_3^- or $COCH_3$. Adapted from (Baik et al. 2012).

Chinese hamster ovary (CHO) cells, the most widely used cells for therapeutic protein production, are good candidates for production of a bioengineered HP. They express many of the enzymes involved in glycosylation; they are relatively safe from biological contamination such as viruses, and they can be adapted to suspension culture and easily scaled up. More importantly, CHO cells produce heparan sulfate (HS), a less sulfated GAG that has same basic disaccharide units as HP, which is typically made by connective tissue type (serosal) mast cells. HS plays many important roles in physiological and pathophysiological processes including angiogenesis (Fuster and Wang 2010), development (Hacker, Nybakken, and Perrimon 2005; Yamaguchi et al. 2010), cell adhesion and proliferation (Tumova, Woods, and Couchman 2000), inflammation (Wang et al. 2005), and viral and bacterial infection (Spear et al. 1992) through its interaction with chemokines, cytokines, and growth factor receptors (Bishop, Schuksz, and Esko 2007). HS has considerably lower anticoagulant activity than HP (Marcum and Rosenberg 1987), but both are mediated through the interaction of a unique pentasaccharide motif, an antithrombin (AT) binding site, with ATIII, a serine-protease inhibitor (Capila and Linhardt 2002; Muszbek et al. 2010) (**Figure 2.2**).

Extensive studies by Lindahl and co-workers have shown that HP and HS are biosynthesized through a similar pathway. HS/HP biosynthesis begins in the

endoplasmic reticulum with the transfer of xylose to a specific serine residue of the core protein (Robinson et al. 1978). Addition of two galactose molecules followed by glucuronic acid gives rise to the common linkage tetrasaccharide, which is modified by a unique glucosaminyltransferase, Extl3. The chains are then polymerized by the sequential addition of D-glucuronic acid (GlcA) and *N*-acetyl-D-glucosamine (GlcNAc), catalyzed by a copolymerase complex consisting of exostosin 1 (Ext1) and exostosin 2 (Ext2) (Esko and Selleck 2002). As the chain polymerizes, a series of modifications takes place starting with *N*-deacetylation and *N*-sulfonation of GlcNAc residues, followed by epimerization of GlcA to IdoA, and finally, the introduction of *O*-sulfo groups at different positions of the glucosamine (GlcN) and uronic acid residues. Complete or nearly complete modification of this nascent GAG chain results in a highly *N*-sulfo, *O*-sulfo, IdoA-rich GAG commonly referred to as HP, which serves as the source of material for further fractionation to generate pharmaceutical HP. HS is characterized by partial modification of the chains resulting in *O*-sulfo poor and GlcNAc, GlcA-rich chains (Casu 1985; Nairn et al. 2007). Many of the enzymes involved in HS biosynthesis have multiple isozymes, which have tissue-specific and developmentally regulated expression (Bai et al. 1999). All of the known enzymes involved in the HS pathway have been cloned and the genes coding for them have been identified from a variety of organisms, including some from Chinese hamster. The expression pattern and activity level of these isozymes presumably determines which particular form of HS will be synthesized.

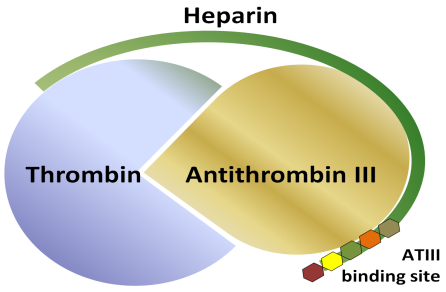

Figure 2.2. Interaction of antithrombin III binding site in heparin with antithrombin, which is required for the anticoagulation process.

Wild type CHO-K1 cells produce simple, less sulfated HS as they lack certain biosynthetic enzymes or exploit different isozymes in comparison with mast cells, which are the native site of HP production. Moreover, CHO cells produce a lower amount of HS compared to other cultured cells such as fibroblasts and some tumor cell lines (Zhang et al. 2006). CHO cells reportedly express two out of four *N*-deacetylase/*N*-sulfotransferases (Ndst), two out of three heparan sulfate 6-*O*-sulfotransferases (Hs6st) and none of seven heparan sulfate 3-*O*-sulfotransferases (Hs3st) (Zhang et al. 2006). CHO cells have been widely used to study different aspects of glycosylation. Mutants lacking certain biosynthetic enzymes were used to determine the components of the HS biosynthetic pathway and their order within the pathway (Zhang et al. 2006). However, CHO cells lack or weakly express Hs3sts and do not produce HS that binds or activates ATIII. Introduction of Hs3st1 or Hs3st5 into CHO cells bestowed ATIII binding activity upon HS produced in the cells (Duncan et al. 2004; Zhang et al. 2001; Zhang et al. 2001), indicating that they have the capacity to generate the ATIII-precursor sequence.

Although many glycosylation-related enzymes related to GAG pathways have been engineered into or genetically inactivated in CHO cells to determine their functions (Bame and Esko 1989; Zhang et al. 2001; Zhang et al. 2001; Bai and Esko 1996), there have been no published efforts to produce HP in CHO cells. Since HP and HS share a common biosynthetic pathway, we hypothesized that CHO cells could be metabolically engineered to produce HP. In this work, the expression levels of metabolic enzymes and isozymes involved in the biosynthetic pathway of HS/HP were evaluated. Stable CHO cell lines that expressed HS/HP key biosynthetic enzymes have been constructed. Finally, the structure and activity of the engineered HS was characterized.

2.2 Results

2.2.1 Evaluation of expression level of enzymes involved in HS/HP biosynthesis

CHO-S host cells were first analyzed to determine the native expression levels of biosynthetic enzymes required for HS/HP production and identify essential biosynthetic enzymes that were absent or in low abundance. Rat mast cells, a native producer of HP, were used as a positive control. As primary mast cells do not divide in culture, they were

freshly isolated from the peritoneal cavity of rats and confirmed by ruthenium red staining, a highly cationic stain (**Figure 2.3**). Ruthenium red binds to the HS anionic sulfo groups, permitting rapid identification of mast cells.

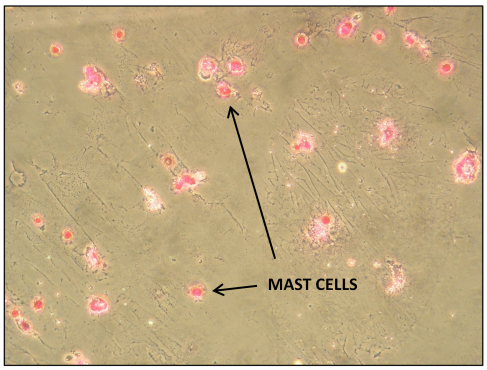

Figure 2.3. Ruthenium red staining of rat mast cells. Rat mast cells were isolated from the peritoneal cavity of adult rats and stained with 0.005% Ruthenium red.

RT-PCR results indicate that Ext1, Ext2, Ndst1, Ndst2, Glce, Hs2st1, Hs3st1, Hs6st1, and Hs6st3 are clearly expressed in rat mast cells (**Figure 2.4** and **Table 2.1**), suggesting the necessity of these enzymes for HP biosynthesis.

Table 2.1. Expression of HS/HP biosynthetic enzymes in rat mast cells and CHO-S cells as determined by RT-PCR and immunoblotting.

Cell type		Ext1	Ext2	Ndst1	Ndst2	Glce	Hs2st1	Hs6st1	Hs6st2	Hs6st3	Hs3st1	Hs3st5
RT-PCR	Rat mast	+	+	+	+	+	+	+	?[a]	+	+	-
	CHO-S	+	+	+	+	+	+	+	-	-	+	-
Immuno-blotting	CHO-S	+	+	n/a[b]	-	+	n/a[c]	+	n/a[b]	+	+	-

[a] RT-PCR of Hs6st2 from rat mast cells yielded a band of incorrect size.
[b] Immunoblotting was not performed for Ndst2 or Hs6st2.
[c] Endogenous expression of Hs2st1 was not detected by commercial antibodies due to lack of species cross reactivity.

RT-PCR with CHO-S cells allowed detection of the transcripts for the Ext1, Ext2, Ndst1, Ndst2, Glce, Hs2st1, Hs3st1, and Hs6st1 enzymes, but not Hs6st2, Hs6st3 and Hs3st5. Immunoblotting results for CHO-S cells showed that Ext1, Ext2, Glce, Hs6st1, Hs6st3, and Hs3st1 are expressed in CHO-S cells, whereas Ndst2 expression was not detected (**Figure 2.5**). Expression of HS biosynthetic enzymes is summarized in **Table 2.1**. The inactivation of Ndst2 in mice has a profound effect on mast-cell HP (Forsberg et al. 1999), leading us to identify it as one of the critical enzymes for introduction into the CHO-S cells.

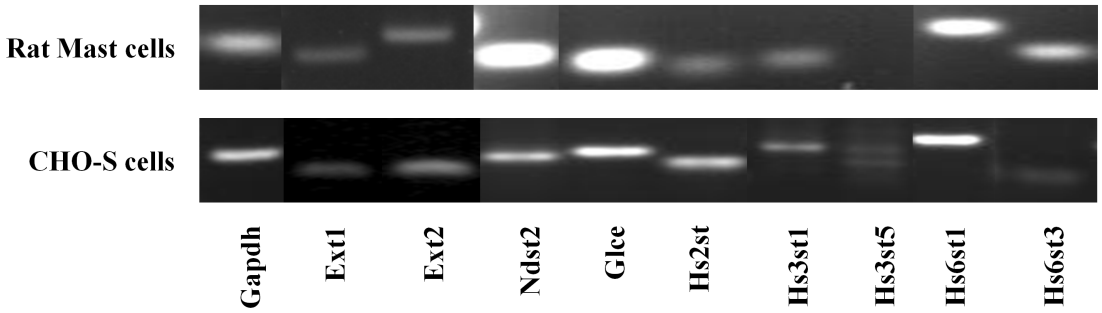

Figure 2.4. Expression of HS/HP biosynthetic enzymes in rat mast cells (top) and CHO-S cells (bottom) detected by RT-PCR.

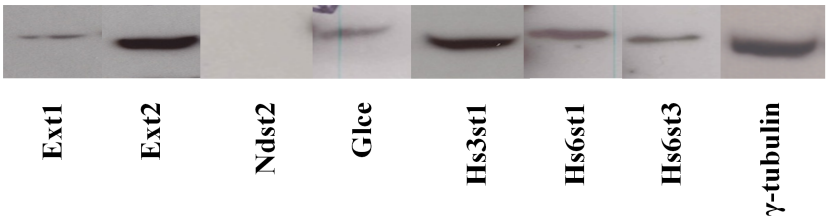

Figure 2.5. Expression of HS/HP biosynthetic enzymes in CHO-S cells determined by immunoblotting.

2.2.2 Development of stable NDST2 and Hs3st1 expressing CHO-S cell lines

Ndst2 and Hs3st1were selected for metabolic engineering, as it has been shown that they are key enzymes for anticoagulant HP biosynthesis (Sugahara and Kitagawa 2002). We observed that Ndst2 expression was not detected in CHO-S cells. *NDST2* and *Hs3st1* genes were engineered sequentially since co-transfection was not successful. At 24 h post-transfection, *NDST2* transfected cells were inoculated into semi-solid media to form colonies for clonal selection. Out of 60 colonies, 10 stable cell lines were successfully established and screened by RT-PCR (data not shown) and western blotting. The NDST2-1 cell line showed the highest level of NDST2 transcription and translation among the NDST expressing clones (**Figure 2.6**) and also sustained these expression levels for at least 30 days; therefore, it was selected for further engineering by expression of Hs3st1.

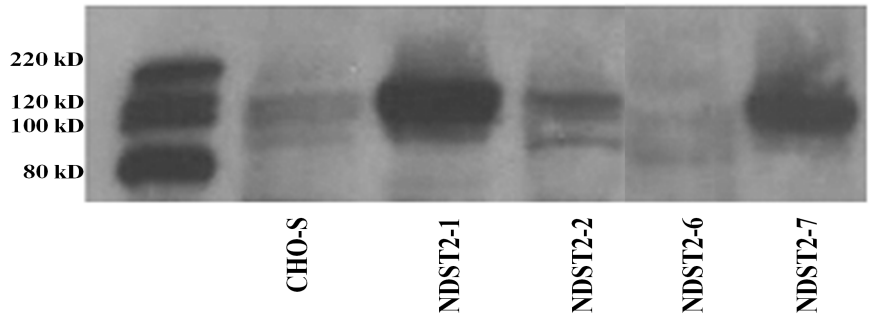

Figure 2.6. Expression of NDST2 enzyme in CHO-S cell clones transfected with *NDST2* detected by immunoblotting. Metabolic engineering of CHO-S cells was done by Dr. J. Y. Baik, SUNY at Albany, College of Nanoscale Science and Engineering, Albany, NY.

The transfection of the *Hs3st1* gene, clonal selection, and screening were carried out in the same manner as *NDST2* transfection. The established dual NDST2 and Hs3st1 expressing cell lines were denoted as Dual-1, Dual-2, etc. Out of 120 colonies from semi-solid media culture, 40 clones were established and screened for Hs3st1 expression by RT-PCR and Western blotting. NDST2 expression was also evaluated to determine if there was a loss of *NDST2* gene expression during the 3 months required to develop dual-expressing cell lines (**Appendix**). Selected cell lines are shown in **Figure 2.7**. Two

highly expressing cell lines, Dual-3 and Dual-29, were selected for characterization of the engineered HS.

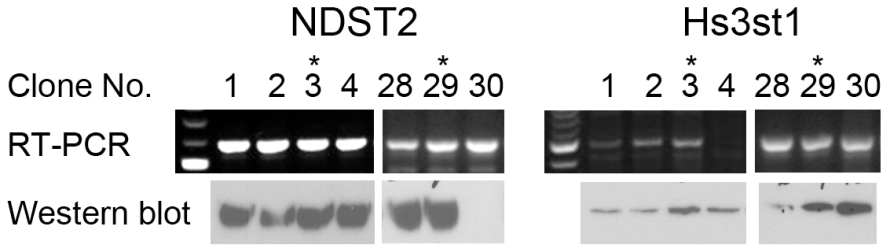

Figure 2.7. Gene and protein expression of NDST2 and Hs3st1 among selected dual-expressing clones. Based on their levels of gene and protein expression, out of 40 NDST2 and Hs3st1 dual-expressing cell lines, Dual-3 and Dual-29 (asterisks) were selected for further characterization. Adapted from (Baik et al. 2012).

2.2.3 Assessment of anticoagulation activity of bioengineered HS

Bioengineered HS was analyzed by an anti-factor Xa anticoagulation assay to determine whether the engineered HS showed increased anticoagulant activity. Since cell-membrane-bound HS proteoglycans can be shed through the action of proteases (Bernfield et al. 1999; Bartlett, Hayashida, and Park 2007), the engineered HS was also purified from the culture medium and analyzed by the anti-factor Xa assay. As shown in **Figure 2.8** the HS extracted from Dual-3 and Dual-29 cell pellets shows significantly increased anticoagulation activity (7.5-fold and 6.8-fold, respectively) compared to the HS from CHO-S host cells, which was 0.2 U/ml. However, the anticoagulant activity of the dual-expressing cells is still considerably lower than that of the pharmaceutical HP. However, the pharmaceutical HP has been fractionated to obtain high anticoagulant activity, whereas the bioengineered HS used in the activity assay was unfractionated, which may explain some of the difference in activity. The HS purified from culture media of Dual-3 and Dual-29 also shows markedly increased anticoagulation activity (52.9-fold and 97.2-fold, respectively) compared to CHO-S cells.

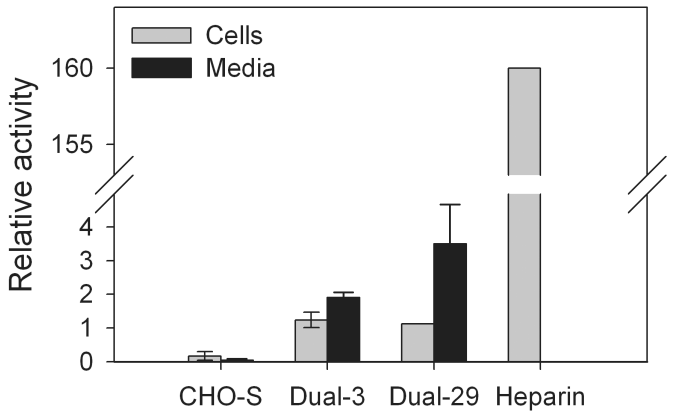

Figure 2.8. Factor Xa assay of dual NDST2 and Hs3st1 expressing cell lines. Pharmaceutical heparin was used as a positive control. Error bars represent 95% confidence intervals. Data was provided by P. Datta, RPI, Center for Biotechnology and Interdisciplinary Studies, Troy, NY.

2.2.4 Disaccharide analysis of engineered HS

The total GAGs were isolated from cells and culture media using a three-step procedure involving protease digestion, strong anion-exchange chromatography on a spin column, followed by salt release to determine the structure of engineered HS. Purified engineered HS was digested by heparin lyase into disaccharides and analyzed by RPIP-UPLC-MS. The amount of total GAG and HS/HP were quantified by carbazole assay and LC-MS, respectively. The results are summarized in **Table 2.2**. In all samples, the amount of HS/HP was higher than chondroitin sulfate/dermatan sulfate (CS/DS). In addition, the dual-expressing cell lines showed a significant increase (4.5-fold to 9-fold) in total GAGs secreted into the medium and >350-fold increase in the amount of HS/HP relative to the amount of CS/DS.

Table 2.2. Amount of total GAG and HS/HP from the cell pellets and culture media. Data was provided by Dr. B. Yang, RPI, Center of Biotechnology and Interdisciplinary Studies, Troy, NY.

	Isolated from cell pellets			Isolated from culture media		
	CHO-S	Dual-3	Dual-29	CHO-S	Dual-3	Dual-29
GAGs (μg)[a]	11.4	10.3	16.9	19.3	85.2	173.2
CS / DS (μg)[b]	2.2	1.3	1.4	0.8	0.01	0.02
HS / HP (μg)	9.2	9.0	15.5	18.5	85.2	173.2
(HS / HP) : (CS / DS)	4.2 : 1	6.9 : 1	11.1 : 1	23.1 : 1	8520 : 1	8660 : 1

The HS/HP disaccharide composition of the CHO-S cell lines is presented in **Figure 2.9**. The quantitative disaccharide composition of HS/HP was determined by calibration with disaccharide standards. For the HS/HP isolated from the CHO-S cells, 0S (88.9%) is the major disaccharide, followed by NS (9.3%) and 6S (2.0%). Interestingly, the HS/HP disaccharide composition of the culture medium for CHO-S cells shows a substantially different composition, with 6S (45.6%) as the predominant disaccharide, followed by 0S (20.3%), NS (18.1%), TriS (9.2%), and NS2S (6.8%). In dual-expressing cell lines, NS (88.3% in Dual-3, 83.7% in Dual-29) was the major disaccharide isolated from the cell pellets, and minor amounts of NS6S and TriS disaccharide were also detected. The major disaccharide from the culture medium for dual-expressing cells was also NS (96.3% in Dual-3 medium, 97.5% in Dual-29 medium). The presence of a 3-*O*-sulfo group containing disaccharide could not be verified because the action of the Hs3st1 enzyme affords a tetrasaccharide that is not cleavable by heparin lyases (Zhao et al. 2011).

[a] Total GAGs were isolated from 5×10^7 cells of each cell line or culture media for the same number of cells.

[b] Chondroitin sulfate/dermatan sulfate comprise the remaining GAGs.

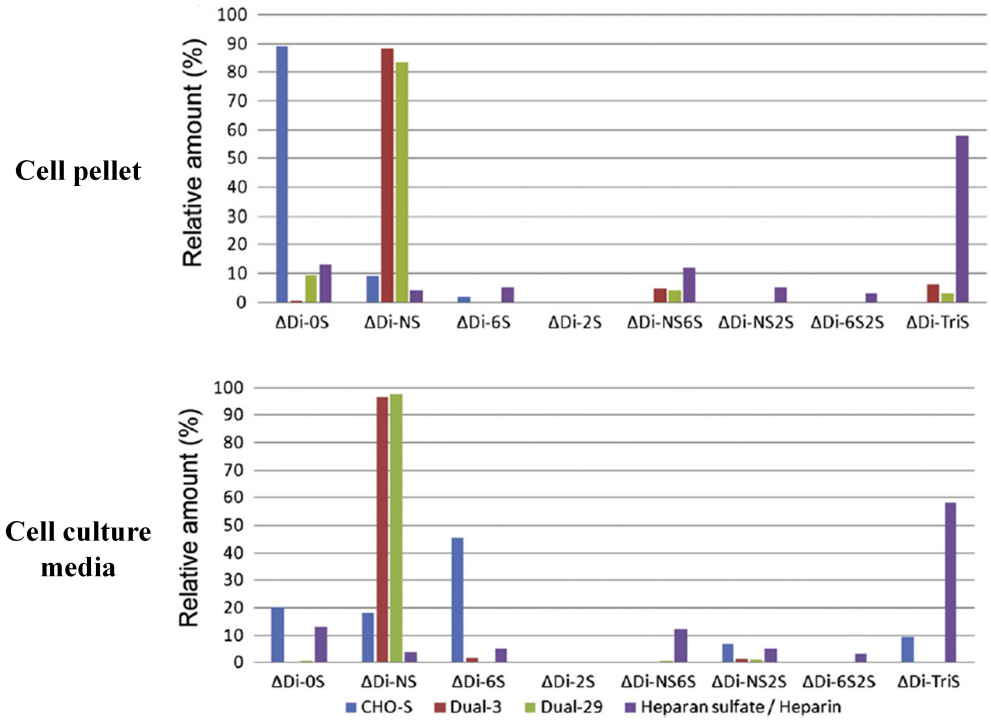

Figure 2.9. Disaccharide analysis of HS/HP from CHO-S, Dual-3 and Dual-29 cell pellets (top) and culture media (bottom) by RPIP-UPLC-MS. Data was provided by Dr. B. Yang, RPI, Center of Biotechnology and Interdisciplinary Studies, Troy, NY.

2.2.5 Expression of sulfatases in CHO-S cells and clones

Disaccharide analysis revealed a decrease in the amount of 6-*O*-sulfonation in Dual-29 clones compared to CHO-S cells. This observation led us to inquire about the activity of sulfatases, Sulf1 and Sulf2, which catalyze the removal of a sulfogroup from carbon-6 of GluNAc/GluNS in HS/HP (Couchman 2010). Immunoblotting confirmed greatly reduced expression of both sulfatases in CHO-S clones Dual-3 and Dual-29 compared to other lines such as HepG2 cells (**Figure 2.10**).

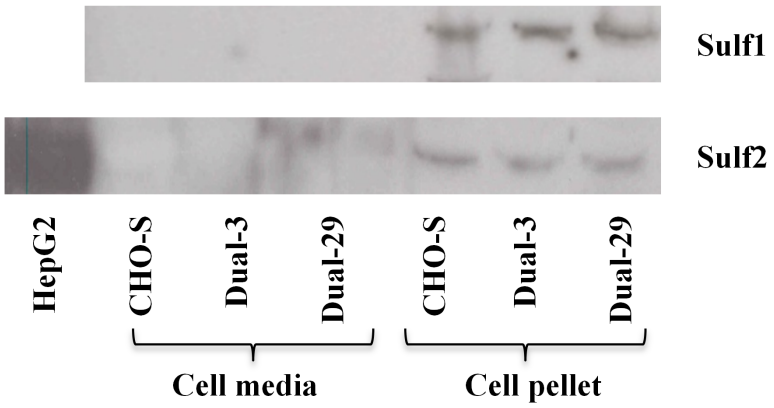

Figure 2.10. Expression of Sulf1 and Sulf2 sulfatases in CHO-S, Dual-3, and Dual-29 cells.

2.3 Discussion

Today, production of HP depends upon extracting GAGs from animal tissues. Despite efforts to synthesize HP chemically or enzymatically (Martin et al. 2009; Linhardt et al. 2007; Kuberan et al. 2003; Noti and Seeberger 2005), the sequence diversity and structural complexity of HP polysaccharides has to date, precluded the development of synthetic laboratory approaches. Some prokaryotic cell strains produce a non-sulfated version of HS/HP, heparosan, which can be used as a precursor for subsequent HP synthesis (Wang et al. 2010). However, that will require many steps of enzymatic modification and purification to obtain the relevant sulfated residues and anticoagulant activity. Therefore, a mammalian cell line was chosen as an alternative producer. Producing HP from mammalian cells is challenging because the production of non-protein macromolecules in mammalian cells has not been investigated intensively, whereas prokaryote strains have been employed to produce many non-protein compounds including polyketides, isoprenoids, bioplastics, and biofuels (Pfeifer et al. 2001; Martin et al. 2003; Aldor and Keasling 2003; Green 2011). Since HS/HP are polysaccharides, which are by nature heterogeneous, it is difficult to control their size and sequence, while protein products are precisely transcribed and translated. In addition, increased production of HS/HP cannot be achieved by genetic amplification in the same manner used for production of most protein therapeutics. It is also necessary to

identify the controlling mechanism of the HP synthesis pathway, which is not fully understood. Moreover, while previous studies have explored CHO cell metabolism (Nolan and Lee 2011; Ahn and Antoniewicz 2011) and engineering CHO cells to enhance cell viability or improve recombinant protein glycosylation (Goh et al. 2010; Yun et al. 2007), there are no reports to date using metabolic engineering to produce non-protein products in CHO cells.

In this study, rat mast cells, natural producers of HP, was used to identify the required expression of HS/HP biosynthetic enzymes and that was compared to CHO-S cells. It was confirmed that CHO-S cells did not express Ndst2 and showed minimal expression of Hs3st1, which are known to be critical for anticoagulant HP biosynthesis. Ndst2 plays an important role in the introduction of *N*-sulfo groups into GlcNAc, which in turn, is important for subsequent sulfonation of the growing HS chain (Sugahara and Kitagawa 2002). Absence of Ndst2 expression can explain the low level of *N*-sulfo groups in CHO-S HS. Hs3st1 is responsible for the formation of the unique ATIII binding pentasaccharide, which makes HP an important anticoagulant therapeutic molecule. It was also established that the CHO-S cell line used in this study expresses Hs6st3, which plays a role in refining of the sulfated structure of HS. This has not been reported for other investigated CHO cell lines.

The development of dual NDST2 and Hs3st1 expressing cell lines was confirmed by RT-PCR and immunoblotting. The disaccharide analysis by RPIP-UPLC-MS showed a significant increase in the *N*-sulfo groups within the disaccharides of the *NDST2* and *Hs3st1* transfected clones, confirming the activity of NDST2. As the available heparin lyases do not cut the HS chain in the 3-*O*-sulfo group containing sequences, RPIP-UPLC-MS could not be used to confirm the activity of Hs3st1. Anti-factor Xa assay showed an increase in HS anticoagulation ability confirming activity of Hs3st1. Quantifying enzyme activity will be necessary to demonstrate the biological activity of the engineered enzymes, but a method is not available at this time.

In the dual-expressing cell lines, the amounts of HS/HP in the media were increased significantly compared to HS/HP extracted from the cells, which implies that HS/HP on the membrane are shed into the medium. Hence, we appear to have increased the metabolic flux through this pathway by metabolic engineering. Increased HS/HP in

the media also supports the hypothesis that bioengineered HS chains will still use the HS core proteins, syndecans and glypicans, for targeting to the outside of the cell. Alternatively, the cells may also express ECM HS proteoglycans. Syndecans are type I transmembrane proteins and glypicans are glycosylphosphatidylinositol-anchored cell-surface proteoglycans. Using these HS core proteins will greatly simplify HP purification as it will eliminate the necessity of cell lysis to recover the HP. Overexpression of the core proteins might also be an option to facilitate increased traffic of bioengineered HS/HP.

From the activity studies, we observed that the engineered HS showed more anticoagulant characteristics compared to normal HS, but there is still room for improvement. In **Figure 2.9**, the relative amounts of disaccharide species in dual-expressing cells show unexpected patterns compared to those of pharmaceutical HP. The major species of dual-expressing cell lines is NS disaccharide, which suggests that the expression level of NDST2 is too high and overwhelms the actions of other enzymes. Despite the fact that enzymes involved in HS biosynthesis have been cloned and expressed, and the relative reaction order in the pathway has been established, many aspects of the biosynthesis such as the type of chain modification, domain placement, and core-protein expression remain poorly understood. The mechanism that controls the HS/HP biosynthetic pathway is also still unclear, but one widely supported hypothesis is that NDST is involved in the termination of sulfonation in HS/HP (Esko and Selleck 2002). Therefore, overexpression of NDST might terminate the sulfonation of HS/HP before other sulfotransferases were able to act on the HS chain, which means that it may be necessary to balance the expression levels of the transgenes with the endogenous genes. In *Escherichia coli* or *Saccharomyces cerevisiae*, the expression levels of enzymes involved in metabolic pathways have been controlled by gene titration, promoter engineering, or transcriptional regulation (Pitera et al. 2007; Alper et al. 2005; Michalodimitrakis and Isalan 2009). Another striking change observed was a decrease in 6-*O*-sulfonation in Dual clone-3 and Dual-29 compared to CHO-S cells. The expression of Sulf1 and Sulf2 was greatly reduced in both Dual-3 and Dual-29, suggesting that the change in 6-*O*-sulfonation we observed is not entirely caused by their activity.

2.4 Conclusions and Future Work

In conclusion, to produce HP from non-animal sources, stable CHO cell lines expressing both NDST2 and Hs3st1 were established. This is an initial study to produce HP, a non-protein therapeutic biomolecule, in mammalian cells by metabolic engineering. The engineered HS extracted from those cell lines and culture media showed that the ratio of NS was significantly increased and anticoagulation activity was increased compared to CHO-S cells. Future work will be directed towards balancing the expression of enzymes along with modification of other factors such as core proteins to achieve a pharmacological HP. Balancing the metabolic engineering to produce an engineered HS identical to the pharmaceutical HP in terms of structure and activity will require understanding the activity of the HS/HP biosynthetic enzymes in the cells. Ideally, a comprehensive model detailing the pathway of HS/HP biosynthesis would inform the work we have established in our system, and guide further analysis. Insights from the model will help direct the development of assays to establish the activity of GAG biosynthetic enzymes and inform manipulation of the HS/HP pathway in the desired direction.

2.5 Materials and Methods

2.5.1 Cell culture

CHO-S cells (Life Technologies) and dual NDST2 and Hs3st1 expressing cell lines were routinely seeded at 2×10^5 cells/ml in 125 ml polycarbonate Erlenmeyer flasks (Corning, Tewksbury, MA) containing 30 ml of culture medium and cultured on orbital shakers agitated at 125 rpm in a humidified 37ºC incubator with 5% CO_2.

2.5.2 Evaluation of the expression of HS/HP biosynthetic enzymes by RT-PCR

2.5.2.1 Isolation of rat mast cells

Peritoneal rat mast cells were isolated from ~ 6-week old adult rats based on a modification of widely used methods for mast cell isolation and staining (Nemeth and Rohlich 1980; Martynova et al. 2005; Gustafson and Pihl 1967). After rats were

sacrificed by CO_2 fixation and decapitation, their abdomens were skinned, followed by injection of ~ 60 ml of sterile phosphate buffered saline (PBS). After a gentle massage of the abdomen, the injected buffer was collected and centrifuged at 120 × g for 10 min. The pellets were re-suspended in 0.5 ml of PBS and layered on the top of a preformed 88% Percoll gradient and centrifuged at 450 × g for 15 min. The mast-cell-containing fraction, which occupied the lower part of the tube, was collected. The presence of the mast cells was confirmed by staining with 0.005% Ruthenium red. The 88% Percoll gradient was prepared by dilution of a 100% Percoll gradient with 1X RPMI-1640. The 100% Percoll gradient was made by adding 10 ml of 10X RPMI-1640 containing 200 mM HEPES/ 1M NaOH to 90 ml of commercial Percoll solution (GE Healthcare, Piscataway, NJ). The tubes were then centrifuged at 12,000 × g for 30 min at 4ºC to make the gradient.

2.5.2.2 RNA extraction, RT-PCR reaction

Total RNA was extracted from the mast cells isolated from 6 rats and from 4×10^6 CHO-S cells using RNeasy mini kits (Qiagen, Germantown, MD) according to the manufacturer‘s instructions. The amount of RNA was assessed by NanoDrop 2000 spectrophotometer (Thermo Fisher Scientific, Waltham, MA). 60 - 90 ng of total RNA per sample was used in reverse transcription and polymerase chain reactions using a SuperScript III Platinum One-Step RT-PCR kit (Life Technologies, Grand Island, NY). A list of primers used is given in **Appendix**. RT-PCR products were separated and visualized by agarose gel electrophoresis using ethidium bromide.

2.5.3 Transfection and selection of NDST2 and Hs3st1 expressing cell lines

The human *NDST2* gene (GenBank: BC035711.1, Thermo Fisher Scientific) was amplified using a primer pair, which includes *BamHI* and *NotI* restriction enzyme sites (forward primer: 5`-GAGCTCGGATCCACTATGCTCCAGTTGTGGAAGGTG-3`; reverse primer: 5`-CTCGAGCGGCCGCTCAGCCCAGACTGGAATGCTG-3`) and inserted into the pcDNA3.1/Neo expression vector (Life Technologies). The mouse

Hs3st1 gene, kindly provided by Professor Jian Liu at University of North Carolina (Xu et al. 2008), was cut by EcoRI and XhoI restriction enzymes and inserted into the pcDNA3.1/Zeo expression vector (Life Technologies). CHO-S cells (2×10^6 cells) were transfected with the *NDST2* gene using a Nucleofector® II (Lonza, Basel, Switzerland) according to the manufacturer's instructions (kit V, program U-024). The transfected cells were seeded at 6.7×10^5 cells/ml and incubated at 37ºC and 5% CO_2 in static 6-well plate cultures (Corning) for 24 hours after transfection. Next, the cells (10^4 cells/ml) were seeded into ClonaCell®-TCS Medium (STEMCELL Technologies, Vancouver, Canada) supplemented with 1 mg/ml of Geneticin® (Life Technologies) and grown at 37ºC and 5% CO_2 for two weeks. Selected NDST2 expressing cell clones were then transfected with the *Hs3st1* gene and inoculated into semi-solid medium supplemented with 1 mg/ml of Geneticin® and 500 μg/ml of Zeocin™ (Life Technologies) in the same manner as for the development of NDST2 expressing cell lines. The host CHO-S cell line and dual NDST2 and Hs3st1 expressing cell lines were maintained in CD CHO medium (Life Technologies) supplemented with 8 mM GlutaMAX™ (Life Technologies) and 15 ml of hypoxanthine/thymidine solution per 500 ml of medium (HT, Mediatech, Manassas, VA). In addition, 1 mg/ml of Geneticin® and 500 μg/ml of Zeocin™ were added to the medium for dual-expressing cell lines.

2.5.4 Screening of *NDST2* / *Hs3st1* transfected cell lines by RT-PCR and immunoblotting

RT-PCR was conducted as described above for wild-type CHO-S cells. For total protein extraction, exponentially growing cells were lysed in Nonidet-P40 lysis buffer (Boston Bioproducts, Ashland, MA) on ice for 30 min in the presence of a cocktail of protease and phosphatase inhibitors (Thermo Fisher Scientific), which contained AEBSF, aprotinin, bestatin, E-64, leupeptin, and pepstatin A. Protein concentrations were determined using BCA assay (Thermo Fisher Scientific). A 40 μg sample of total protein was loaded and separated on 4-20% polyacrylamide gels (Thermo Fisher Scientific) at 150 V. Tris-Hepes-SDS buffer was used as the running buffer. Proteins were transferred onto a PVDF membrane (Bio-Rad Laboratories, Hercules, CA), probed with relevant primary antibodies (described below), and then detected using the appropriate HRP-

conjugated secondary antibody and chemiluminescent (Super Signal West Pico ECL substrate, Thermo Fisher Scientific) exposure on high performance chemiluminescence film (Amersham Hyperfilm ECL, GE Healthcare). The primary and secondary antibodies used are the following: anti-gamma-tubulin (T3320, Sigma-Aldrich, St. Louis, MO); anti-Ndst2 (sc-16764, Santa Cruz Biotechnology, Santa Cruz, CA), anti-Hs3st1 (sc-104313, Santa Cruz Biotechnology), anti-Hs6st1 (sc-109943, Santa Cruz Biotechnology), anti-Hs6st3 (sc-84308, Santa Cruz Biotechnology); anti-Glce (H00026035-B01P, Abnova, Taipei City, Taiwan); anti-Sulf1 (sc-98325, Santa Cruz Biotechnology), anti-Sulf2 (sc-68435, Santa Cruz Biotechnology), goat anti-rabbit HRP-conjugated (31460), goat anti-mouse HRP-conjugated (31430, Thermo Fisher Scientific); donkey anti-goat HRP-conjugated (sc-2020, Santa Cruz Biotechnology).

2.5.5 Anticoagulant-activity analysis of bioengineered HS by anti-Factor Xa assay

The anti-factor Xa anticoagulation activity was based on a chromogenic assay from a published method (Chen et al. 2005) with a heparin anti-FXa assay kit (HemosIL^{TM}, Instrumentation Laboratory, Bedford, MA). In brief, the GAGs purified as described below from CHO cell lines or a HP standard (at various concentrations) were dissolved in Tris-EDTA buffer (50 mM Tris, 7.5 mM EDTA, and 175 mM NaCl, pH 8.4). The reaction mixture, which consisted of 25 µl of ATIII stock solution (1 IU/ml) and 25 µl of the GAGs or HP, was incubated at 37°C for 2 min. 25 µl of Factor Xa (13.6 nkat/ml) was added. After incubating at 37°C for 4 min, 25 µl of chromogenic substrate S-2765 (0.75 mg/ml) was added. The absorbance of the reaction mixture was measured at 405 nm continuously for 10 min in a 96-well plate reader (SpectraMax M5, Molecular Devices, Sunnyvale, CA).

2.5.6 Disaccharide analysis of engineered HS

2.5.6.1 Isolation and purification of GAGs from cells and culture media

Disaccharide analysis of engineered HS/HP was carried out as described previously (Yang et al. 2011). The cell samples were individually subjected to proteolysis at 55°C

with 10% (w/v) of actinase E (20 mg/ml in HPLC grade water, Kaken Biochemicals, Tokyo, Japan) for 20 h. After proteolysis, particulates were removed from the resulting solutions by passing each through a 0.22 μm membrane syringe filter. Samples were then concentrated using Microcon YM-10 centrifugal filter units (10 kDa molecular weight cutoff, Millipore) by centrifugation at 12,000 × g and washed with 15 ml of distilled water to remove peptides. The retentate was collected and lyophilized. Samples were dissolved in 0.5 ml of 8 M urea containing 2% CHAPS (pH 8.3). A Vivapure Mini Q H spin column (Viva Science, Edgewood, NJ) was prepared by equilibrating with 200 μl of 8 M urea containing 2% CHAPS (pH 8.3). To remove any remaining proteins, the clarified, filtered samples were loaded onto and run through the Vivapure MINI Q H spin columns under centrifugal force (700 × g). The columns were then washed with 200 μl of 8 M urea containing 2% CHAPS at pH 8.3, followed by five washes with 200 μl of 200 mM NaCl. GAGs were released from the spin column by washing three times with 50 μl of 16% NaCl. GAGs were desalted with YM-10 spin columns. The GAGs were lyophilized and stored at room temperature for future use.

2.5.6.2 Enzymatic digestion and reverse-phase ion-pairing ultra-performance liquid chromatography mass spectrometry (RPIP-UPLC-MS)

The GAGs recovered from cells and media were quantified by microcarbazole assay (Zhang et al. 2009) and then used to prepare a stock solution from which 5 μg of analyte could be removed. Cloning, *Escherichia coli* expression, and purification of recombinant heparin lyase I (EC 4.2.2.7), heparin lyase II (no EC assigned), and heparin lyase III (EC 4.2.2.8) from *Flavobacterium heparinum* were performed as described previously (Shaya et al. 2006; Yoshida et al. 2002; Godavarti et al. 1996). Heparin lyase I, II, and III (5mU each, assayed prior to use) in 5 μl of 25 mM Tris 500 mM NaCl, and 300 mM imidazole buffer (pH 7.4) were added to 5 μg of GAG sample in 25 μl of distilled water and incubated at 37°C for 10 h to completely degrade the GAG sample. The products were recovered by centrifugal filtration using a YM-10 microconcentrator, and the HS/HP disaccharides were recovered in the flow-through and lyophilized. The digested GAG disaccharides were redissolved in water at a final concentration of 50 to 100 ng/μl for LC–MS analysis.

LC–MS analyses were performed on an Agilent 1200 LC/MSD instrument (Agilent Technologies, Wilmington, DE) equipped with a 6300 ion trap and a binary pump followed by a UV detector equipped with a high-pressure cell. The column used was an Acquity UPLC BEH C18 column (2.1 × 150 mm, 1.7 μm, Waters, Milford, MA). Eluent A was water/acetonitrile (85:15, v/v), and eluent B was water/acetonitrile (35:65, v/v). Both eluents contained 12 mM tributylamine (TrBA) and 38 mM NH_4OAc with pH adjusted to 6.5 with acetic acid. Disaccharide analysis was performed using a gradient of solution A for 10 min, followed by a linear gradient from 10 to 40 min (0–50% solution B) at a flow rate of 100 μl/min. The column effluent entered the source of the electrospray ionization (ESI)–MS for continuous detection by MS. The electrospray interface was set in negative ionization mode with a skimmer potential of – 40.0 V, a capillary exit of – 40.0 V, and a source temperature of 350°C to obtain the maximum abundance of the ions in a full-scan spectrum (200–1500 Da). Nitrogen (8 l/min, 40 psi) was used as a drying and nebulizing gas.

Quantification analysis of HS/HP disaccharides was performed using calibration curves constructed by separation of increasing amounts of unsaturated HS/HP disaccharide standards (2, 5, 10, 15, 20, 30, 50, and 100 ng per disaccharide). Unsaturated disaccharides standards of HS/HP (0S: ΔUA-GlcNAc, NS: ΔUA-GlcNS, 6S: ΔUA-GlcNAc6S, 2S: ΔUA2S-GlcNAc, NS2S: ΔUA2S-GlcNS, NS6S: ΔUA-GlcNS6S, 2S6S: ΔUA2S-GlcNAc6S, triS: ΔUA2S-GlcNS6S) were obtained from Iduron (Manchester, UK). Linearity was assessed based on the amount of disaccharide and peak intensity in MS. All analyses were performed in triplicate.

3. MURINE MASTOCYTOMA CELLS AS A MODEL TO STUDY HEPARAN SULFATE/HEPARIN BIOSYNTHETIC PATHWAY

3.1 Introduction

Heparin (HP) is one of the most widely used therapeutic anticoagulant molecules. Consequently, there is a necessity for a model to study its biosynthetic pathway in greater detail. HP is biosynthesized in the same pathway as heparan sulfate (HS) (Esko, Kimata, and Lindahl 2009). Although the enzymes and their position within the involved pathway are known, it is a challenge to manipulate the pathway for the production of HP of clinically acceptable quality. This was demonstrated using a system engineered to produce HP in Chinese hamster ovary (CHO) cells expressing two crucial enzymes of the pathway, NDST2 and Hs3st1. Our results showed that the resultant HS/HP chains displayed low anticoagulant activity (Baik et al. 2012)

Connective tissue mast cells naturally produce HP, and have potential for study of HP biosynthesis and its biological role. However, isolation, propagation and maintenance of primary connective tissue mast cells is challenging. These issues have rendered research into the role of mast cells in HS/HP production problematic. Primary mast cells have primarily been used for the study of various aspects of inflammatory processes (Young et al. 1987; Theoharides and Cochrane 2004). Mice deficient in Ndst2 produced mast cells of modified morphology that contained undersulfated HP (Forsberg et al. 1999). A study using mutant mouse mast cells deficient in C5-Epimerase highlighted its importance for *O*-sulfonation of HP (Feyerabend et al. 2006). The immortalized mast cell line, C57.1, was shown to express the transcript for Hs3st (Shworak et al. 1997), but little else has been established within the HS/HP pathway in that cell line.

Furth murine mastocytoma cells were isolated and a tumor cell suspension was produced in order to study HP biosynthesis. Designated as MST, they were used to study the biological role of HP. MST cells express the proteoglycan serglycin that has heparin along with a minor fraction of chondroitin sulfate (CS) E GAG chains (Lidholt, Eriksson, and Kjellen 1995). HP chain structure produced by MST cells was similar to commercial HP except that it lacked 3,6-*O*-sulfonation and anticoagulant activity, which are essential for the biological function of HP. It has also been shown that GAGs are

associated with cytoplasmic granules (Montgomery et al. 1992). Heparin is processed by heparinase, which exhibits endoglucuronidase activity and is localized outside of granules. Heparinase does not act on CS/DS (Ogren and Lindahl 1971).

Murine mastocytoma cells were used to study localization of HS/HP and CS/DS biosynthetic enzymes within the Golgi apparatus. Cells were treated with Brefeldin A (BFA), which is a fungal metabolite that disrupts Golgi structure in a way that *cis*-, *medial*- and *trans*-Golgi fuse back with the endoplasmic reticulum, whereas the *trans*-Golgi network remains unaffected. This drug makes it possible to distinguish molecules residing in the Golgi from those residing in the *trans*-Golgi network. This technique made it possible to associate HS/HP biosynthetic enzymes with the proximal Golgi, whereas CS/DS enzymes were mainly localized within the *trans*-Golgi network. Although the cells were still able to produce both GAGs, both molecules were undersulfated in cells treated with BFA. This suggested that enzymes involved in GAG chain modification were mainly localized in the distal portion of the Golgi. It was also observed that CS chains were shorter than in control cells, whereas HS/HP chains were longer than in control cells. The fact that both types of GAG were synthesized but the total level was decreased suggested, that even though HS/HP biosynthetic enzymes localize primarily to the proximal Golgi and CS enzymes to the distal Golgi, those enzymes were actually dispersed throughout the entire Golgi (Klausner, Donaldson, and Lippincott-Schwartz 1992; Misumi et al. 1986; Uhlin-Hansen et al. 1997)**.** Association of CS/DS biosynthetic enzymes with the *trans*-Golgi network was established in other cell lines including human melanoma (Uhlin-Hansen et al. 1997) and rat ovarian granulosa cells (Uhlin-Hansen et al. 1997).

From mast and mastocytoma cell studies, it was revealed that HS/HP biosynthetic enzymes are in complexes called GAGosomes. These include XylT and GalT (Schwartz 1975), Ext1 and Ext2 (Kobayashi et al. 2000), C5-Epimerase and Hs2st (Pinhal et al. 2001), and possibly Ext2 and Ndst1 (Presto et al. 2008).

MST cells and their various subclones are suitable models for elucidation of the minutiae of the HS/HP biosynthetic pathway. We used MST cells and MST-10H cells, which is an MST clone with HS3ST1 transfected, to gain insight into various aspects of HP biosynthesis. We examined expression levels of the GAG chain polymerization and

modification enzymes, their intracellular localization, and the expression of their relevant core proteins. We also assessed the effect that modification of the pathway in MST-10H cells produced on the structure and activity of the newly biosynthesized HS/HP chains. We compared those data with the results obtained from studies using CHO cells with the aim to establish the essential elements for anticoagulant HP production.

3.2 Results

3.2.1 Murine mastocytoma cells express sulfated GAGs.

MST and MST-10H cells grow as aggregates in static suspension conditions (**Figure 3.1 A**). In order to confirm that they express sulfated GAGs, which are negatively charged, staining with the positively charged stain ruthenium red, was performed (**Figure 3.1 B**). This technique indicated that both cell lines contain sulfated GAGs.

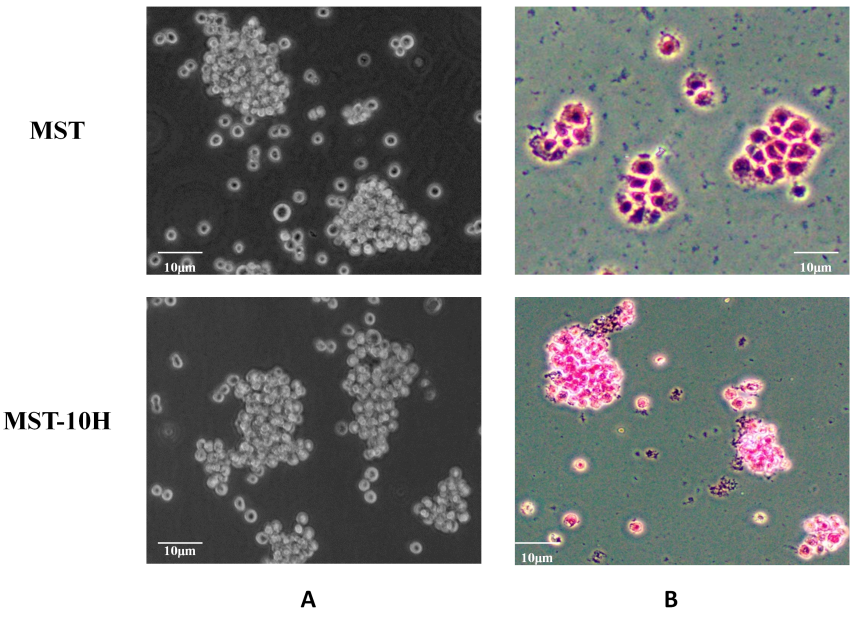

Figure 3.1. Murine mastocytoma cells. A. Bright field images of MST and MST-10H cells. **B.** Ruthenium red staining of MST and MST-10H cells.[a]

[a] Difference in the color of Ruthenium Red stain between MST and MST-10H is due stain drying.

3.2.2 Expression profile of HS/HP biosynthetic enzymes in MST and MST-10H cells is different from wild-type CHO-S and Dual-29 cells.

mRNA levels of the HS/HP biosynthetic enzymes in MST and MST-10H cells were established by RT-PCR analyses, and results are shown in **Figure 3.2**. For comparison, RT-PCR results for the same enzymes from wild-type (wt) CHO-S and the Dual-29 clone are also shown. Expression of all HS/HP biosynthetic enzymes, except Hs3st5, was detected in MST and MST-10H cells. CHO-S (wt) and Dual-29 express all of the tested enzymes excluding Hs6st2, Hs6st3 and Hs3st5, and these results are summarized in **Table 3.1**.

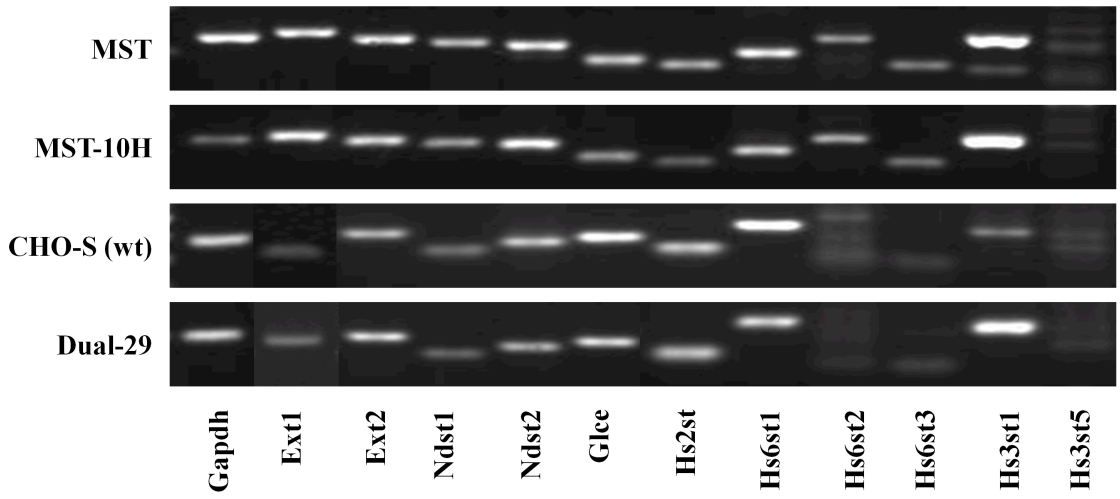

Figure 3.2. Expression of HS/HP biosynthetic enzymes in MST, MST-10H, CHO-S (wt) and Dual-29 cells detected by RT-PCR.

Immunoblotting was performed to confirm expression of the HS/HP biosynthetic enzymes and to establish a correlation with the expression of the mRNA of the enzymes using MST and MST-10H cells. We measured expression of the Ext1, Ext2, Ndst2, Glce, Hs6st1, Hs6st3 and Hs3st1 enzymes (**Figure 3.3**). The expression of Ext1 was detected in both MST and MST-10H cells, and its expression in MST-10H cells was lower, but detectable. The expression of Ext2, Glce and Hs6st1 could not be detected in either cell line. Both cell lines were shown to express Ndst2. The expression of Hs3st1

was detected in MST-10H cells, but not in MST cells. In contrast, the expression of Hs6st3 was detected in MST cells, but not in MST-10H cells.

For comparison, the expression of Ext1, Ext2, Hs6st1, Hs6st3, and Hs3st1 was detected in CHO-S (wt) and Dual-29 cells. Ndst2 expression was detected only in Dual-29 cells, and not in CHO-S (wt). In contrast, Glce was expressed in CHO-S (wt) and not in Dual-29 cells (**Figure 3.3**).

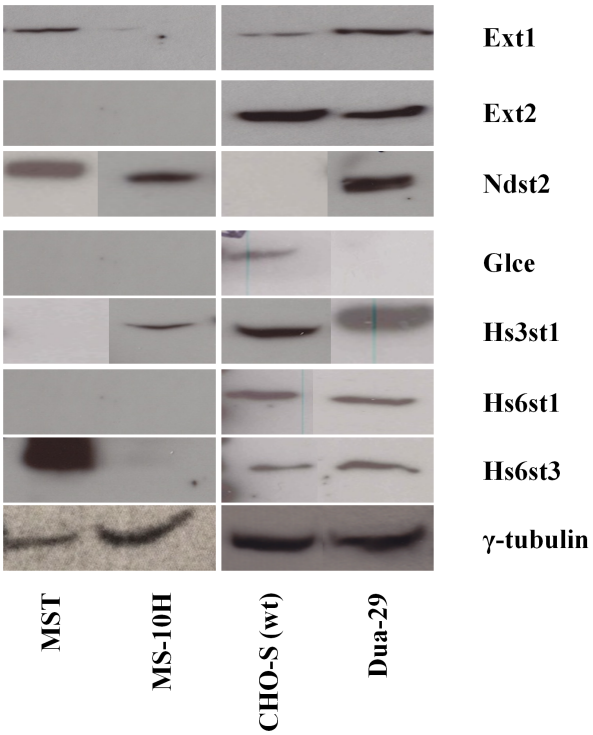

Figure 3.3. Expression of HS/HP biosynthetic enzymes in MST, MST-10H, CHO-S (wt) and Dual-29 detected by immunoblotting.

Table 3.1. Expression of HS/HP biosynthetic enzymes in MST, MST-10H, CHO-S (wt) and Dual-29 cells determined by RT-PCR.

Cell type	Ext1	Ext2	Ndst1	Ndst2	Glce	Hs2st	Hs6st1	Hs6st2	Hs6st3	Hs3st1	Hs3st5
MST	+	+	+	+	+	+	+	+	+	+	?[a]
MST-10H	+	+	+	+	+	+	+	+	+	+	?[a]
CHO (wt)	+	+	+	+	+	+	+	-	-	+	-
Dual-29	+	+	+	+	+	+	+	-	-	+	-

3.2.3 Intracellular localization of Ndst2 and Hs3st1 enzymes.

Cellular localization of the key HS/HP biosynthetic enzymes, Ndst2 and Hs3st1, had been previously assayed in MST and MST-10H cells (data not shown). Localization of those enzymes was tested in CHO-S (wt) and Dual-29 cells to compare with MST and MST-10H cells. CHO-S (wt) and Dual-29 cells were fractionated, and different fractions were isolated, including Golgi and ER. A schematic of the cell fractionation is presented in **Figure 3.4**. Identity of the Golgi fraction was checked by detecting the expression of the 58 kDa Golgi marker protein (**Figure 3.5**). The marker protein was localized in intact CHO-S (wt) and Dual-29 cells juxtaposed with the nucleus, thereby confirming its Golgi association. The marker was also expressed in membranes isolated from both cell types confirming their Golgi origin. In CHO-S (wt) and Dual-29 cells, Ndst2 was detected in the Golgi fraction. In Dual-29 cells, Hs3st1 protein was localized to the Golgi fraction, but no signal was detected in Golgi isolated from CHO-S (wt) cells (**Figure 3.6**).

[a] RT-PCR of Hs3st5 from MST and MST-10H cells yielded a band of incorrect size.

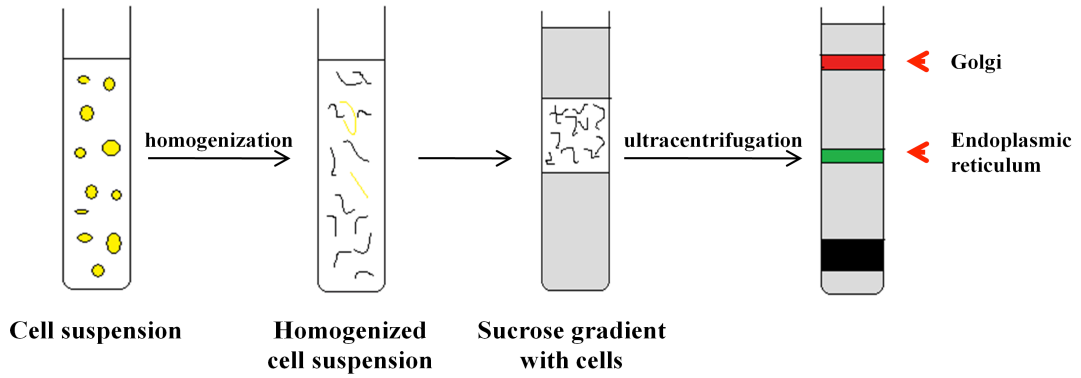

Figure 3.4. Subcellular fractionation of CHO-S (wt) and Dual-29 cells for Golgi membrane isolation.

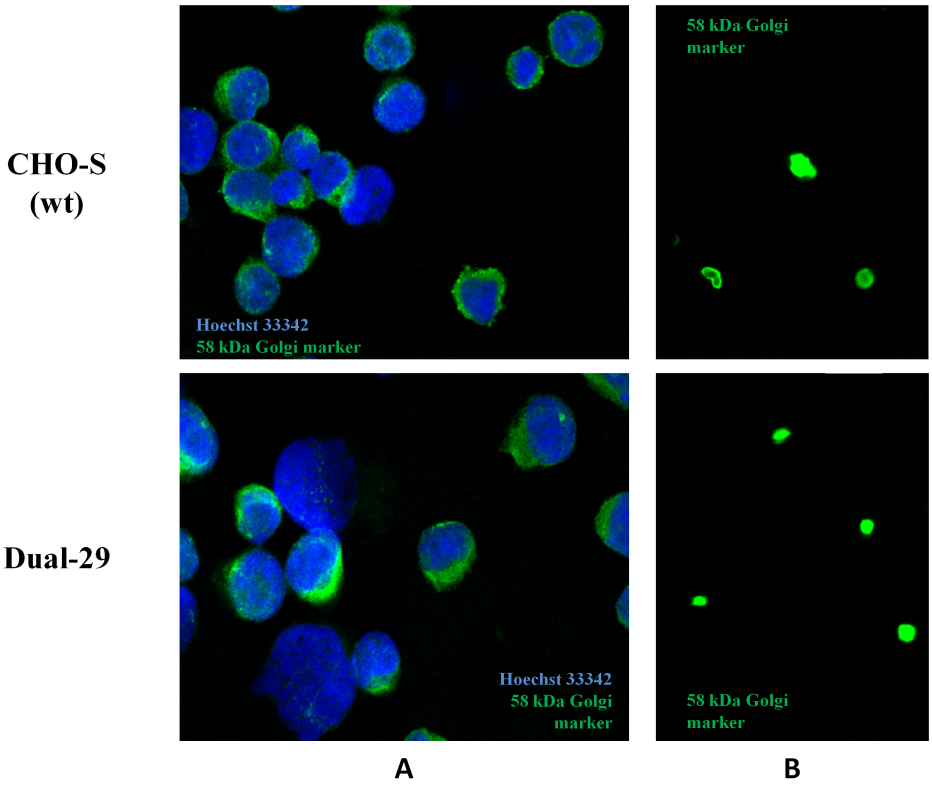

Figure 3.5. Expression of 58 kDa Golgi protein marker in CHO-S (wt) and Dual-29 cells (A) and in Golgi membranes isolated from CHO-S (wt) and Dual-29 cells (B).

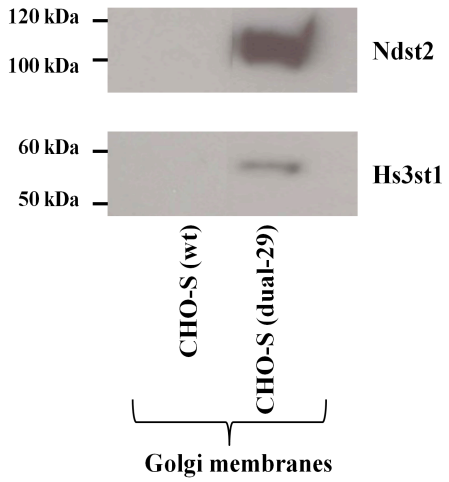

Figure 3.6. Expression of Ndst2 and Hs3st1 in Golgi membranes of CHO-S (wt) and Dual-29 cells detected by immunoblotting. Samples of Golgi fractions was provided by Dr. T. Gemmill, SUNY at Albany, College of Nanoscale Science and Engineering, Albany, NY.

3.2.4 Expression of HS/HP core proteins changes in MST-10H and Dual-29 cells

Syndecans and glypicans are core proteins that carry HS chains in cells, whereas HP is attached to serglycin (Esko, Kimata, and Lindahl 2009). There are 4 transmembrane proteins that belong to the syndecan family (1-4) (Tkachenko, Rhodes, and Simons 2005; Couchman 2010). The expression of syndecan-1 was detected in both MST and MST-10H cells, and syndecan-3 was detected only in MST-10H cells, while syndecan-2 and -4 were not detected in either cell type. A similar pattern was observed for the expression of syndecans in CHO-S (wt) and Dual-29 cells. Syndecan-1 and -3 were expressed in both CHO-S (wt) and Dual-29 cells, while syndecan-2 and -4 were not detected in either cell line. The conditioned media in which CHO cells were grown was also examined for the presence of syndecans in order to assess the possibility that they are shed out of the cell and into the media. Results showed no syndecans in the media. Due to the interference of constituent protein components of the media used to culture MST and MST-10H cells, it was not possible to check for syndecans in the media (**Figure 3.7**).

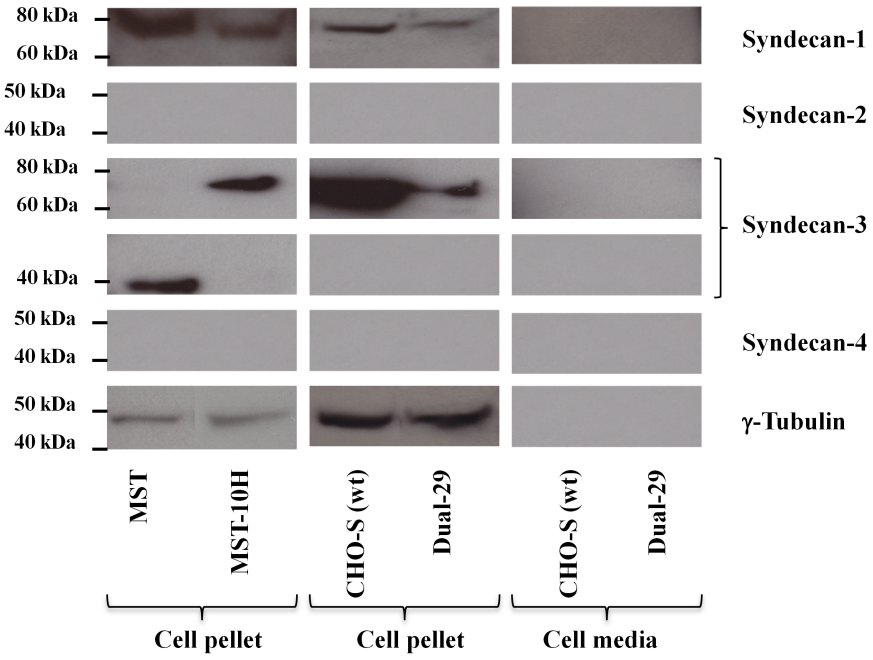

Figure 3.7. Expression of syndecans in MST, MST-10H, CHO-S (wt) and Dual-29 cells detected by immunoblotting.

There are 6 members of GPI-anchored proteins (glypican-1-6) belonging to the glypican family (Filmus, Capurro, and Rast 2008). Glypican-1 was expressed in both MST and MST-10H cells, while expression of glypican-2, -3 and -5 were detected in MST-10H cells and not in MST cells, whereas glypican-4 and -6 were not detected in either cell line. In contrast, CHO-S (wt) and Dual-29 cells were shown to express glypican-1, -5, and -6. Dual-29 cells express glypican-2 and -3 whereas CHO-S (wt) did not express either. The expression of glypican-4 was not detected in either CHO cell line (**Figure 3.8).** As with syndecans, the media CHO-S (wt) and Dual-29 cells were cultured in was assayed for possible shedding of the glypicans. Only glypican-6 was detected in the media from CHO-S (wt). Again, it was not possible to perform this assay for MST and MST-10H cells.

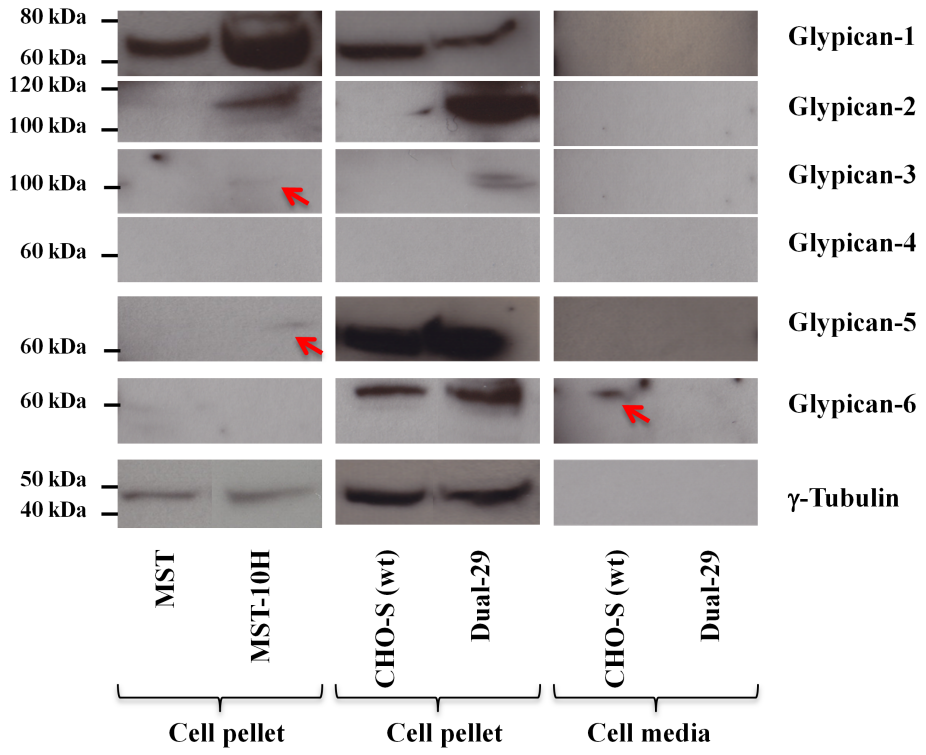

Figure 3.8. Expression of glypicans in MST, MST-10H, CHO-S (wt) and Dual-29 cells detected by immunoblotting.

Serglycin is an HP core protein that been shown to be expressed in mouse mastocytoma cells (Lidholt, Eriksson, and Kjellen 1995). Its expression in our mastocytoma cell lines MST and MST-10H was confirmed by RT-PCR (**Figure 3.9**). Serglycin transcript was detected in both MST and MST-10H cells. We also confirmed the expression of serglycin message in CHO-S (wt) and Dual-29 cells.

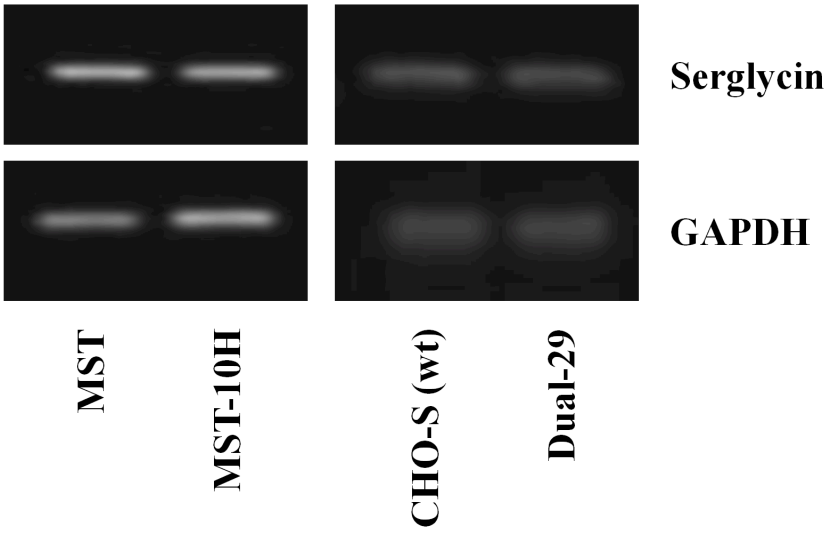

Figure 3.9. Expression of serglycin in MST, MST-10H, CHO-S (wt) and Dual-29 cells detected by RT-PCR.

3.2.5 HS/HP disaccharide structure of MST-10H cells approximates the commercial HP structure.

In order to establish the structure of the HS/HP chains synthesized by MST and MST-10H cells, GAG chains were isolated, digested and the resultant disaccharides were collected and analyzed by LC-MS (**Figure 3.10**). HS/HP levels from the cell pellet fraction and from cell culture media were assessed. Bovine lung HP was used as a positive control. Heparin expresses all 8 disaccharides that can be detected by LC-MS, the majority being TriS. In the MST cell pellet, all disaccharides were detected, excepting 2S6S, with the majority being TriS (41.8%). NS6S comprised 18.3%, NS2S 9.1%, NS 14.2%, 6S 8.9%, 2S 1.2% and 0S 6.5%. In HS/HP isolated from culture media of MST cells, TriS and 2S comprised the majority of the disaccharides (30.8% and 20.3%, respectively), whereas NS6S comprised 17.5%, NS2S 10.5%, NS 10%, 6S 3.9%, 0S 6.9%. Results for MST-10H cells showed that TriS and NS6S comprised the largest population of disaccharides (63.3% and 20.6%, respectively). NS2S disaccharides comprised 4.3%, NS 7.2%, 6S 2.1%, 2S 0.7% and 0S 1.8%. HS/HP isolated from culture media of MST-10H cells consisted of TriS disaccharides (30.8%), NS6S (18.8 %), NS2S (11.4%), NS (11.7%), 6S (4.5%), 2S (10.5%) and 0S (12.3%). This data is summarized

in **Table 3.2**. The total quantity of GAG isolated from the MST cell pellet was 1.9 $\mu g/10^7$ cells, and MST culture media was 8.1 $\mu g/10^7$ cells. In MST-10H cells, the amount of GAG found in the culture media was much greater (49.5 $\mu g/10^7$ cells) than in cells (6.1 $\mu g/10^7$ cells). Since CS/DS and HS/HP share early stages of their biosynthetic pathways, we also determined the ratio between these classes of GAGs in MST and MST-10H cells. The quantity of HS/HP was higher than CS/DS in the cell pellet fraction from MST and MST-10H (14:1 and 4:1, respectively). In contrast, CS/DS quantity was greater than HS/HP in culture media from both MST and MST-10H cells with the [HS/HP]/[CS/DS] ratio being 1:27 and 1:32, respectively. These results could be compared to HS/HP disaccharide compositions obtained from the cell pellet fraction and culture media of CHO-S (wt) and Dual-29 cells (see **Table 2.2** and **Figure 2.9**).

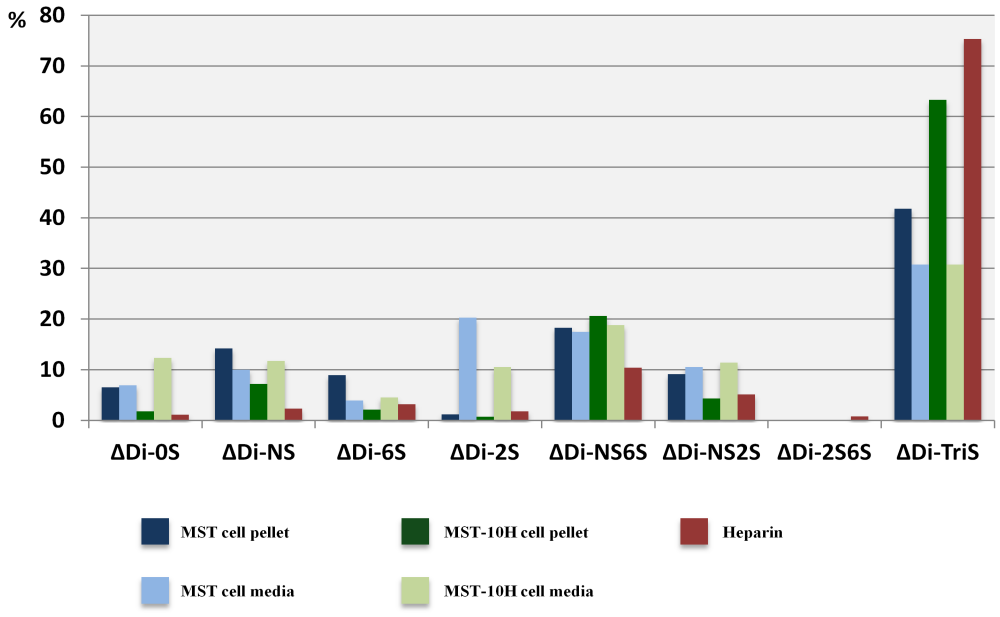

Figure 3.10. Disaccharide composition of HS/HP isolated from MST (cell pellet and media), MST-10H (cell pellet and media) and bovine lung heparin. LC-MS data has been provided by Dr. B. Yang, RPI, Center of Biotechnology and Interdisciplinary Studies, Troy, NY.

Table 3.2. Structure of HS/HP isolated from MST and MST-10H cells. LC-MS data has been provided by Dr. B. Yang, RPI, Center of Biotechnology and Interdisciplinary Studies, Troy, NY.

Samples	Total amount of GAG (μg/10^7 cells)	HS/HP disaccharides								Ratio of HS/HP to CS/DS
		0S	NS	2S	6S	NS2S	NS6S	2S6S	TriS	
MST cell pellet	1.9	6.5	14.2	1.2	8.9	9.1	18.3	n/d[a]	41.8	14:1
MST cell media	8.1	6.9	10.0	20.3	3.9	10.5	17.5	n/d[a]	30.8	1:27
MST-10H cell pellet	6.1	1.8	7.2	0.7	2.1	4.3	20.6	n/d[a]	63.3	4:1
MST-10H cell media	49.5	12.3	11.7	10.5	4.5	11.4	18.8	n/d[a]	30.8	1:32

3.2.6 HS/HP isolated from MST-10H cells express tetrasaccharide structures similar to AT-binding sites.

Anticoagulant activity of HP is determined by the presence of the AT binding sites, which are pentasaccharides of defined sequence, of which 3-*O*-sulfonation is an essential feature. It is known that the primary AT binding site structure is uronic acid -> glucosamine (*N*-acetyl/*N*-sulfo) 6-*O*-sulfo -> glucuronic acid -> glucosamine *N*-sulfo 3-*O*-sulfo (6-*O*-sulfo) -> iduronic acid 2-*O*-sulfo -> glucosamine *N*-sulfo 6-*O*-sulfo (Shworak et al. 1997). HS/HP from MST and MST-10H cells was checked for the presence of this sequence by tetrasaccharide analysis. This technique allows us to establish the presence of variations of the AT binding sequence. Bovine lung HP was used as a positive control, and it expresses 5 variations of the AT sequence that are converted by heparin lyase II to five tetrasaccharides: 1) ΔUA-GlcNAc6S-GlcA-GlcNS3S; 2) ΔUA-GlcNS-GlcA-GlcNS3S6S; 3) ΔUA-GlcNS6S-GlcA-GlcNS3S; 4) ΔUA-GlcNAc6S-GlcA-GlcNS3S6S; 5) ΔUA-GlcNS6S-GlcA-GlcNS3S6S. HP isolated

[a] 2S6S disaccharide structure was not detected in any samples.

from MST-10H cells expressed all above mentioned sequences in varying amounts (**Table 3.3**). Distribution of the various tetrasaccharides was similar in bovine lung HP and HS isolated from MST-10H cells. The most common tetrasaccharide structure was structure 2 (3.6% and 6.7% for bovine lung HP and HS from MST-10H cells, respectively), followed by 3 (3.1% and 2.1% for bovine lung HP and HS from MST-10H cells, respectively), 4 (1.4% and 3.4% for bovine lung HP and HS from MST-10H cells, respectively), 5 (1.2% and 0.4% for bovine lung HP and HS from MST-10H cells, respectively) and 1 (0.4% and 0.3% for bovine lung HP and HS from MST-10H cells, respectively) for both bovine lung HP and HS from MST-10H cells. None of those sequences were detected in MST cells, CHO-S (wt) or Dual-29 cells. Tetrasaccharide analysis was also performed with HS/HP isolated from culture media of CHO-S (wt) and Dual-29 cells. None of the 3-*O*-sulfonated sequences were detected in those culture media samples.

Table 3.3. Distribution of 3-*O*-sulfo group containing tetrasaccharide structures in bovine lung heparin and MST-10H cells. LC-MS data has been provided by Dr. B. Yang, RPI, Center of Biotechnology and Interdisciplinary Studies, Troy, NY.

Samples	1[a] (%)[b]	2 (%)	3 (%)	4 (%)	5 (%)	Total (%)
Bovine lung HP	0.4	3.6	3.1	1.4	1.2	9.7
MST-10H cells	0.3	6.7	2.1	3.4	0.4	12.9

3.3 Discussion

Heparin is a widely used and important therapeutic. Applications include use during heart surgeries (cardiopulmonary bypasses), hemodialysis and treatment of atrial fibrillation (Doty et al. 1979; Langenecker et al. 1994; Billett et al. 2010). HP is biosynthesized in the same pathway as HS (Esko, Kimata, and Lindahl 2009). We attempted to produce HP in CHO cells, taking advantage of their natural HS biosynthetic pathway. Even though we transfected enzymes necessary for anticoagulant HP production, NDST2 and Hs3st1, we observed only modestly increased anticoagulant

[a] Structures of the sequences are in the text.
[b] Amount of each tetrasaccharide structure is given as a percent from total amount of both disaccharide and tetrasaccharides detected by LC-MS for given sample.

activity (Baik et al. 2012). Next, we decided to study the details of HS/HP biosynthetic pathway in mast cells, which are natural producers of HP, with the aim to gain greater understanding of the pathway in order to apply this knowledge to other systems that might potentially be used for HP production. Use of primary mast cells is complex due to the difficulties associated with their isolation and propagation. Therefore, we used Furth murine mastocytoma cells (MST), which produce HP that is comparable in structure to therapeutic HP (Montgomery et al. 1992)**,** and do not have the same drawbacks as primary mast cells. Since the MST cell line produced HP lacking anticoagulant properties, the MST-10H cell line was engineered by transfecting the HS3ST1 gene into MST cells. Both cell lines stained positive for oversulfated GAG. We then studied the expression of HS/HP biosynthetic enzymes, their intracellular localization, and the expression of HS/HP core proteins. We also examined the structure of the HS/HP chains biosynthesized by both cell lines as well as the presence of the ATIII binding site.

HS/HP chain polymerization and chain modification enzymes were all detected at the message level excepting Hs3st5 in both MST and MST-10H cells. In CHO-S (wt) and Dual-29 cells, mRNA for all enzymes was expressed, excluding Hs6st2, Hs6st3 and Hs3st5. When we studied the protein expression, we were surprised to find that only a few of those enzymes were detected. Ndst2 was detected in both MST and MST-10H cells, whereas the expression of Ext1 and Hs6st3 decreased in MST-10H cells. The expression of Ext2, Glce, and Hs6st1 was not detected in either cell line. As expected, Hs3st1 was expressed in MS-10H cells, as that line is transfected with the gene for that enzyme. In contrast, both CHO cell lines expressed many of the HS/HP chain polymerization and modification enzymes, including Ext1, Ext2, Hs6st1 and Hs6st3. As expected, Ndst2 and Hs3st1 were overexpressed in Dual-29 cells, whereas Glce was only detected in CHO-S (wt) cells. These results suggest that the presence of the HS/HP biosynthetic enzymes alone is not enough to produce anticoagulant HP, and that additional factors might be required.

One of the factors that could potentially affect the structure of HP produced by MST and MST-10H cells is intracellular localization of the HS/HP biosynthetic enzymes. These enzymes are all known to be transmembrane proteins, save Hs3st1 (Carlsson and

Kjellen 2012). It has been previously shown that in murine mastocytoma cells HS/HP biosynthetic enzymes localize in various parts of Golgi (Uhlin-Hansen et al. 1997). To check whether there is a difference in localization of HS/HP biosynthetic enzymes in CHO cells, which could lead to the differences in the GAG structure, cell fractions were isolated from CHO cells and the presence of Ndst2 and Hs3st1 was checked in those fractions. In Dual-29 cells, Ndst2 and Hs3st1 were localized to the Golgi, whereas none of the enzymes were detected in the Golgi in CHO-S (wt) cells. Taken together, we have demonstrated that Dual-29 cells exhibit a localization pattern of key HS/HP biosynthetic enzymes similar to that of oversulfated HP producing MST cells. Nevertheless, the structure of the final HS/HP chain is distinct in Dual-29 from that observed in MST cells.

Another important element to consider is the expression of core proteins for HS and HP, and we turned our attention to this factor next. HS is synthesized on a core consisting of syndecans and glypicans (Esko, Kimata, and Lindahl 2009). HP uses serglycin, which also can carry CS E chains, as a core protein (Lidholt, Eriksson, and Kjellen 1995). The syndecan family of transmembrane proteins consists of four members. The extracellular domain of syndecan-1 and -3 carries HS and CS chains, whereas the extracellular domain of syndecan-2 and -4 carries only HS chains (Tkachenko, Rhodes, and Simons 2005). Syndecans are known to dimerize, and this has been shown to be important for their activity (Choi et al. 2005). Based on the molecular weight of expressed proteins we can conclude that MST cells express a dimeric version of syndecan-1 and monomeric syndecan-3, while MST-10H cells express dimeric versions of both syndecan-1 and -3. In contrast, both CHO-S (wt) and Dual-29 cells express dimeric syndecan-1 and -3. The expression of syndecan-3 is lower in Dual-29 cells. Glypicans are GPI-anchored proteins with 6 members in the family (Filmus, Capurro, and Rast 2008). In MST cells, the expression of only glypican-1 was detected, whereas MST-10H cells use glypican-1, -2, -3, and -5. In CHO-S (wt) cells, the expression of glypican-1, -5 and -6 was detected, and in Dual-29 cells glypican-2, and-3 were also detected. CHO-S cells do not naturally produce HP, but do produce HS. When NDST2 and Hs3st1 were transfected into Dual-29 cells, the total amount of both cell-associated and extracellular GAG was increased compared to CHO-S (wt). The ratio of

HS/HP to CS/DS was increased in Dual-29 cells, suggesting that the observed increase in total GAG was actually due to an augmentation in the amount of HS. This might explain the observed overexpression of glypicans in Dual-29 as HS carriers. The glypican increase also might be compensating for the decrease in syndecan-3 expression. As syndecan-3 carries both HS and CS chains, overexpressing glypicans over syndecans could be a more efficient way for cells to handle transport and presentation to the extracellular space an increased HS load. In contrast, mastocytoma cells normally produce HP, which could explain why MST cells express only one of each active form of syndecan and glypican. Upon transfection with Hs3st1 (MST-10H cells), the aggregate amount of cell-associated and extracellular GAG was increased. The amount of CS is greater than HS in culture media from MST cells. The ratio of CS/HS is even greater for GAGs isolated from culture media of MST-10H cells. The ratio of HS/CS in MST-10H cells is decreased compared to MST cells. Taken together, this implies that the increase in total GAG (both cell-associated and extracellular) is predominantly due to the increase in CS chains. This also suggests that the increase in the expression of syndecan-3 in MST-10H cells could be a way for cells to handle the increased levels of CS chains. The increase in glypicans might be explained by the fact that the increase in the HS/HP amount is chiefly a result of an increase in HS rather than HP. Detecting no change in the expression of serglycin, the core protein for HP, supports the conclusion that MST-10H cells produce more CS compared to MST cells. The precise mechanism resulting from the transfection of Hs3st1 that could lead to that outcome remains unclear.

HS/HP chains isolated from both MST and MST-10H cell lines resemble commercial HP in that they all contain a high amount of trisulfated disaccharides. MST-10H cells have the highest amount of trisulfated disaccharides, nearly to the level of observed in commercial HP. In contrast, Dual-29 cells transfected with NDST2 and Hs3st1 exhibited an increase in *N*-sulfo disaccharides, with only a minor increase in the quantity of the trisulfated versions. HP chains isolated from MST-10H cells have 3-*O*-sulfo group containing tetrasaccharide structures, which are found in anticoagulant HP. This suggests that HP from MST-10H is functionally active. In contrast, 3-*O*-sulfo group-containing sequences were not found in HP from Dual-29 cells. The reason

transfection of Hs3st1 has a different effect on the level of trisulfation and 3-*O*-sulfonation of HS/HP chains in Dual-29 cells and MST-10H cells remains unsettled.

Despite the fact that there was not a striking difference in the expression and intracellular localization of the HS/HP biosynthetic enzymes between CHO cells and mastocytoma cells, the latter do produce HS/HP chains that structurally resemble commercial HP. The HS/HP biosynthetic pathway is a complex system with complex interplay among a large array of enzymes. Some of these have isozymes that have distinct spatial and temporal distribution. Others are known to complex with one another to function properly. Perhaps there is an interaction between Hs3st1 and other sulfotransferases, as transfection of Hs3st1 results in an increase in NS6S2S sulfonation. Therefore, one intriguing possible explanation of the observation that transfection of Hs3st1 resulted in the appearance of 3-*O*-sulfo group containing sequences in MST-10H cells but not in Dual-29 cells, is that the need for additional protein factors that could be required for correct Hs3st1 localization in the Golgi for proper function. As CHO cells are not normally HP producers, they might be missing that protein and transfected Hs3st1 is not properly localized in the compartment of Golgi that it would normally do. That can potentially explain the fact that overexpression of Hs3st1 in Dual-29 cells results in detection of it in additional cellular locations apart from the Golgi.

3.4 Conclusions and Future Work

Altogether, the findings of this research confirm that the HS/HP biosynthetic pathway is a complex yet elegant system, where changing one constituent can affect other components. In light of all of the research already conducted on the details of the pathway by diverse research groups, there are still remain many unanswered questions. Would targeting Hs3st1 to the Golgi be enough to ensure its activity? And what exactly is the molecular mechanism of the transfected Ndst2 and Hs3st1 enzymes? These and numerous other lines of research require intensive investigation. Gaining profound insight into the details of the HS/HP pathway will help us to manipulate it with endgame goals not only to controllably produce the pharmaceutically relevant heparin molecule, but also to generate HS with various structures. This latter goal is particularly enticing as

it stands to provide the ability to control cell fate, as it has been shown that different structures of HS interact with different signaling molecules. In order to accomplish this, we must first come to know how the various structures of HS affect cell fate.

3.5 Materials and Methods

3.5.1 MST and MST-10H cell culture

Mastocytoma cell lines MST and MST-10H were generous gifts from Dr. J. Esko (USCD, La Jolla, CA). Cells were grown as aggregates in static suspension conditions in complete media containing DMEM/F12 (Life Technologies, Grand Island, NY) and 15% fetal bovine serum (Life Technologies). In addition, culture media for MST-10H cells contained Geneticin® at a final concentration of 400 µg/ml. Cells were cultured at 37°C in a humidified atmosphere with 5% CO_2.

3.5.2 Ruthenium red staining

Cells were smeared onto a microscope slide, air-dried and stained with 0.005% Ruthenium red (Sigma-Aldrich, St. Louis, MO) for 30 min at room temperature and examined using brightfield microscopy (Gustafson and Pihl 1967).

3.5.3 Total RNA isolation and qRT-PCR reactions

Total RNA was extracted from the MST and MST-10H cells using RNeasy mini kits (Qiagen, Germantown, MD) according to the manufacturer‘s instructions. The amount of RNA was assessed via UV on a NanoDrop 2000 spectrophotometer (Thermo Fisher Scientific). 60-90 ng of total RNA per sample was used in reverse transcription and polymerase chain reactions using a SuperScript III Platinum One-Step RT-PCR kit (Life Techonologies). A list of primers is supplied in **Appendix**. RT-PCR products were separated by agarose gel electrophoresis and visualized using ethidium bromide.

3.5.4 Protein isolation, quantification and immunoblotting

For total protein extraction, exponentially growing cells were lysed in Nonidet-P40 lysis buffer (Boston Bioproducts, Ashland, MA) on ice for 30 min in the presence of a cocktail of protease and phosphatase inhibitors, (Thermo Fisher Scientific) which comprise AEBSF, aprotinin, bestatin, E-64, leupeptin, and pepstatin A. Protein concentrations were determined using the BCA assay (Thermo Fisher Scientific). A total protein sample of 40 μg was loaded and separated on 4-20% polyacrylamide gels (Thermo Fisher Scientific) at 150 V, with Tris-HEPES-SDS buffer used as the running buffer. Proteins were transferred onto a PVDF membrane (Bio-Rad Laboratories, Hercules, CA), probed with relevant primary antibodies (described below), and subsequently detected using the appropriate HRP-conjugated secondary antibody with chemiluminescent (Super Signal West Pico ECL substrate, Thermo Fisher Scientific) exposure on high performance chemiluminescence film (Amersham Hyperfilm ECL, GE Healthcare). The primary and secondary antibodies used were the following: anti-γ-tubulin (T3320, Sigma-Aldrich); anti-Ext1 (sc-11039, Santa Cruz Biotechnology, Santa Cruz, CA), anti-Ext2 (sc-11045, Santa Cruz Biotechnology), anti-Ndst2 (sc-16764, Santa Cruz Biotechnology), anti-Hs3st1 (sc-104313, Santa Cruz Biotechnology), anti-Hs6st1 (sc-109943, Santa Cruz Biotechnology), anti-Hs6st3 (sc-84308, Santa Cruz Biotechnology), anti-Glce (H00026035-B01P, Abnova, Taipei City, Taiwan); anti-58K Golgi protein (ab27043, Abcam, Boston, MA), anti-syndecan-1 (sc-5632, Santa Cruz Biotechnology), anti-syndecan-2 (sc-15348, Santa Cruz Biotechnology), anti-syndecan-3 (ab63932, Abcam), anti-syndecan-4 (ab104568, Abcam), anti-glypican-1 (sc-66909, Santa Cruz Biotechnology), anti-glypican-2 (ab129526, Abcam), anti-glypican-3 (ab129381, Abcam), anti-glypican-4 (ab100843, Abcam), anti-glypican-5 (sc-84278, Santa Cruz Biotechnology), anti-glypican-6 (ab71343, Abcam), goat anti-rabbit HRP-conjugated (31460), goat anti-mouse HRP-conjugated (31430, Thermo Fisher Scientific); donkey anti-goat HRP-conjugated (sc-2020, Santa Cruz Biotechnology).

3.5.5 TCA precipitation of proteins

CHO-S (wt) and Dual-29 cells were spun at 200 x g for 5 min and the supernatant was examined for the enzymes of interest. An equal amount of cold 20% Trichloroacetic acid was added to the supernatants and kept at 4°C for 4 h. This mixture was centrifuged at 15,000 x g for 15 min at 4°C. Chilled acetone was added to the pellet and incubated at 4°C for 15 min, and then centrifuged at 13,000 x g for 15 min at 4°C. The resulting pellet was air-dried and resuspended in SDS loading buffer.

3.5.6 Immunocytochemistry

CHO-S (wt) and Dual-29 cell suspension was smeared on microscope slide (poly-L-lysine treated) and air dried for 30 min. Slides were fixed with 4% paraformaldehyde (Thermo Fisher Scientific) for 10 minutes at room temperature and blocked with DPBS-Triton 100-X solution supplemented with 5% Bovine Serum Albumin (BSA) (Life Technologies). They were incubated at room temperature for 1 h with primary antibody diluted in DPBS-Triton X-100 solution supplemented with 1% BSA. After several washes with DPBS, slides were incubated with secondary antibody (A11001, goat anti-mouse Alexa Fluor 488, Life Technologies) diluted in DPBS Triton X-100 solution supplemented with 1% BSA at room temperature for 1 h. Cells were washed several times with DPBS and stained with Hoechst 33342 for 5 min at room temperature. Slides were washed in DPBS and air dried for 30 min. ProLong Gold antifade reagent was added to each slide and covered with a cover slip and incubated overnight at room temperature in the dark. The following day, slides were sealed and analyzed with a Zeiss 510 Meta multiphoton confocal microscope. The primary antibody was anti-58K Golgi protein (ab27043, Abcam).

3.5.7 Subcellular fractionation and isolation of Golgi fractions

Subcellular fractionation of CHO-S (wt) and Dual-29 cells was performed with modifications as described in (Balch et al. 1984). In short, cells were homogenized using a Dounce homogenizer in 0.25 M sucrose (Sigma-Aldrich) containing 10 mM Tris-HCl

(pH 7.4) by crushing them 40-60 times. Crude cell homogenate was brought to a concentration of 1.4 M sucrose (10 mM Tris-HCl, pH 7.4) and layered on the following sucrose gradient (from bottom to top): 2 M sucrose (1 mL), 1.6 M sucrose (1.5 mL), 1.4 M sucrose (cell homogenate, 4 mL), 1.2 M sucrose (5 ml), and 0.8 M sucrose (all the way to the top). Subcellular fractions were separated by ultracentrifugation of the sucrose gradient at 90,000 x g for 2 h at 4°C. The bottom three fractions were collected in separate tubes and flash frozen in liquid nitrogen and stored at -80°C. The top fraction was transferred to a fresh ultracentrifuge tube and covered with 0.8 M sucrose (Tris-HCl, pH 7.4) all the way to the top of the tube. After ultracentrifugation at 90,000 x g for 1 h at 4°C, the bottom fraction (Golgi fraction) was collected and flash frozen in liquid nitrogen and stored at -80°C.

3.5.8 Isolation, purification and enzymatic depolymerization of GAGs.

Isolation and purification of GAGs from liver tissue, urine and CHO cells techniques were previously described (Yang et al. 2011; Zhang et al. 2006). The cell samples were individually subjected to proteolysis at 55°C with 10% (w/v) of actinase E (20 mg/ml in HPLC grade water, Kaken Biochemicals, Tokyo, Japan) for 20 h. After proteolysis, particulates were removed from the resulting solutions by passing each through a 0.22 μm membrane syringe filter. Samples were then concentrated using Microcon YM-10 centrifugal filter units (10 kDa molecular weight cutoff, Millipore) by centrifugation at 12,000 × g and washed with 15 ml of distilled water to remove peptides. The retentate was collected and lyophilized. Samples were dissolved in 0.5 ml of 8 M urea containing 2% CHAPS (pH 8.3). A Vivapure Mini Q H spin column (Viva science, Edgewood, NJ) was prepared by equilibrating with 200 μl of 8 M urea containing 2% CHAPS (pH 8.3). To remove any remaining proteins, the clarified, filtered samples were loaded onto and run through the equilibrated Vivapure Mini Q H spin columns under centrifugal force (700 × g). The columns were then washed with 200 μl of 8 M urea containing 2% CHAPS at pH 8.3, followed by five washes with 200 μl of 200 mM NaCl. GAGs were released from the spin column by washing three-times with 50 μl of 16% NaCl, and desalted using YM-10 spin columns. Finally, the GAGs were lyophilized.

The recovered GAGs were next completely depolymerized using polysaccharides lyases. Chondroitin lyase ABC (5 m-units) and chondroitin lyase ACII (2 m-units) in 10 µl of 0.1% BSA were added to an ~ 5 µg GAG sample in 25 µl of distilled water and incubated at 37°C for 10 h. The enzymatic products were recovered by centrifugal filtration at 13,000 x g. CS/DS disaccharides that passed through the filter were freeze-dried for LC-MS analysis. GAGs remaining in the retentate were collected by reversing the filter and spinning at 13,000 x g, followed by incubation with 10 m-units of heparin lyase I, II, and III at 37°C for 10 h. The products were recovered by centrifugal filtration using a YM-10 spin column, and the disaccharides were collected in the flow-through and freeze-dried. Cloning, overexpression in *Escherichia coli*, and purification of the recombinant heparin lyase I (EC 4.2.2.7), heparin lyase II (no EC assigned), and heparin lyase III (EC 4.2.2.8) from *Flavobacterium heparinum* were all performed as previously described (Shaya et al. 2006; Yoshida et al. 2002).

3.5.9 Derivatization of unsaturated disaccharides with AMAC

The freeze-dried biological sample containing GAG-derived disaccharides (~ 5 µg) or a mixture of 17 disaccharide standards (5 µg/ per each disaccharide or 0.5 nmol/ per each disaccharide) was added to 10 µl of 0.1 M AMAC solution in acetic acid (AcOH)/dimethyl sulfoxide (DMSO) (3:17, v/v) and mixed by vortexing for 5 min. Next, 10 µl of 1 M $NaBH_3CN$ was added to the reaction mixture and incubated at 45°C for 4 hours (Kitagawa, Kinoshita, and Sugahara 1995). Finally, the AMAC-tagged disaccharide mixtures were diluted to various concentrations (0.5-100 ng) using 50% (v/v) aqueous DMSO, and LC-MS analysis was performed.

3.5.10 LC-MS disaccharide composition analysis of CS/DS and HS/HP

LC-MS analyses were performed on an Agilent 1200 LC/MSD instrument (Agilent Technologies, Inc. Wilmington, DE) equipped with a 6300 ion-trap and a binary pump. The column used was a Poroshell 120 C18 column (2.1 × 150 mm, 2.7 µm, Agilent, USA) at 45°C. Eluent A was 80 mM ammonium acetate solution (20 mM, 40 mM, 60

mM, 80 mM, 100 mM) and eluent B was methanol. Solution A and 15% solution B were flowed (150 μl/min) through the column for 5 min followed by a linear gradients from 15-30% solution B from 5 to 30 min. The column effluent entered the ESI-MS source for continuous detection by MS. The electrospray interface was set in negative ionization mode with a skimmer potential of -40.0 V, a capillary exit of -40.0 V, and a source temperature of 350°C, to obtain the maximum abundance of the ions in a full-scan spectrum (150-1200 Da). Nitrogen (8 l/min, 40 psi) was used as a drying and nebulizing gas (Yang et al. 2012).

Quantification analysis of AMAC-labeled disaccharides was performed using calibration curves constructed by separation of increasing amounts of unsaturated disaccharide standards (0.1, 0.5, 1, 5, 10, 20, 50, 100 ng/each disaccharide or 0.02, 0.03, 0.05, 0.1, 0.2, 0.3 nM/each disaccharide). Linearity was assessed based on amount of disaccharide and peak intensity in UV255 nm, mass spectrometry total ion chromatography (TIC) and extract ion chromatography (EIC).

3.5.11 Tetrasaccharide mapping

For tetrasaccharides analysis, the heparin lyase II (40 mU in 20 μL of 25 mM Tris, 500 mM NaCl, 300 mM imidazole buffer (pH 7.4)) was added to 50-100 μg of GAG sample in 40 μl of distilled water and incubated at 35°C for 10 h. The products of enzymatic degradation were freeze-dried for further LC-MS analysis.

LC-MS analyses were performed on an Agilent 1200 LC/MSD instrument (Agilent Technologies, Inc. Wilmington, DE) equipped with a 6300 ion trap and a binary pump followed by a UV detector equipped with a high-pressure cell. The column used was a Poroshell 120 C18 column (2.1 × 100 mm, 2.7 μm, Agilent, USA). Eluent A was water/acetonitrile (85:15) v/v, and eluent B was water/acetonitrile (35:65) v/v. Both eluents contained 12 mM tributylamineand 38 mM NH_4OAc with pH adjusted to 6.5 with acetic acid. Solution A for 2 min followed by a linear gradient from 2 to 40 min (0-30% solution B) was used at a flow rate of 150 μl/min. The column effluent entered the source of the ESI-MS for continuous detection by MS. The electrospray interface was set in negative ionization mode with a skimmer potential of -40.0 V, a capillary exit of -

40.0 V, and a source temperature of 350°C, to obtain the maximum abundance of the ions in a full-scan spectrum (200-1500 Da). Nitrogen (8 l/min, 40 psi) was used as a drying and nebulizing gas.

4. TERATOCARCINOMA CELLS AS A MODEL TO STUDY FUNCTION OF DIFFERENT GAG STRUCTURES DURING DIFFERENTIATION PROCESSES

4.1 Introduction

New strategies in medical therapies, such as induced differentiation of cancer cells to block metastasis, require deeper understanding of all aspects of cellular behavior including epigenomic, transcriptomic, proteomic and glycomic. This information will provide researchers the ability to redirect cell behavior. In addition, optimizing the efficacy of cell-based therapies in a multicellular environment will require an understanding of how the cellular glycome can respond. In disease states, an inappropriate glycome may also provide abnormal cellular capabilities for a given tissue environment by facilitating new signaling pathways. Systematic analysis can help to provide a database of responses that can predict cellular outcomes.

Glycosaminoglycans (GAGs) comprise a large fraction of the cellular glycome and localize mainly to the external membrane of cells, and also reside within the extracellular matrix. The biosynthetic pathways and enzymes involved in GAG biosynthesis are well defined and the enzymes and their isoforms have been found to be differentially expressed in various cell types (Esko 1991; Linhardt 2003; Skidmore et al. 2008; Sugahara and Kitagawa 2002). GAGs are linear, sulfated and highly charged heterogeneous polysaccharides consisting of a repeating disaccharide unit. Polysaccharide length and fine structure, in addition to the placement of protein-binding domains, are critical to the functioning of proteoglycans (PGs) in cell signaling. Four distinct types of GAGs are present in eukaryotic cells: chondroitin sulfate/dermatan sulfate (CS/DS), heparan sulfate/heparin (HS/HP), keratan sulfate (KS), and hyaluronan (HA). They are attached to core proteins to form cellular PGs that are critical for a variety of cell signaling and migration roles as well as mammalian organ development (Davies, Fisher, and Barnett 2001; Linhardt and Toida 2004). GAGs act as molecular co-

---

This chapter previously appeared as: Gasimli, L., H. E. Stansfield, A. V. Nairn, H. Liu, J. L. Paluh, B. Yang, J. S. Dordick, K. W. Moremen, and R. J. Linhardt. 2012. Structural remodeling of proteoglycans upon retinoic acid-induced differentiation of NCCIT cells. *Glycoconj. J.* Oct 2.

receptors in cell signaling for cell–cell interactions and as regulators of cell adhesion, cell growth and differentiation (Linhardt and Toida 2004; Lanctot, Gage, and Varki 2007). By defining temporal changes in GAG profiles on cells during cellular quiescence, proliferation, and lineage differentiation, we refine our global view of development in the multicellular environment. This is particularly critical for novel therapeutic applications with stem cells or tissue progenitors as well as efforts to optimize the *in vitro* stem cell niche for cell, tissue and organ based therapies (Linhardt and Toida 2004; Lanctot, Gage, and Varki 2007).

Teratocarcinomas are malignant germ cell tumors consisting of embryonal carcinoma (EC) cells. They are malignant equivalents of normal pluripotent embryonic cells from the pre-implantation stage of embryos (Andrews et al. 2005; Damjanov 1990). Single embryonal carcinoma cells from teratocarcinomas develop into tumors that contain a mixed population of more than two dozen well-differentiated adult tissues from all three germ layers, including brain, muscle, bone, teeth, bone marrow, eyes, secretory glands, skin and intestine, as well as placental and yolk sac tissue. The ability of *in vitro* cultured embryonal carcinoma cells to form organized structures that resemble the developing embryo has promoted their use as a model system for the study of early embryonic development (Pierce 1985). The widely studied NCCIT cell line, derived from a mediastinal mixed germ cell tumor, has been shown to differentiate into derivatives of all three embryonic germ layers (ectoderm, mesoderm, and endoderm) and extraembryonic cell lineages (Teshima et al. 1988). The NCCIT line is responsive to retinoic acid (RA), inducing cellular differentiation accompanied by the disappearance of oligosaccharide surface antigens associated with pluripotency (Damjanov, Horvat, and Gibas 1993). For these reasons, coupled with their ease of manipulation, NCCIT cells are a useful model to quantify the concomitant changes to the glycan profile upon RA treatment to reveal promotive and/or restrictive changes associated with the action of this morphogen for inducing loss of pluripotency and increased lineage restriction.

Modification of GAG profiles upon RA treatment to induce the loss of pluripotency and lineage commitment has not been previously studied. Such information on a well-studied morphogen is vital to obtain a more complete understanding of the underlying cellular signaling pathways that are immediately affected. As such, the NCCIT cell line

affords an important model to discern changes in GAG accompanying pluripotency loss and commitment to multi-lineage differentiation. In this research, changes to the pluripotent cellular glycome that resulted from RA-induced differentiation have been analyzed. Changes in gene transcript and protein abundance for GAG biosynthesis pathways were quantified and examined using qRT-PCR and Western analysis, respectively. Disaccharide compositional analysis, utilizing liquid chromatography/mass spectrometry (LC/MS), was used to determine changes in GAG chain modifications for CS/DS and HS/HP pathways in response to RA-induced differentiation and concurrent loss of pluripotency.

4.2 Results

4.2.1 Changes in cell population upon RA treatment

NCCIT teratocarcinoma cells were treated with RA (10 μM) for up to 40 days to induce differentiation. As observed previously with RA treatment (Damjanov, Horvat, and Gibas 1993), growth of NCCIT cells slowed in response, (**Figure 4.1 A**) and differentiation followed.

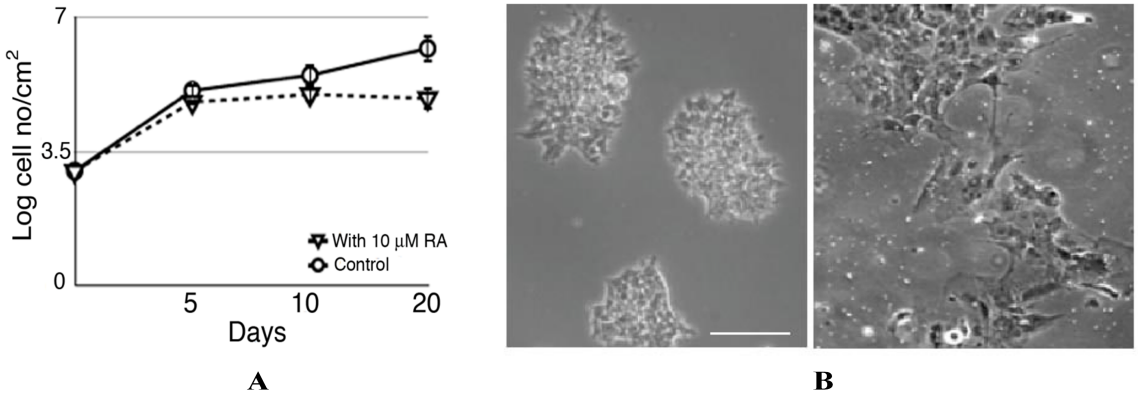

Figure 4.1. Differentiation of NCCIT cells by RA. A. Growth curves of untreated and RA treated NCCIT cells. Growth retardation of cells treated with 10μM RA is evident at day 5. **B.** Morphology changes in NCCIT cells upon differentiation. Left panel shows phase contrast image of NCCIT cells unexposed to RA. Right panel shows phase contrast image of NCCIT cells after 20 days RA treatment, revealing distinct morphological changes consistent with differentiation. Adapted from (Gasimli et al. 2012).

NCCIT cells are known to undergo multilineage differentiation upon treatment with RA (Damjanov, Horvat, and Gibas 1993; Packer et al. 2000; Lee, Chan, and Chan 2002; Kumar and Duester 2010). Expression of markers for pluripotency, along with lineage-specific markers was monitored using qRT-PCR (**Table 4.1** and **Table 4.2**) and Western blot (data not shown).

Table 4.1. Changes in expression of lineage specific markers in NCCIT cells upon RA treatment.

Markers	Fold-change, RA/Control[a]	Markers	Fold-change, RA/Control
OCT3/4	-3.0	KRTAP3-2	1.0
Nestin	3.0	MYH6	Decreased[b]
Beta-III-Tubulin	1.0	RET9	-6.0
Olig2	1.0	HOXA5	14000
GFAP	n/a[c]	AFP	1.0
PTX2	25.0	PDX1	2.0

In addition, immunofluorescence (**Figure 4.2**) was used to monitor differentiation towards neuronal and glial lineages. Samples for qRT-PCR were taken at days 0, 14, 21, 29 and 40 days of RA treatment. Results for qRT-PCR reported are from day 40 of RA treatment. The rounded morphology of EC cells is altered drastically upon differentiation (**Figure 4.1 B**). We observed flattened cells, including some with branched elongated cytoplasmic processes typical of neuronal morphology. Changes in morphology were accompanied by 3-fold reduced expression of Oct3/4 (**Figure 4.2** and

[a] Fold-change of transcript abundance for NCCIT-RA compared to untreated NCCIT cells. A fold-change <1 indicates that the transcript is more abundant in the control cells than in the RA-treated population and a fold-change >1 indicates that the transcript is more abundant in the treated cells than in the controls. A fold change equal to 1 indicates no changes in the transcript level upon RA treatment.
[b] Expression was not detected at day 40 of RA treatment.
[c] Expression was not detected at any time point.

Table 4.1), which has been shown to be a pluripotency marker (Lanctot, Gage, and Varki 2007). The expression of Nestin, a marker for neural differentiation (Dahlstrand et al. 1992), increased 3-fold, suggesting proliferation of neural progenitor cells. There were no changes in expression of β-III-tubulin (mature neuronal marker) or Olig2 (oligodendrocyte marker) observed, whereas expression of glial fibrillary acidic protein (GFAP), a type III intermediate filament protein common to cells of the central nervous system (particularly astrocytes), was not detected.

Table 4.2. RT-PCR primers for NCCIT characterization.[a]

Gene	Accession Number	Primer Forward	Primer Reverse
Ribosomal protein S18 (RPS18)	NM_022551.2	aatccacgccagtacaagatccca	tcttcacggagcttgttgtccaga
Glial fibrillary acidic protein (GFAP)	NM_001131019.1	agagggacaatctggcaca	cagcctcaggttggtttcat
Myelin basic protein (MBP)	NM_001025081.1	agccctctgccctctcat	ggagccgtagtgagcagttc
Keratin associated protein 3-2 (KRTAP3-2)	NM_031959.2	attgccatggattgctgtg	aggatttgtcggaggagca

Expression of keratin associated protein 3-2 remained unchanged. An example marker of mesodermal origin, RET9, had decreased 6-fold decreased expression. Expression of MYH6 was low at the beginning of the treatment and was not detectable later during differentiation. Markers for endodermal lineages such as PDX1 displayed a 2-fold increase in expression with no change in expression of AFP. The most dramatic increase was observed in expression of PITX2 (ectodermal marker) and HOXA5 (endodermal marker), 25-fold and 14,000-fold respectively. Our analysis indicates that RA treatment was redirecting cells from pluripotency and allowing for multiple

[a] Primers for GAG biosynthetic enzymes are described previously (Nairn et al. 2007) Supplementary Table.

differentiation pathways to execute. NCCIT cells treated in RA for 20 days were used for transcript analysis of GAG biosynthetic enzymes, as complete loss of pluripotency was observed at this point.

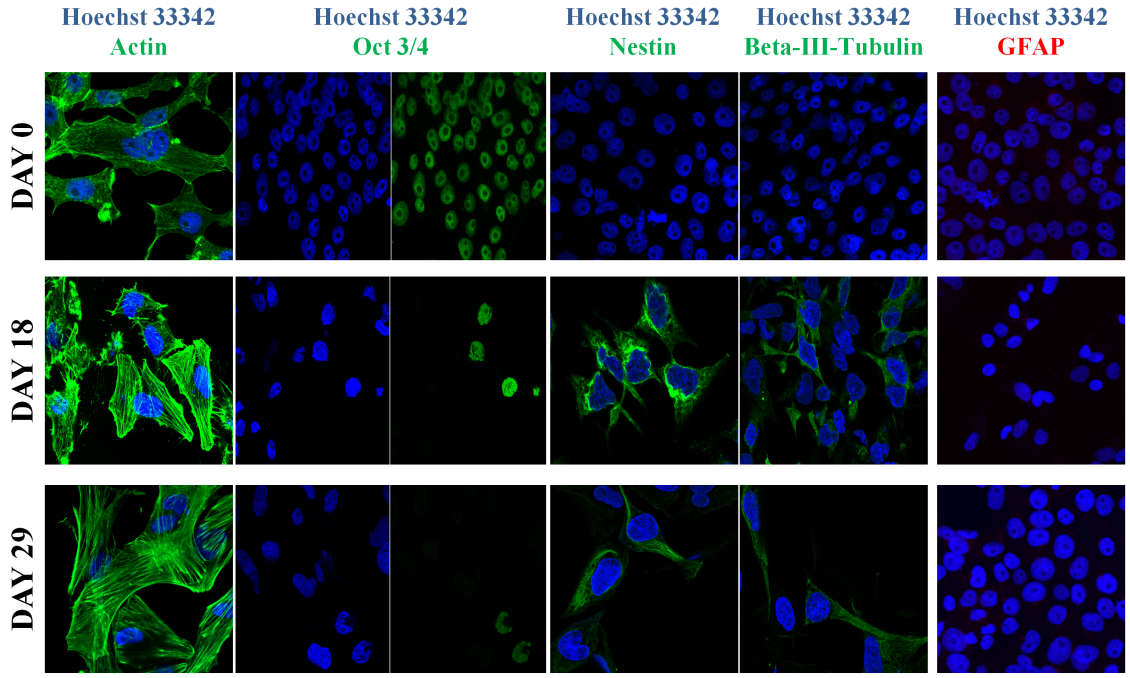

Figure 4.2. Expression of the markers associated with neural lineage in differentiated NCCIT cells. Immunofluorescence of NCCIT cells at 0, 18 and 29 days of RA treatment. RA-dependent decrease in expression of Oct3/4 and increased expression in Nestin and β-III-tubulin is observed. Expression of glial associated proteins GFAP was undetectable. Actin staining is shown as a positive control. Adapted from (Gasimli et al. 2012).

4.2.2 Changes in expression of core proteins carrying GAG chains upon RA treatment

The transcript abundance of genes encoding GAG core proteins were examined in RA-treated (day 20) and compared to untreated control NCCIT cells and fold-change determined (**Table 4.3** and **Figure 4.3**). Levels of selected core proteins were also examined using Western blot analysis (**Figure 4.4**). The transcript levels for core proteins for CS/DS were assessed, revealing that lumican (1500-fold) and decorin (2800-fold) increased, while fibromodulin, procollagen and versican showed no change in transcript level. Decreased expression of transcripts for CS/DS included biglycan (48-

fold), aggrecan and neurocan (each 10-fold) as well as neuroglycan, bamacan, brevican, thrombomodulin, epican (CD44) and macrophage migration inhibitory factor (CD74) (range of 2-8 fold). Expression level of HS core protein messages changed in RA-treated NCCIT cells in comparison to untreated NCCIT cells. In RA-treated NCCIT cells, elevated message levels for glypican-5 (68-fold), glypican-3 (12-fold) and glypican-6 (8-fold) were observed. No change in expression was detected for agrin, syndecan-1, syndecan-2 or syndecan-4. Significant reductions in serglycin (17-fold) and glypican-4 (21-fold) messages were also observed, as well as minor reductions (range of 2-6 fold) for perlecan, syndecan-3, glypican-1 and glypican-2. We next examined core proteins to determine if the magnitude of changes in their transcript levels corresponded to a concomitant increase in their expressed protein levels. Western blotting analysis (**Figure 4.4**) demonstrated the most dramatic changes for expression of lumican, decorin and glypican-5. Lumican and decorin, each which displayed thousand-fold increases in transcript levels, were of particular interest. Immunoblotting confirmed a steady-state increase in protein levels for production of lumican and decorin in RA-treated NCCIT cells. In contrast, expression of glypican-5 fluctuated throughout the course of RA treatment, decreasing at day 4 and day 15 of the treatment and increasing at day 9. Biglycan proteins remained at an undetectable level in pluripotent NCCIT cells and RA treated cells (**Figure 4.4**). Recombinant human biglycan was used as a positive control to confirm that the Western had worked, and that the negative results observed were reliable (data not shown).

Table 4.3. Change in expression of core proteins of CS/DS and HS/HP in NCCIT cells upon RA treatment. qRT-PCR data has been provided by Dr. A. Nairn, UGA, Complex Carbohydrate Research Center, Athens, GA.

Protein	Fold-change, RA/Control[a]	GAGs attached	Protein	Fold-change, RA/Control[a]	GAGs attached
Lumican	1500.0	CS/KS	CD74	-7.4	CS
Fibromodulin	1.0	CS/KS	Serglycin	-17.0	HP/CS_E
Aggrecan-1 (CSPG1)	-10.0	CS	Perlecan	-2.0	HS/CS
Versican (CSPG2)	1.0	CS	Agrin	1.0	HS
Neurocan (CSPG3)	-10.00	CS	Syndecan-1	1.0	HS
NG2 (CSPG4)	1.0	CS	Syndecan-2 (HSPG1)	1.0	HS
Neuroglycan (CSPG5)	-2.0	CS	Syndecan-3	-2.0	HS
Bamacan	-2.0	CS	Syndecan-4	1.0	HS
Brevican (CSPG7)	-2.0	CS	Glypican-1	-3.5	HS
Decorin	2800.0	CS/DS	Glypican-2 (cerebroglycan)	-6.4	HS
Biglycan	-48.00	CS/DS	Glypican-3	12.0	HS
Procollagen 1Xa2	1.0	CS	Glypican-4	-21.0	HS
Thrombomo-dulin	-4.4	CS	Glypican-5	68.0	HS
Epican (CD44)	-5.1	CS	Glypican-6	8.0	HS

[a] Fold-change of transcript abundance for NCCIT-RA compared to untreated NCCIT cells. A fold-change <1 indicates that the transcript is more abundant in the control cells than in the RA-treated population and a fold-change >1 indicates that the transcript is more abundant in the treated cells than in the controls. A fold-change equal to 1 indicates no changes in the transcript level upon RA treatment.

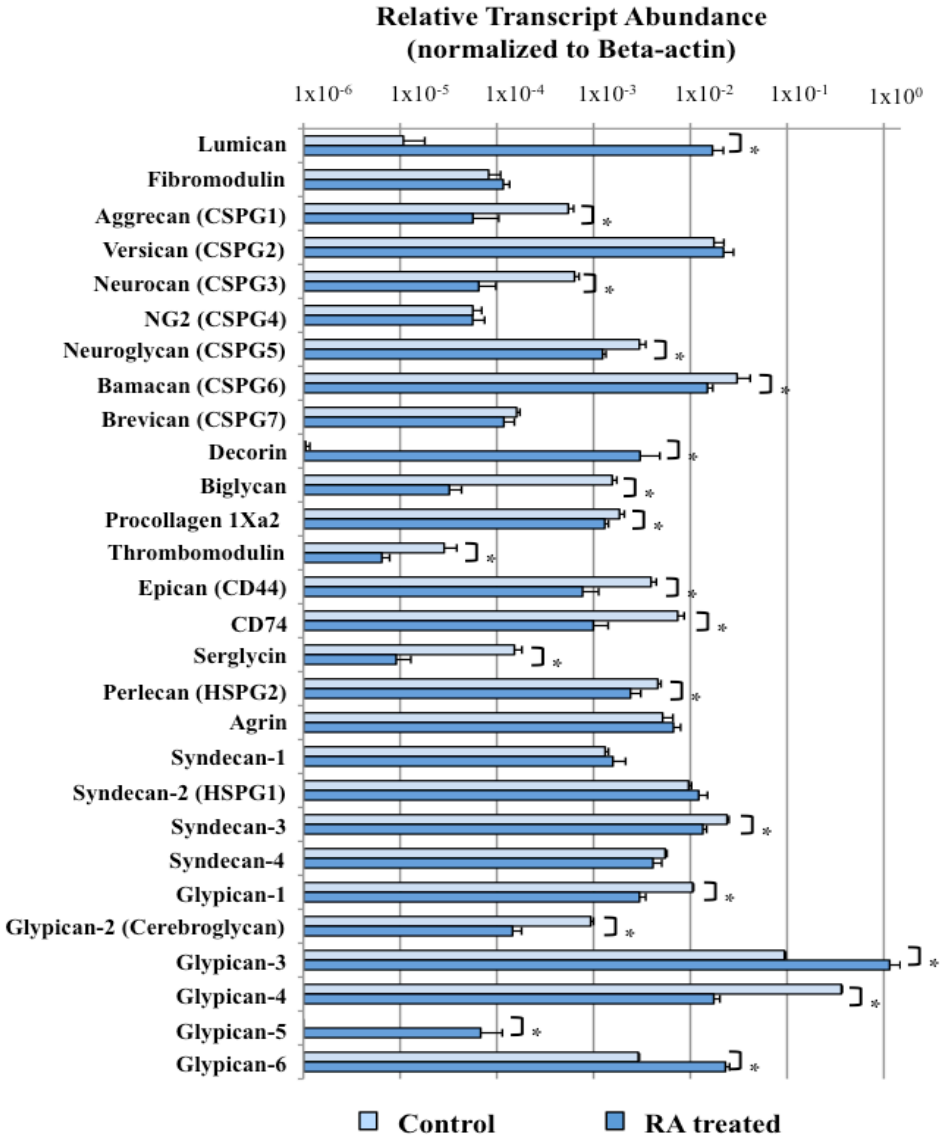

Figure 4.3. Expression of core proteins of CS/DS and HS/HP in NCCIT cells. The relative transcript abundance of CS/DS and HS/HP core proteins as normalized to β-actin. Relative transcript abundance for NCCIT untreated control pluripotent cells and NCCIT RA-differentiated cells plotted on a $\log_{10}$ scale for each gene assayed. qRT-PCR data has been provided by Dr. A. Nairn, UGA, Complex Carbohydrate Research Center, Athens, GA. Adapted from (Gasimli et al. 2012).

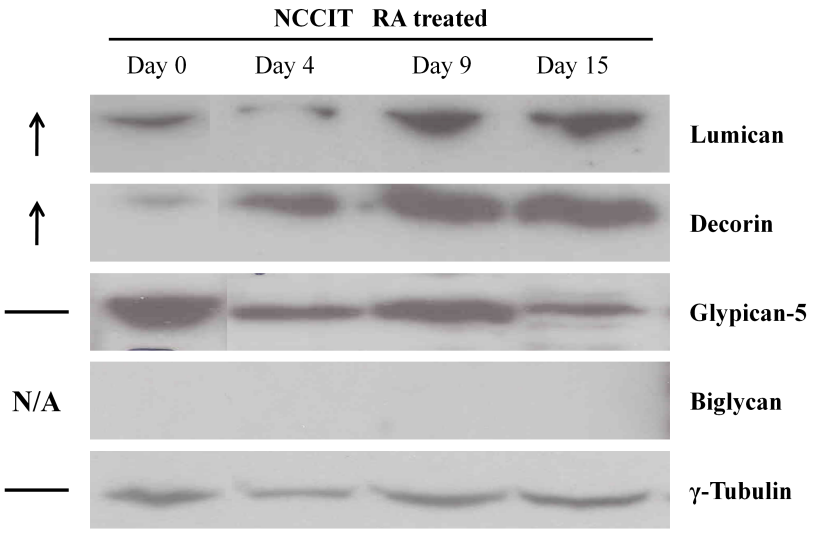

Figure 4.4. Change in expression level of lumican, decorin, glypican-5 and biglycan in NCCIT cells after differentiation detected by western blotting. Arrows to the left of the panel indicate an increase in protein expression following RA treatment, while a horizontal bar indicates no change with treatment and "N/A" indicates that no protein was detected with the selected antibody. γ-tubulin is shown as a loading control. Adapted from (Gasimli et al. 2012).

4.2.3 RA effects on expression levels of enzymes involved in linkage region biosynthesis and chain extension

Pathways for early and late enzymatic reactions leading to the synthesis of CS/DS and HS/HP GAG chains were scrutinized. Early stage biosynthesis of both CS/DS and HS/HP occurs by initialization of GAG chains on core proteins within shared and distinct branched pathways (**Figure 4.5 A**). Several genes encode enzymes that regulate the early steps of CS/DS and HS/HP biosynthesis. These include xylosyl transferases (XYLT1 and XYLT2), β4-galactosyltransferase (β4GALT7), β3-galactosyltransferase (β3GALT6), and β3-glucuronosyltransferase (β3GAT3). The biosynthesis of CS/DS and HS/HP diverge in the chain extension and modification steps. For HS/HP linkage region biosynthesis and chain extension, α-N-acetylglucosaminyltransferases (EXTL2, EXTL3), α-N-acetylglucosaminyl-β-glucuronosyl transferases (EXT1, EXT2), and the combined action of the enzymes EXT1/EXT2, EXTL1, and EXTL3 are required. CS/DS linkage region biosynthesis and extension is accomplished by the activity of β-4-N-

acetylgalactosamine transferases (CSGALNACTs) and chondroitin synthases (CHSY1, CHPF1, CHPF2, CHSY3). Relative transcript abundance was examined as a function of β-actin change (RA/Control, untreated) (**Table 4.4** and **Figure 4.5 B**). Essentially no significant changes were observed in expression levels of enzymes involved in the common linkage region sequences. In the HS/HP pathway, only EXTL1 displayed a large change in expression, decreasing approximately 19-fold in RA-treated cells. A small, but statistically significant change in EXT2 (~ 2-fold) was detected, but no changes were detected in the levels of EXT1, EXTL2, or EXTL3. Examination of the expression of genes encoding the enzymes involved in the linkage region synthesis, chain initiation and extension of CS/DS revealed an approximate 8-fold decrease in transcript level of CSGALNACT1 in RA-treated cells.

Table 4.4. Change in expression of genes coding for CS/DS and HS/HP biosynthetic enzymes in NCCIT control versus RA-differentiated NCCIT cells. qRT-PCR data has been provided by Dr. A. Nairn, UGA, Complex Carbohydrate Research Center, Athens, GA.

Gene	Fold-change, RA/Control[a]	Gene	Fold-change, RA/Control[a]	Gene	Fold-change, RA/Control[a]
XYLT1	1.0	EXT1	1.0	CHSY1	-2.0
XYLT2	1.0	EXT2	-2.0	CHPF1	2.0
B4GALT7	1.0	EXTL1	-19.0	CHSY3	-2.0
B3GALT6	1.0	EXTL3	1.0	CHPF2	2.0
B3GAT3	1.0	CSGALNACT1	-8.0	DSE1	2.0
EXTL2	1.0	*CSGALNACT2*	1.0	*DSE2*	-2.0

[a] Fold-change of transcript abundance for NCCIT-RA compared to untreated NCCIT cells. A fold-change <1 indicates that the transcript is more abundant in the control cells than in the RA-treated population and a fold-change >1 indicates that the transcript is more abundant in the treated cells than in the controls. A fold-change equal to 1 indicates no changes in the transcript level upon RA treatment.

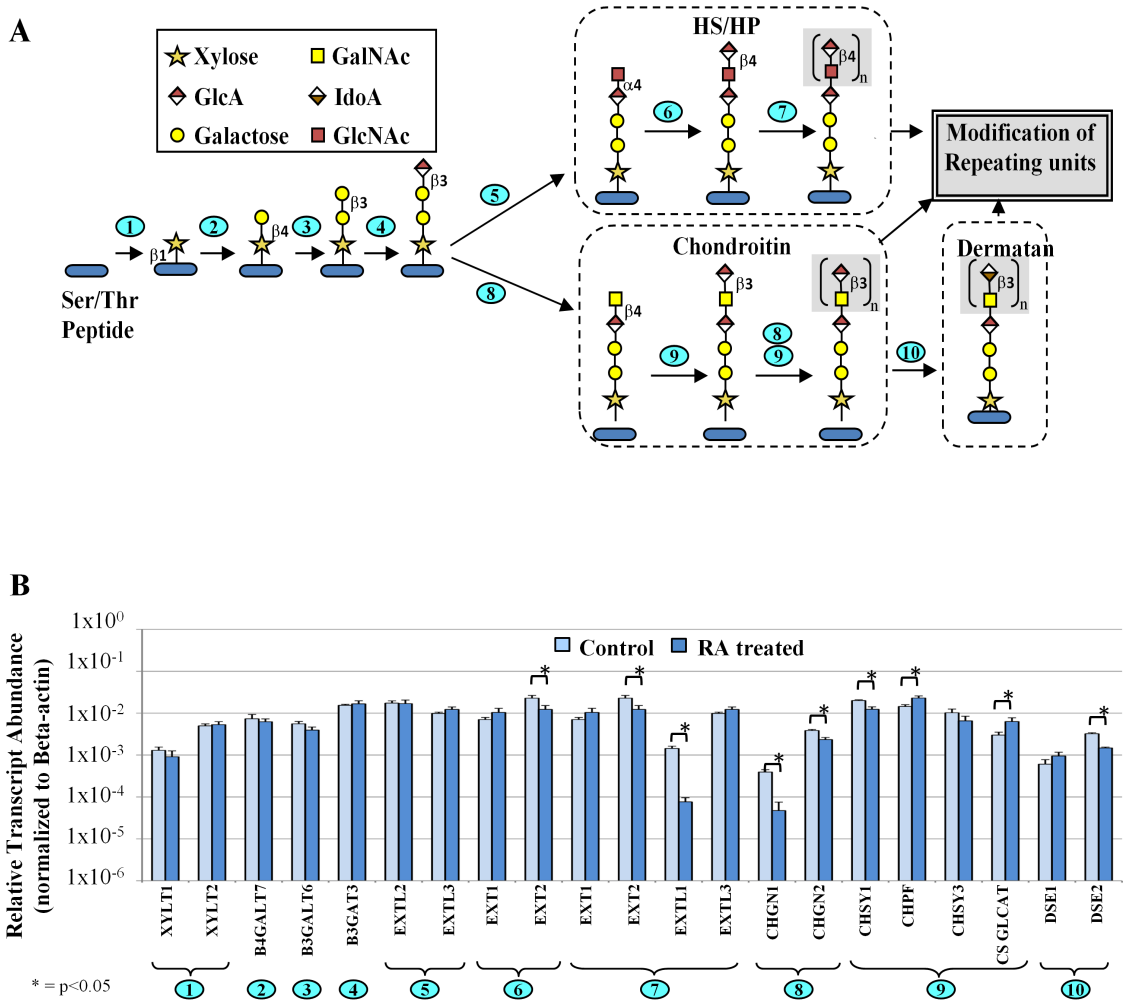

Figure 4.5. Change in expression of HS/HP and CS/DS biosynthetic enzymes. A. Graphic diagram of GAG core tetrasaccharide biosynthesis showing the branch in formation of HS/HP and CS/DS families. The Ser/Thr-containing polypeptide core protein is glycosylated and modified through ten enzymatic reactions occurring in the endoplasmic reticulum and Golgi. Numbered steps correspond to the reactions catalyzed by enzymes coded by (1): XYLT1, XYLT2, (2): B4GALT7, (3): B3GALT6, (4): B3GALT3, (5): EXTL2, EXTL3, (6): EXT1, EXT2, (7): EXT1, EXT2, EXTL1, EXTL3, (8): CSGALNACT1, CSGALNACT2, (9): CHSY1, CHPF1, CHSY3, CHPF2, and (10): DSE1, DSE2. **B.** Relative transcript levels for genes coding CS/DS and HS/HP chain initiation and elongation enzymes. Plotted as described for Figure 4.3. qRT-PCR data has been provided by Dr. A. Nairn, UGA, Complex Carbohydrate Research Center, Athens, GA. Adapted from (Gasimli et al. 2012).

Small (2-fold) changes in CHSY1, CHPF1, CHSY3 and CHPF2 were observed, and modest changes in transcript levels of dermatan sulfate epimerase (DSE1 and DSE2), which converts glucuronic acid (GlcA) to iduronic acid (IdoA) in DS biosynthesis, were noted.

4.2.4 Effect of RA on expression of genes for enzymes involved in HS/HP and CS/DS GAG chain modifications.

The enzymatic pathways for HS/HP and CS/DS are shown in **Figures 4.6 A** and **4.7 A**, respectively. The combined action of *N*-deacetylase/*N*-sulfotransferases (NDSTs), C5-epimerase (GLCE), 2-*O*-sulfotransferase (HS2ST1), 6-*O*-sulfotransferases (HS6STs) and 3-*O*-sulfotransferases (HS3STs) are responsible for modification of HS/HP repeating units. We observed increased transcript levels for generally all enzymes involved in chain modification of HS/HP except for a few of the seven HS3ST isoforms assayed (**Table 4.5** and **Figure 4.6 B**).

Table 4.5. Change in expression of genes coding for HS/HP chain modification enzymes in NCCIT control and RA-treated cells. qRT-PCR data has been provided by Dr. A. Nairn, UGA, Complex Carbohydrate Research Center, Athens, GA.

Gene	Fold-change, RA/Control[a]	Gene	Fold-change, RA/Control[a]	Gene	Fold-change, RA/Control[a]
NDST1	1.0	HS2ST1	2.6	HS3ST2	1.0
NDST2	1.0	HS6ST1	2.2	HS3ST3B1[b]	-2.2
NDST3	8.0	HS6ST2	3.4	HS3ST4	-3.5
NDST4	4.0	HS6ST3	20.0	HS3ST5	-3.0
GLCE	2.5	HS3ST1	2.5	HS3ST6	-2.0

[a] Fold-change of transcript abundance for NCCIT-RA compared to untreated NCCIT cells. A fold-change <1 indicates that the transcript is more abundant in the control cells than in the RA-treated population and a fold-change >1 indicates that the transcript is more abundant in the treated cells than in the controls. A fold-change equal to 1 indicates no changes in the transcript level upon RA treatment.
[b] Transcript level for HS3ST3A1 was not assayed.

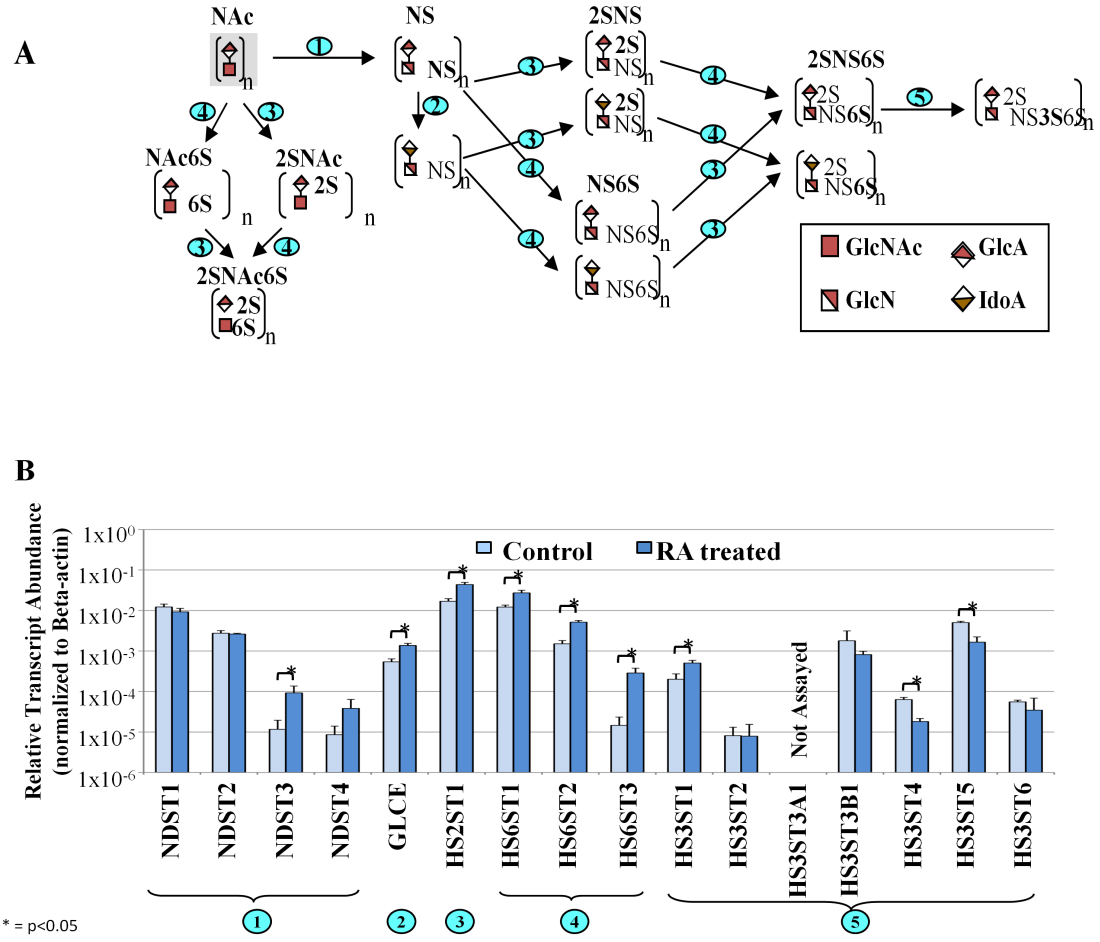

Figure 4.6. Change in expression of HS/HP chain modification enzymes in NCCIT cells upon RA treatment. **A.** Graphic diagram of the modification of the repeating units in the HS/HP chain. Numbers on steps correspond to the reactions catalyzed by enzymes coded by (1): NDST1, NDST2, NDST3, NDST4, (2): GLCE, (3): HST2T1, (4): HS6ST1, HS6ST2, HS6ST3, and (5): HS3ST1, HS3ST2, HS3ST3A1, HS3ST3B1, HS3ST4, HS3ST5, HS3ST6. **B.** Relative transcript abundance for genes involved in HS/HP chain modifications for RA-treated and control NCCIT cells. Plotted as described for Figure 4.3. Multiple names for an enzymatic step are tissue specific isoforms. qRT-PCR data has been provided by Dr. A. Nairn, UGA, Complex Carbohydrate Research Center, Athens, GA. Adapted from (Gasimli et al. 2012).

Of the four isoforms of NDST, only two showed changes of significance. The levels of the NDST3 and NDST4 transcripts increased 8-fold and 4-fold, respectively. Transcript levels for the GLCE, HS2ST1, HS6ST1 and HS6ST2 enzymes, and HS3ST1 increased slightly (<5-fold) in RA-treated cells. However, a large increase in transcript abundance of ~ 20-fold was detected for the HS6ST3 isoform following treatment with RA. Transcript levels for the HS3ST3B1, HS3ST4 and HS3ST5 isoforms decreased marginally in RA treated cells. In contrast, RA treatment resulted in fewer changes to transcript levels of genes involved in the modification of CS/DS GAG repeating units (**Table 4.6** and **Figure 4.7 B**). Introduction of the sulfation pattern characteristic of CS and DS requires chondroitin 4-O-sulfotransferases (CHST11 and CHST12), a dermatan 4-O-sulfotransferase (D4ST1), chondroitin uronosyl sulfotransferase (UST), chondroitin 6-O-sulfotransferases (CHST3 and CHST7), and N-acetylgalactosamine 4S, 6S transferase (CHST15). A subset of the genes displayed limited changes (<5-fold) in expression in RA treated cells, compared to control untreated NCCIT cells. However, an ~ 8-fold decrease in transcript abundance was observed for CHST15 following RA treatment.

Table 4.6. Change in expression of genes coding for CS/DS chain modification enzymes in NCCIT control and RA-treated cells. qRT-PCR data has been provided by Dr. A. Nairn, UGA, Complex Carbohydrate Research Center, Athens, GA.

Gene	Fold-change, RA/Control[a]	Gene	Fold-change, RA/Control[a]
CHST11	2.4	CHST3	3.4
CHST12	1.0	CHST7	-4.3
D4ST1	1.0	CHST15	-7.9
UST	-2.2		

[a] Fold-change of transcript abundance for NCCIT-RA compared to untreated NCCIT cells. A fold-change <1 indicates that the transcript is more abundant in the control cells than in the RA-treated population and a fold-change >1 indicates that the transcript is more abundant in the treated cells than in the controls. A fold-change equal to 1 indicates no changes in the transcript level upon RA treatment.

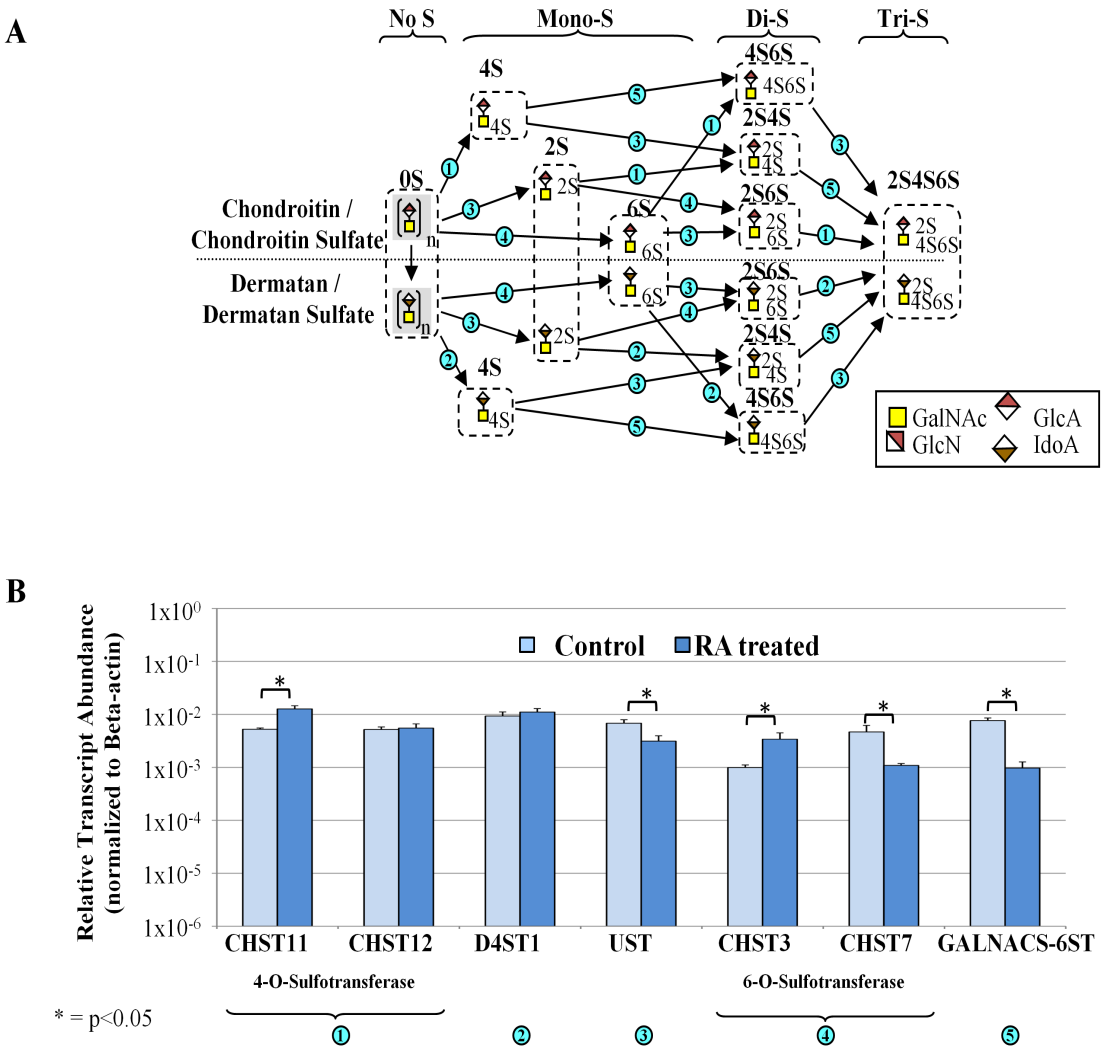

Figure 4.7. Change in expression of CS/DS chain modification enzymes in NCCIT cells upon RA treatment. A. Graphic representation of the modification of the repeating units of CS/DS. Numbers on steps correspond to the reactions catalyzed by enzymes coded by (1): CHST11, CHST12, (2): D4ST1, (3): UST, (4): CHST3, CHST7, and (5): CHST15. **B.** Relative transcript abundance for genes involved in CS/DS chain modifications for RA-treated and control NCCIT cells. Steps with multiple names for an enzymatic step are tissue specific isoforms. qRT-PCR data has been provided by Dr. A. Nairn, UGA, Complex Carbohydrate Research Center, Athens, GA.

4.2.5 Disaccharide analysis of GAGs from untreated pluripotent NCCIT and RA-induced cell derivatives.

Composition of disaccharides of GAGs was studied to provide detailed structural information on the appearance of chain variations. Cell-associated GAGs were isolated from untreated NCCIT cells and RA-treated differentiated NCCIT cell populations at 4, 7, 15 and 25 days after the start of treatment. Isolated GAGs were then digested with selected polysaccharide lyases (heparin lyase I, II and III and chondroitin lyases ACII, and ABC) to obtain disaccharides for LC-MS analysis of HS/HP and CS/DS. Disaccharide analysis of HS/HP revealed the presence of two different disaccharide components comprising the HS/HP GAGs in the untreated pluripotent NCCIT cells. Nonsulfated (0S) HS/HP disaccharide was the major component of NCCIT cells with 6S being present in much smaller amounts. The disaccharide composition remained unchanged with RA treatment (**Figure 4.8 A**). CS/DS disaccharide analysis revealed that 4S comprised nearly 98%, with only limited amounts of detectable 6S disaccharide. The 4S was also the major disaccharide following RA treatment, but a slight drop in the amount of 6S disaccharide occurred attendant with the appearance of 4S6S disaccharides (**Figure 4.8 B).** Thus, RA treatment of NCCIT cells results in slightly modified CS/DS GAG composition, but no detectable changes in HS/HP GAG composition.

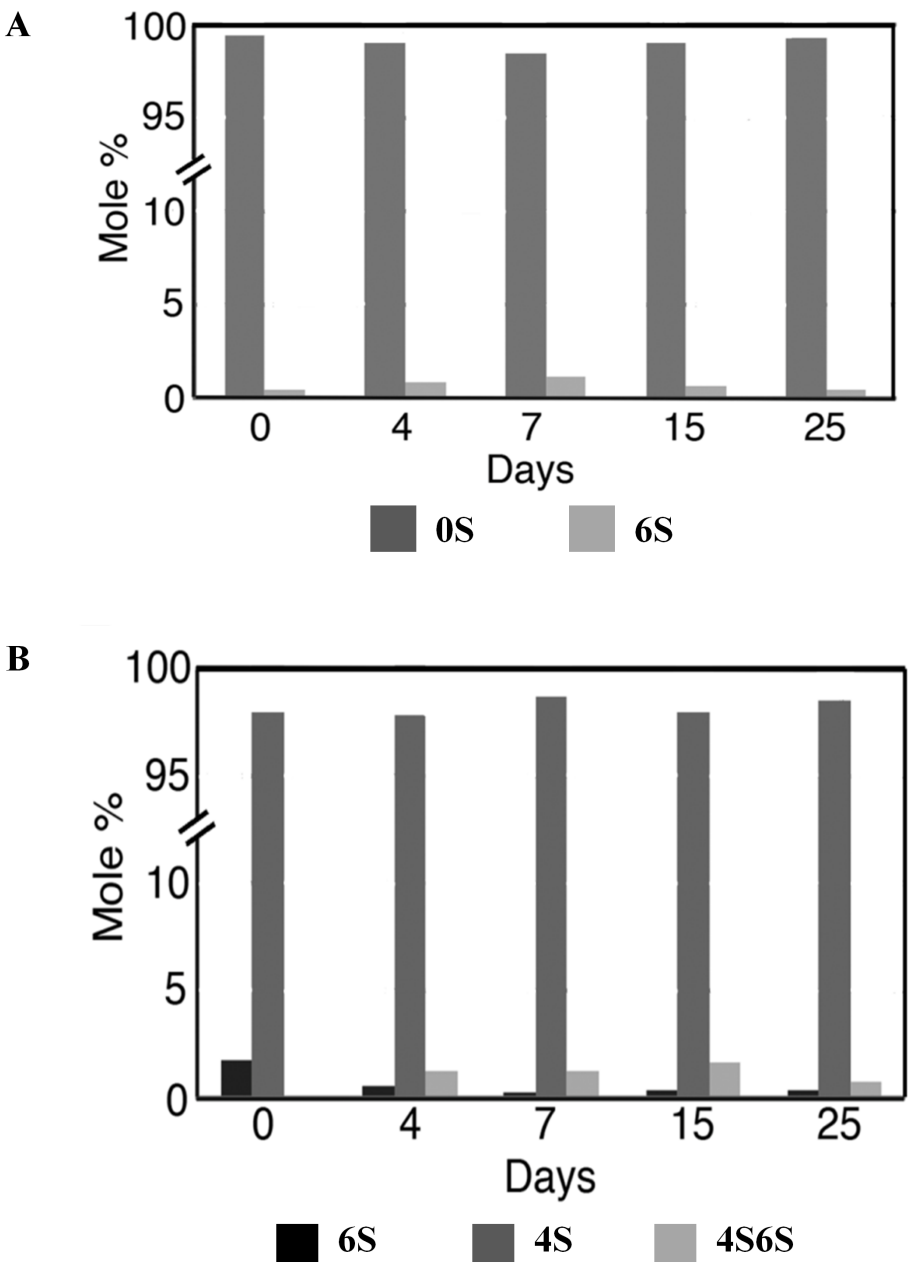

Figure 4.8. Changes in glycan composition of NCCIT cells during differentiation. A. Levels of HS/HP disaccharides at various time points during RA treatment of NCCIT cells by mole percent. Dark grey bars represent 0S disaccharides and light grey bars represent 6S disaccharides. **B.** Levels of CS/DS disaccharides at various time points during RA treatment of NCCIT cells by mole percent. Black bars represent 6S disaccharides, dark grey bars represent 4S disaccharides, and light grey bars represent 4S6S disaccharides. LC-MS data has been provided by Dr. B. Yang, RPI, Center of Biotechnology and Interdisciplinary Studies, Troy, NY. Adapted from (Gasimli et al. 2012).

4.3 Discussion

How GAGs contribute to developmental regulation of cell signaling upon interaction with morphogens remains an important unanswered question that has repercussions in the medical field as well as the study of development. NCCIT cells, like pluripotent embryonic stem cells, have the ability to differentiate into representatives of all germ layers. RA treatment directs these cells along multiple lineages, reflective of its role in early tissue formation. Detailed analysis of the cellular glycome of the pluripotent teratocarcinoma line NCCIT upon RA-induced treatment reveals changes at the mRNA and protein levels. These results provide evidence for quantitative transcriptional changes to core proteins and enzymes involved in early to late linkage region biosynthesis, chain extension, and chain modification. In addition, we performed disaccharide composition analysis of the CS/DS and HS/HP GAGs from pluripotent NCCIT and its RA-treated derivatives. This research provides the first GAG profile for the action of the RA morphogen that drives loss of pluripotency and the remodeling of the cellular glycome that accompanies multi-lineage differentiation.

Our knowledge of the biological functions of core proteins remains in its infancy. However, it is known that these proteins are of great interest in growth regulation, cell attachment, cell-cell interaction and cell motility (Couchman 2010; Esko, Kimata, and Lindahl 2009). In the CS/DS PG core proteins, RA-induced differentiation of NCCIT resulted in a dramatic increase in transcript and protein levels for the decorin core protein. Decorin plays a role in axon formation and can also suppress the expression of inhibitory CS PGs such as neurocan, brevican, phosphacan and NG2 to promote axonal growth (Hanemann et al. 1993; Minor et al. 2008). The ability to suppress inhibitory pathways for differentiation while initiating or promoting differentiation suggests dual roles for remodeling. In cancer, low levels of decorin are associated with poor prognosis and large tumor size (Troup et al. 2003). Biglycan has been shown to have inhibitory effects on axonal growth (Lemons et al. 2005) and on the growth of pancreatic cancer cell lines via G1-phase cell cycle arrest (Weber et al. 2001). We observed a decrease in biglycan transcript level contemporaneous with increased decorin. However, biglycan protein expression was not detected at any time point. This suggests that the baseline quantity of protein is low, which makes detection upon differentiation challenging.

Lumican expression increased as a result of RA treatment and has been shown to play a role in slowing the growth of retinal cells of neural epithelial origin. Its high expression may therefore facilitate differentiation through cell cycle changes. Similar to decorin, low levels of lumican are associated with poor prognosis and large tumor size in breast cancer, negative estrogen receptor and progesterone receptor status and increased inflammatory response (Troup et al. 2003). Although not as dramatic, we observed changes in HSPG core proteins such as increased glypican-5 transcript levels upon differentiation. However the increased transcript level did not seem to affect protein expression, as glypican-5 expression fluctuated throughout the RA treatment period, with a final decrease observed on day 15 of the treatment. Glypicans are thought to play an important role in development and differentiation through the interaction with growth factors and morphogens (Saunders, Paine-Saunders, and Lander 1997). Overexpression of glypican-5 increases cell proliferation by potentiating basic fibroblast growth factor (FGF), hepatocyte growth factor and Wnt1A, resulting in mesodermal inducing effects (Williamson et al. 2007). Glypican-5 is expressed in adult brain tissue and localized in neurons as well as in fetal brain, lung and liver tissues. Glypican-3 was also overexpressed in RA induced differentiated NCCIT cells and has been implicated in cancers by providing FGF and bone morphogenic protein-7, as well as stimulating Wnt signaling in hepatocarcinomas (Capurro et al. 2005). It also inhibits hepatomas and is silenced in mesotheliomas and ovarian and breast cancers (Filmus 2001; Sung et al. 2003). Glypican-3 may exert these effects through its HS chains (Lai et al. 2008) or core protein (Filmus 2001; Bishop, Schuksz, and Esko 2007).

Chain composition and length are known to be important effectors of cell signaling through mediation of interactions of various growth factors and chemokines. Upon loss of pluripotency by RA treatment, we observed several changes in the transcript abundances of NCCIT genes encoding enzymes involved in early to late linkage region biosynthesis and chain extension. Overall, for CS/DS and HS/HP chain initiation and elongation following differentiation, we observed no dramatic changes in transcript abundance. Two exceptions to this are EXTL1 and CSGALNACT1, which encode enzymes that play roles in chain elongation of HS and CS/DS respectively, both of which showed changes in message levels. HS chain modification enzymes function as

multiple tissue-specific isoforms, which are responsible for the heterogeneous structure of HS. We found that isoforms encoded by NDST3 and NDST4 were upregulated. Expression of these isoforms has been shown during embryonal development, and it has been suggested that NDST3 may play a role in development of brain, liver, kidney and heart. Both isozymes have restricted distribution in adult organisms. In the adult mouse, NDST3 is found in the brain and heart. A small amount of NDST4 is found in brain tissue (Aikawa and Esko 1999; Aikawa et al. 2001; Grobe et al. 2002). C5-Epimerase (GLCE) and HS2ST1 are thought to work in concert to produce HP, an oversulfated variant of HS found in mast cells. HP uses serglycin as a core protein. Following differentiation, the transcript levels for GLCE and HS2ST1 increased only slightly and transcripts for serglycin declined. Overall, this indicates that HP production does not change during treatment of NCCIT cells with RA. HS6ST3 is the only one of the three isoforms of the 6-*O*-sulfotranferases that displayed an ample increase in transcript abundance following RA treatment. It has broad tissue distribution, but its sub-specificity is not well understood (Kusche-Gullberg and Kjellen 2003). Only slight changes in HS3ST isoform transcript levels were observed. The HS3ST isoforms generate subtle modifications in HS structure resulting in the formation of recurring pentasaccharide patterns in the chain structure characteristic of HP. This pentasaccharide sequence is the source of the anticoagulant activity of HP. Even though transcripts for all of the sulfotransferases were detected in NCCIT cells during their differentiation, disaccharide compositions of HS chains were primarily non-sulfated and showed little complexity. Taken together, our findings suggest that transcripts of the enzymes involved in HS/HP and CS/DS biosynthesis are produced at a steady-state level. The fluctuation in factors such as the level of transcripts encoding core proteins does not carry over into cell-associated GAG structural changes. The same disaccharide composition was observed throughout the entire treatment and is consistent with the lack of change in the transcript levels observed for the majority of HS/HP biosynthetic enzymes. Transcript abundance of the gene encoding the CS/DS chain modification enzyme GalNac4S-6ST dropped upon differentiation, even though disaccharide analyses revealed a slight increase in 4S6S structural disaccharides in CS/DS glycans. This result could be explained by our focus upon cell-associated CS/DS chains, whereas some

portion of GAG chains are associated with core proteins that get secreted into the media. This result could also suggest that other factors or pathways may contribute to this structural profile at the glycome level.

Analysis of HS/HP and CS/DS disaccharides in the teratocarcinoma line NCCIT indicates significant changes occur in biosynthesis of specific core proteins of CS/DS and HSPGs. This may in part reflect neuronal commitment, which occurred in a subpopulation of NCCIT cells and which has been shown to involve these changes. However, the detected changes in actual disaccharide composition of CS/DS and HS/HP were insignificant. The HS/HP and CS/DS GAGs examined here are known to be important in many signaling pathways such as FGF, Wnt, BMP, and Hedgehog (Capurro et al. 2008; Kraushaar, Yamaguchi, and Wang 2010; Lanctot, Gage, and Varki 2007). Since cell-associated GAG was the only form analyzed in this study, future experiments analyzing the structure and composition of GAG chains from PGs that are secreted into the media would provide additional relevant data. This study also did not examine whether changes in hyaluronic acid and keratan sulfate composition might also contribute to RA-induced morphogen effects on differentiation of NCCIT cells. Keratan sulfate has specific distribution, found in such tissues as the cornea and cartilage. However, little is known about its role in cell development (Funderburgh 2002; Funderburgh, Caterson, and Conrad 1986). Hyaluronan has been shown to be important in morphogenesis via its physical properties as well as through signaling pathways including CD44. Hyaluronan is crucial in early morphogenesis of the prostate and kidney and in formation and modeling of blood vessels (Brown and Papaioannou 1993; Toole 2001). The contribution of hyaluronan and keratan sulfate remains to be determined in future studies.

4.4 Conclusions and Future Work

In summary, analysis of GAG profiles of pluripotent NCCIT and RA-treated cells reveals that suppression of inhibitory pathways is accompanied by the activation of differentiation-enhancing pathways. How significant these reported changes are to this remodeling is unknown at this time. It is possible that multiple glycocalyx options are

initiated that are then refined through environmental reinforcement. Future analysis of these questions along with comparative analysis of GAG profiles induced by use of other morphogens will help to clarify the mechanisms. Such analyses combined with transcriptome, epigenome and proteome profiles will help uncover the complex circuitry regulating cell fate with environmental influences for pluripotent and differentiated cell states. NCCIT cells were used specifically because of their ability to differentiate along multiple lineages as a model for pluripotent cells. However, it would also be interesting to analyze pluripotent cells which have differentiated into various lineages in order to obtain pure cell populations for GAG profiling, and to compare findings. As we gain greater understanding of the precise contribution of GAGs to signaling pathways, such analyses will be critical to predict, track and control cell fate. This capability is important not only for *in vivo* cell-based therapies, but also *in vitro* in order to improve the artificial cell environment in order to promote cell lineages as well as assembly of more complex multi-dimensional tissue and organ structures.

4.5 Materials and Methods

4.5.1 NCCIT cell culture and RA treatment

Teratocarcinoma cell line NCCIT (ATCC, Manassas, VA) was grown in RPMI-1640 medium (Mediatech, Manassas, VA) containing 10% fetal bovine serum (Life Technologies, Grand Island, NY) and 100 U/ml penicillin and streptomycin (Life Technologies) and cultured at 37°C in a humidified atmosphere with 5% CO_2. NCCIT cell differentiation was induced by adding 10 μM *trans*-RA (Sigma-Aldrich, St. Louis, MO) every three days for up to 40 days.

4.5.2 Total RNA isolation, cDNA synthesis and qRT-PCR reactions

Four biological replicates of untreated and RA-differentiated NCCIT cell samples were harvested after 9 and 20 days of growth, flash frozen in liquid nitrogen and stored at -80°C until use. For measurement of PG-related gene expression levels, RNA was isolated from cell lysates on day 20 of differentiation using the RNeasy Plus kit (Qiagen,

Valencia, CA) and cDNA synthesis was performed using Superscript III First Strand Synthesis (Life Technologies) as previously described (Li et al. 2011). The qRT-PCR reactions, done in triplicate for each gene analyzed, cycling conditions and analysis of amplimer products were performed as described. Briefly, reactions contained 1.25 µl of diluted cDNA template (1:10), 1.25 µl of primer pair mix (125 µM final concentration) and 2.5 µL iQ SYBR Green Supermix (BioRad, Hercules, CA) added to 96-well microtiter plates. Primers for the control gene, β-actin (NM 001101), were included on each plate to control for run variation and to normalize individual gene expression. Primer pairs for GAG-related genes were designed within a single exon (Nairn et al. 2007; Nairn et al. 2008) and primer design validated previously using the standard curve method (Nairn et al. 2007; Pfaffl 2001). Primer sequences and accession numbers for genes can be found in **Table 4.2**.

4.5.3 Calculation of relative gene expression levels and statistical analysis

An average of the triplicate Ct values for each gene was determined and the standard deviation calculated. Samples were rerun if the standard deviation value was >0.5 Ct units. The logarithmic average Ct value for the control gene and each tested gene was converted to a linear value by the equation 2^{-Ct}. Converted values were normalized to β-actin by dividing individual gene value by control gene value. Normalized values were scaled so that genes below the level of detection were given a value of 1×10^{-6}, and this value was used as the lower limit on histograms. A non-parametric Mann-Whitney test (GraphPad InStat3, v3.1) was used to determine statistically significant changes ($p<0.05$) in transcript abundance between undifferentiated and RA-treated samples. Fold change was calculated by dividing normalized values of tested genes in RA-treated cells by those in untreated control cells.

4.5.4 Protein isolation, quantification and immunoblotting

Cells were lysed in Nonidet-P40 lysis buffer (Boston Bioproducts, Ashland, MA) on ice for 30 min in the presence of a cocktail of protease and phosphatase inhibitors (Thermo

Fisher Scientific), which contained AEBSF, aprotinin, bestatin, E-64, leupeptin, and pepstatin A. Protein concentration was determined using the BCA assay (23227, Pierce). Approximately 40 μg of total protein was loaded and separated on a 4-20% gradient polyacrylamide gel. After transfer to a PVDF membrane, proteins of interest were detected using relevant primary and HRP-conjugated secondary antibodies followed by chemiluminescent (Pierce, Super Signal West Pico ECL substrate) exposure on high performance chemiluminescence film (GE Healthcare, Little Chalfont, UK, Amersham Hyperfilm ECL). Primary antibodies used were anti-γ-tubulin (T3320, Sigma Aldrich), anti-decorin (H00001634-B01P, Abnova, Walnut, CA), anti-lumican (H00004060-D01P, Abnova), anti-biglycan (H00000633-D01P, Abnova,), and anti-glypican-5 (sc-84278, Santa Cruz Biotechnology, Santa Cruz, CA).

4.5.5 Immunofluorescence

NCCIT cells were grown in Lab-Tek chamber slides and treated with 10 μM *trans*-RA every 3 days. Media from cells on days 0, 18 and 29 of RA treatment was washed off and cells were fixed with 4% paraformaldehyde. Cells were blocked with DPBS-Triton 100-X solution supplemented with 5% Bovine Serum Albumin (BSA). They were incubated overnight at 4°C with primary antibody diluted in DPBS-Triton X-100 solution supplemented with 1% BSA. The following day, after several washes with DPBS, cells were incubated with secondary antibody (A11001, A21244, goat anti-mouse Alexa Fluor 488, goat anti-rabbit Alexa Fluor 647, Life Technologies) diluted in DPBS-Triton X-100 solution supplemented with 1% BSA at room temperature for 1 h. After several washes with DPBS, cells were stained with Hoechst 33342 for 5 min at room temperature. After several washes, slides were detached from chambers and incubated overnight with ProLong Gold antifade reagent covered with a cover slip. The following day slides were sealed and analyzed with a Zeiss 510 Meta multiphoton confocal microscope. Primary antibodies used were anti-Oct3/4 (611202, BD Biosciences, Franklin Lakes, NJ), anti-nestin (ab6320, Abcam, Boston, MA), anti-β-III-tubulin (ab7751, Abcam), anti-GFAP (H00001634-B01P, Millipore, Billerica, MA). Alexa

Fluor 488 conjugated phalloidin stain was used for actin staining (A12379, Life Technologies).

4.5.6 Isolation and purification of total and cell surface GAGs

For total GAG recovery, 1×10^8 pluripotent NCCIT and RA-differentiated cells were harvested at the indicated time points, washed in PBS three times, and centrifuged to pellet cells. Isolation and purification of GAGs was performed as previously described with some modifications (Li et al. 2011; Zhang et al. 2006). Specifically, cell pellets were resuspended in 1 ml water and subjected to proteolysis at 55°C in 2 mg/ml actinase E (Kaken Biochemicals, Tokyo, Japan) for 20 h. After proteolysis, particulates were removed by using a 0.22 μm syringe-top filter. Peptides were removed from the samples using Microcon Centrifugal Filter Units YM-10 (10k MWCO, 15 ml, Vivascience, Ridgewood, NJ). Samples were collected from the top layer of the filtration membrane and lyophilized, then dissolved in 8 M urea containing 2% CHAPS (pH 8.3, Sigma-Aldrich). A Vivapure MINI Q H spin column was prepared by equilibrating with 200 μl of 8 M urea containing 2% CHAPS (pH 8.3). To remove any remaining proteins, the clarified, filtered samples were loaded onto and run through the Vivapure MINI Q H spin columns under centrifugal force (700 × g). The columns were then washed with 200 μl of 8 M urea containing 2% CHAPS at pH 8.3, followed by five washes with 200 μl of 200 mM NaCl. GAGs were released from the spin column by washing three times with 100 μl of 16% NaCl, and desalted with a Microcon Centrifugal Filter Unit YM-3 (3,000 MWCO, Millipore) spin column. The isolated GAG samples were freeze-dried for future analysis.

4.5.7 Enzymatic depolymerization of GAGs for CS/DS and HS/HP analysis

Isolated GAG samples were incubated with chondroitin lyase ABC (10 m-units, Seikagaku Corporation, Tokyo, Japan) and chondroitin lyase ACII (5 m-units, Seikagaku Corporation) at 37°C for 10 h and the enzymatic products were recovered by centrifugal filtration as described above, but at 13,000 x g. CS/DS disaccharides that passed through

the filter were freeze-dried for LC-MS analysis. GAGs remaining in the retentate were collected by reversing the filter and spinning at 13,000 x g, followed by incubation with 10 m-units of heparin lyase I, II, and III at 37°C for 10 h. The products were recovered by centrifugal filtration and the HS/HP disaccharides collected and freeze-dried for LC-MS analysis. Cloning, overexpression in *Escherichia coli*, and purification of the recombinant heparin lyase I (EC 4.2.2.7), heparin lyase II (no EC assigned), and heparin lyase III (EC 4.2.2.8) from *Flavobacterium heparinum* were all performed as previously described (Shaya et al. 2006; Yoshida et al. 2002).

4.5.8 Reverse-phase ion-pairing ultra-performance liquid chromatography mass spectrometry (RPIP-UPLC-MS) disaccharide composition analysis of CS/DS and HS/HP

LC-MS analyses were performed on an Agilent 1200 LC/MS instrument (Agilent Technologies, Inc. Wilmington, DE) equipped with a 6300 ion trap with two separate systems for the CS/DS disaccharide analysis and HS/HP disaccharide analysis. Unsaturated disaccharide standards of CS/DS, ΔUA-GalNAc (0S), ΔUA-GalNAc4S (4S), ΔUA-GalNAc6S (6S), ΔUA2S-GalNAc (2S), ΔUA2S-GalNAc4S (2S4S), ΔUA2S-GalNAc6S (2S6S), ΔUA-GalNAc4S6S (4S6S), ΔUA2S-GalNAc4S6S (2S4S6S) and unsaturated disaccharide standards of HS/HP, ΔUA-GlcNAc (0S), ΔUA-GlcNS (NS), ΔUA-GlcNAc6S (6S), ΔUA2S-GlcNAc (2S), ΔUA2S-GlcNS (NS2S), ΔUA-GlcNS6S (NS6S), ΔUA2S-GlcNAc6S (2S6S), ΔUA2S-GlcNS6S (NS2S6S) were obtained from Seikagaku America-NorthStar BioProducts (East Falmouth, MA) and Iduron (Manchester, UK). The column used was a 1.7 μm Acquity UPLC BEH C18 column (2.1 × 150 mm, Waters, Milford, MA). For CS/DS disaccharide analysis, solutions A and B for UPLC were 0 and 75% acetonitrile, respectively, containing the same concentration of 15 mM HXA as an ion-pairing reagent and 100 mM HFIP as an organic modifier. The column temperature was maintained at 45°C. For disaccharide analysis, solution A was used for 10 minutes, followed by a linear gradient from 10 to 40 min of 0 to 50% (v/v) solution B at a flow rate of 100 μl/min. The electrospray interface was set in positive ionization mode with the skimmer potential 40.0 V, capillary exit 40.0 V, and the temperature set at 350°C to obtain maximum abundance of the ions in a full-scan

spectra (350–1500 Da, 10 full scans/s) (Solakyildirim, Zhang, and Linhardt 2010). Nitrogen was used as a drying gas (8 l/min) and a nebulizing gas (40 psi). For HS/HP disaccharide analysis, eluent A was water/acetonitrile (85:15) v/v, and eluent B was water/acetonitrile (35:65) v/v. Both eluents contained 12 mM tributylamine (TrBA) and 38 mM NH_4OAc with pH adjusted to 6.5 with acetic acid. The column temperature was maintained at 45°C. For disaccharide analysis, solution A was used for 10 min, followed by a linear gradient from 10 to 40 min of 0 to 50% (v/v) solution B at the flow rate of 100 μl/min. The electrospray interface was set in negative ionization mode with the skimmer potential and capillary exit of -40.0 V, with a temperature of 350°C to obtain maximum abundance of the ions in a full-scan spectra (350–1500 Da, 10 full scans/s). Nitrogen was used as a drying gas (8 l/min) and nebulizing gas (40 psi) (Yang et al. 2011).

Quantification analysis of HS/HP disaccharides was performed using calibration curves constructed by separation of increasing amounts of unsaturated HS / heparin disaccharide standards (2, 5, 10, 15, 20, 30, 50, and 100 ng per disaccharide). Unsaturated disaccharide standards of HS/HP (0S: ΔUA-GlcNAc, NS: ΔUA-GlcNS, 6S: ΔUA-GlcNAc6S, 2S: ΔUA2S-GlcNAc, NS2S: ΔUA2S-GlcNS, NS6S: ΔUA-GlcNS6S, 2S6S: ΔUA2S-GlcNAc6S, triS: ΔUA2S-GlcNS6S) were obtained from Iduron (Manchester, UK). Linearity was assessed based on the amount of disaccharide and peak intensity in MS. All analyses were performed in triplicate.

5. ROLE OF GAG STRUCTURES IN FATE COMMITMENT OF HUMAN EMBRYONIC STEM CELLS

5.1 Introduction

Embryonic stem cells (ESCs) have prodigious potential in translational medicine, both directly and indirectly. ESCs might one day be used to replenish tissues that have been damaged in various diseases including Parkinson's and diabetes, and in this way provide a direct clinical use. Indirectly, ESCs are used as targets for drug development and also as models for the study of developmental processes. Their use is more favorable over primary, immortalized tumor, or genetically transformed cells as ESCs can be maintained in culture for extended periods of time, giving rise to uniform and genetically normal cell populations. The distinctiveness of ESCs is inherent in their pluripotency, which imparts the ability to differentiate into cell types of all germ layers: ectoderm, mesoderm and endoderm. Another important feature of ESCs is their capability to undergo asymmetric division, the result of which yields one cell that maintains pluripotency, while the other cell differentiates into a progenitor of defined cell type. As a result, there is always a pool of cells that retain "stemnity" whereas the rest provide cell types of interest (Schuldiner et al. 2001; Kehat et al. 2001; Hay et al. 2008; Amit et al. 2000).

Controlled effects of cell-extrinsic (He, Nakada, and Morrison 2009) and cell-intrinsic signals direct signaling pathways determining the embryonic stem cell state. It is a tightly controlled network of transcription factors (Boyer et al. 2005; Kim et al. 2008; Chen et al. 2008), interacting with the microRNA network (Marson et al. 2008; He et al. 2005; Wang et al. 2008; Lichner et al. 2011; Tay et al. 2008; Melton, Judson, and Blelloch 2010), that processes information received from the extracellular environment and in turn regulates the expression of genes required for maintenance of pluripotency or else driving differentiation towards a specific lineage.

Proteoglycans (PG) reside primarily in the extracellular space, as they are associated with the cell membrane, or else comprising a large fraction of the extracellular matrix. PGs consist of protein core with glycosaminoglycan (GAG) chains attached (Ly, Laremore, and Linhardt 2010). PGs interact with chemokines, growth factors, and morphogens, and they are important for modulating signaling pathways such as FGF,

Wnt, and BMP (Lander and Selleck 2000; Kjellen and Lindahl 1991; Bernfield et al. 1999; Yoneda and Couchman 2003; Linhardt and Toida 2004; Esko, Kimata, and Lindahl 2009), which are important in determination of stem cell fate. The principal activity of PGs has been associated with their GAG chains, although the core protein can also possess some activity of its own (Horowitz et al. 1999; Oh et al. 1998). GAGs are linear polymers consisting of repeating disaccharides, and can be divided into 4 classes: heparan sulfate (HS)/heparin (HP), chondroitin sulfate (CS)/dermatan sulfate (DS), keratan sulfate (KS) and hyaluronan (HA). These classes differ in the structure of the repeating disaccharides, and so also in their function (Ly, Laremore, and Linhardt 2010).

The role of diverse elements in stem cell fate determination including transcription factors, microRNAs, and chromatin modifiers have been extensively studied, but the function of proteoglycans (PG) remains less clearly defined. There have been limited studies considering the connection between PGs and stem cell fate. Even fewer studies have been done to link the structure of GAG chains to stem cell commitment towards the various lineages. The bulk of studies of PGs have been accomplished using neural stem cells, satellite cells and hematopoetic stem cells. The importance of HSPGs with regards to cell exit from the pluripotency state has been demonstrated, as cells missing HS failed to differentiate (Johnson et al. 2007). PGs such as neurocan, phosphacan, neuroglycan C, tenascin C (Garcion et al. 2004), aggrecan (Kabos et al. 2004), and NG2 (Ida et al. 2006; Nishiyama, Yang, and Butt 2005; Belachew et al. 2003) have been found in the rat ventricular zone of the telencephalon, where neural progenitor cells reside. Decorin, biglycan, and betaglycan regulate proliferation of bone marrow stromal cells (Bi et al. 2005)**.** NG2 has also been associated with epithelial and hair follicle stem cells (Kadoya et al. 2008)**.** The requirement for syndecan-3 for proper myoblast fusion and fiber structure has been proven (Cornelison et al. 2004)**.** Serglycin was shown to be important for neurogenesis (Damjanov, Horvat, and Gibas 1993)**.** ESCs express simple, *N*-sulfonated HS (Johnson et al. 2007). Upon differentiation toward embryoid bodies, levels of 6-*O*-sulfo groups increases (Nairn et al. 2007), and differentiation toward a neuronal fate is accompanied by elevated levels of *N*-, 2-*O*-, and 6-*O*-sulfo groups (Johnson et al. 2007). 3-*O*-sulfonation was shown to be important for transitioning of

pluripotent mouse SCs to mouse epiblast stem cells (Hirano, Van Kuppevelt, and Nishihara 2013).

The role of proteoglycans and their GAG chains in the direction of stem cell differentiation towards hepatic and pancreatic lineages has not been extensively studied. It has been implied that PGs modulate differentiation of stem cells towards hepatocytes through the mediating of the interaction between hepatic growth factor (HGF) and the c-Met receptor (Deakin and Lyon 1999). Understanding the role of GAGs in genesis of hepatocytes and Isl-1 cells would enable researchers to control those differentiation processes with the aim to utilize those cells for regenerative medicine as well as drug development. In this research, pluripotent embryonic stem cells have been differentiated into Isl-1 cells, which possess multipotential developmental capacity and are localized to the developing pancreas, and hepatocytes. They can also be differentiated into hepatic, adipocytic, osteocytic (Eberhardt et al. 2006), as well as the majority of heart cell types (Bu et al. 2009). Changes in HS/HP chain composition, expression of core proteins and HS/HP biosynthetic enzymes were examined to establish changes in the cellular glycome accompanying differentiation towards hepatic and Isl-1 cell types.

5.2 Results

5.2.1 Experimental hESCs WA09 (H9) possess normal karyotype and express pluripotency markers.

Pluripotent WA09 (H9) cells were grown on matrigel and exhibited morphology typical of non-differentiated stem cells (**Figure 5.1 A**). They were routinely karyotyped to ensure that no chromosomal abnormalities developed during stem cell maintenance (**Figure 5.1 B**). Their pluripotency was monitored by checking for expression of relevant markers including Oct3/4, SSEA-4, and Nestin. Our H9 cell line expresses Oct3/4 and SSEA-4, confirming their pluripotency (**Figure 5.1 C**). Nestin, which is associated with early neural differentiation (Dahlstrand et al. 1992), was not expressed, further confirming pluripotency (**Figure 5.1 D**).

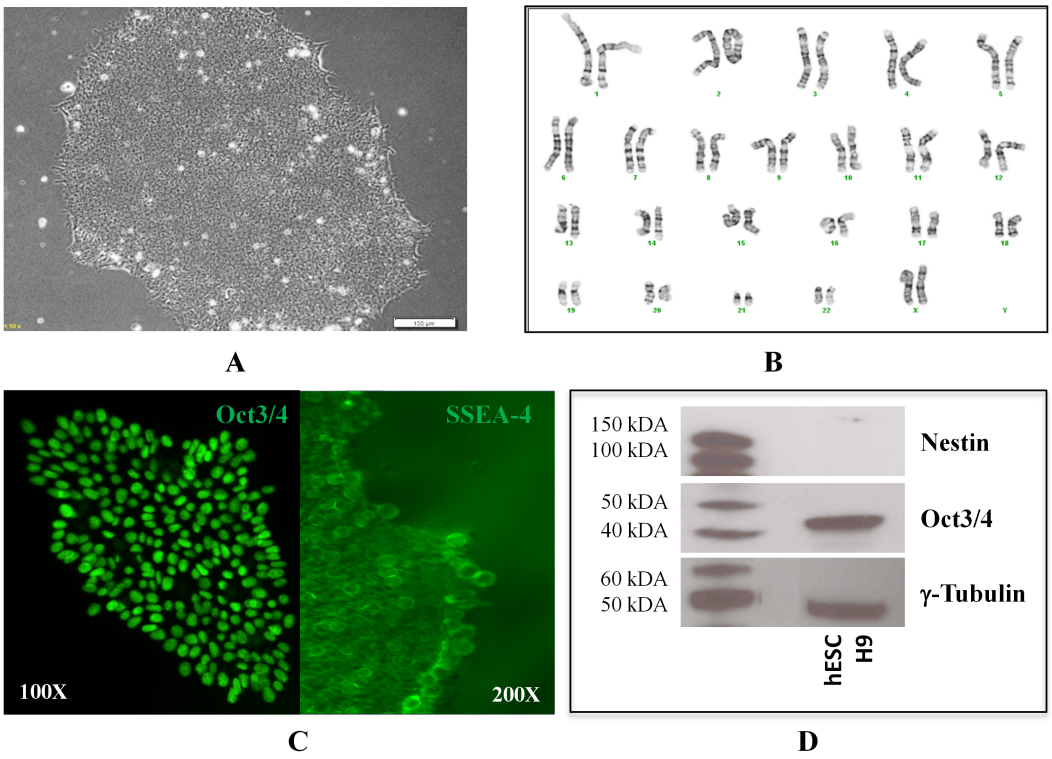

Figure 5.1. Expression of pluripotency markers and karyotyping of hESC cell line H9. Pluripotent H9 cells express typical morphology **(A)** and normal karyotype[a] **(B)** when grown on matrigel substrate with mTeSR1 media. They also express the pluripotency markers Oct3/4 and SSEA-4, as detected by immunocytochemistry **(C)** and do not express the early differentiation marker Nestin, as detected by immunoblotting **(D).**

5.2.2 Differentiation of hESC line H9 towards mesendodermal Isl-1 cells

Differentiation of H9 cells towards Isl-1 cells was completed in Dr. S. Dalton's Lab at the University of Georgia at Athens, and was confirmed by confirming the expression of pluripotency marker Nanog, as well as the Isl-1 cell marker, Isl (**Figure 5.2 A**). As expected, the expression of the Nanog transcription factor was high in non-differentiated H9 cells, whereas it decreased upon differentiation. In contrast, pluripotent H9 cells did not express the Isl marker, but an increased level of that protein was observed in Isl-1 cells (**Figure 5.2 B**), confirming their differentiation.

[a] Karyotyping of WA09 cells was done by Cell Line Genetics Inc., Madison, WI.

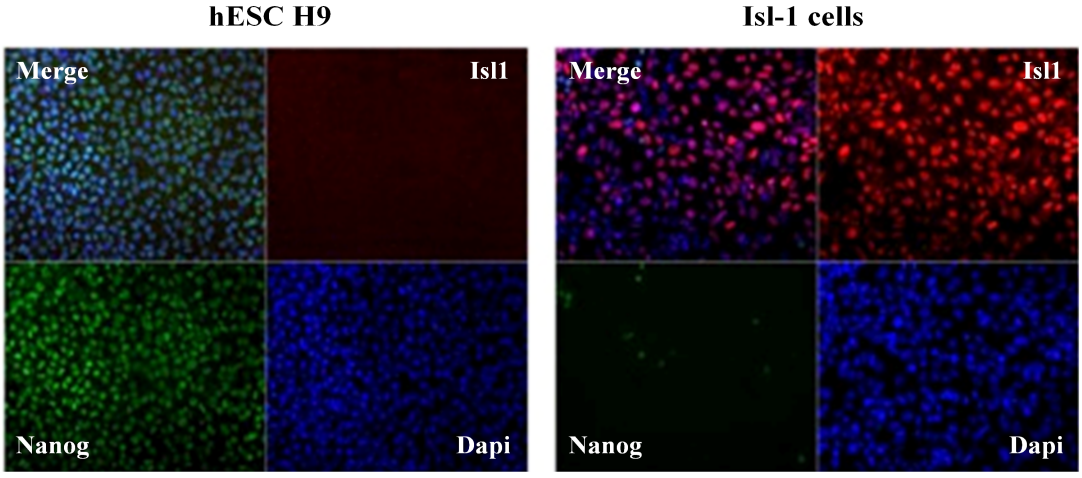

Figure 5.2. Differentiation of H9 cells towards Isl 1 cell type is confirmed by decreased expression of Nanog (A) and an increase in the level of Isl protein (B). Data was provided by Dr. S. Dalton lab, UGA, Athens, GA.

5.2.3 Differentiation of the hESC line H9 towards hepatocyte cell type

During differentiation, hESCs traverse several stages, including specified hepatic cells, hepatoblasts and hepatocytes (**Figure 5.3**).

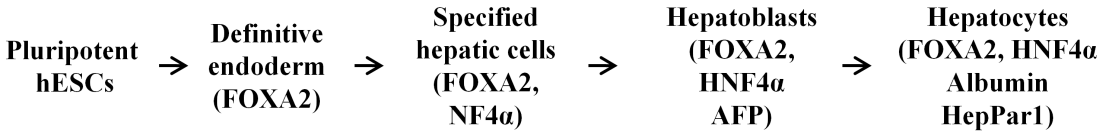

Figure 5.3. Scheme of the stages observed during differentiation of hESCs towards hepatocytes and markers expressed at each stage.

Each of those cell types varies in their morphological structure and present typical protein marker expression. During differentiation, we observed several cell types in differentiated H9 cell populations, including those that morphologically resembled hepatocytes (**Figure 5.4**). Pluripotent H9 cells had round cells packed tightly into colonies. During differentiation, polygonal shaped cells appeared, which is closer to the

morphology of hepatocytes. In addition, cells morphologically resembling epithelial and neuronal cells were observed in the population of differentiated cells.

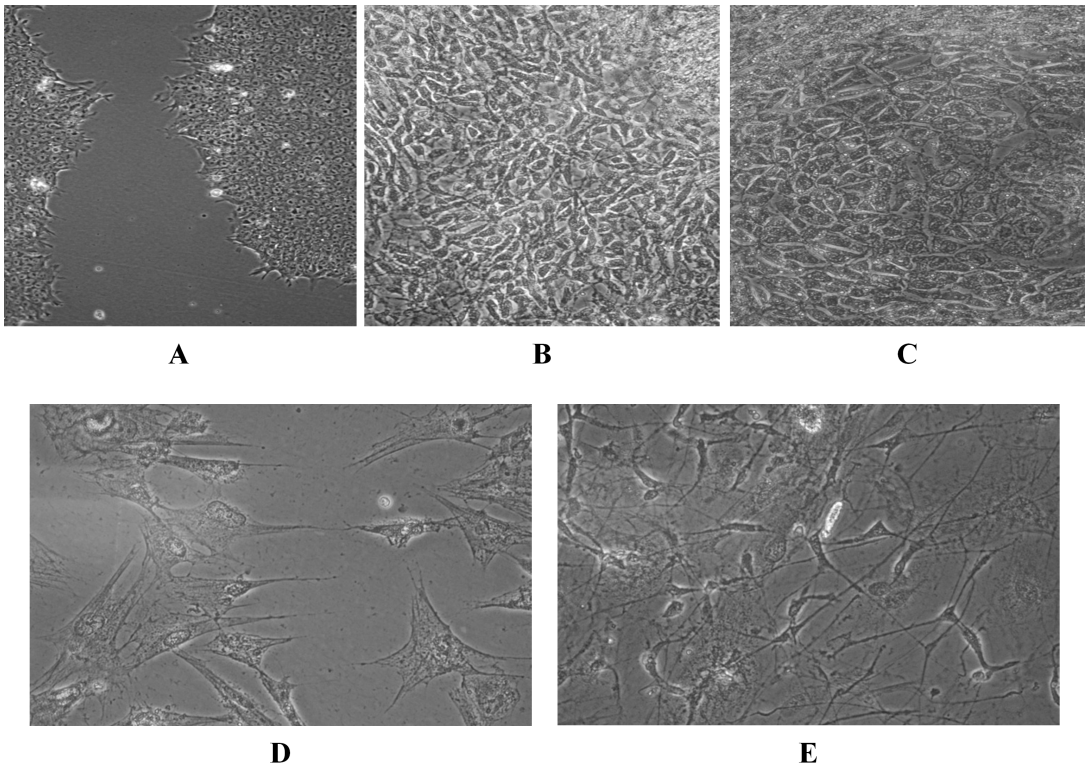

Figure 5.4. Cell types observed during differentiation of H9 cells during differentiation towards hepatocytes: pluripotent H9 cells (A), cells resembling early hepatocytes (B), cells resembling mature hepatocytes (C), and other cell types (D, E). Sample was provided by Dr. A. M. Hickey, RPI, Center of Biotechnology and Interdisciplinary Studies, Troy, NY.

Expression of the pluripotency marker Oct3/4 was not detected in a differentiated H9 cell population, confirming the impression that they had lost pluripotency. Hepatocyte nuclear factor (HNF) 3β (FOXA2) is a transcription factor that regulates expression of α-fetoprotein (AFP) protein in the early stages of hepatic differentiation (Wederell et al. 2008). Both FOXA2 and AFP were expressed in our differentiated H9 cells, confirming that differentiation was primed towards an endodermal fate. HNF4α is a transcription factor that regulates the expression of albumin (Hayhurst et al. 2001), one of the most abundant proteins in mature hepatocytes. Expression levels for both HNF4α

and albumin were low in differentiated H9 cells. Yet another marker for mature hepatocytes, HepPar1 (Fan et al. 2003) was also not detected (**Figure 5.5**).

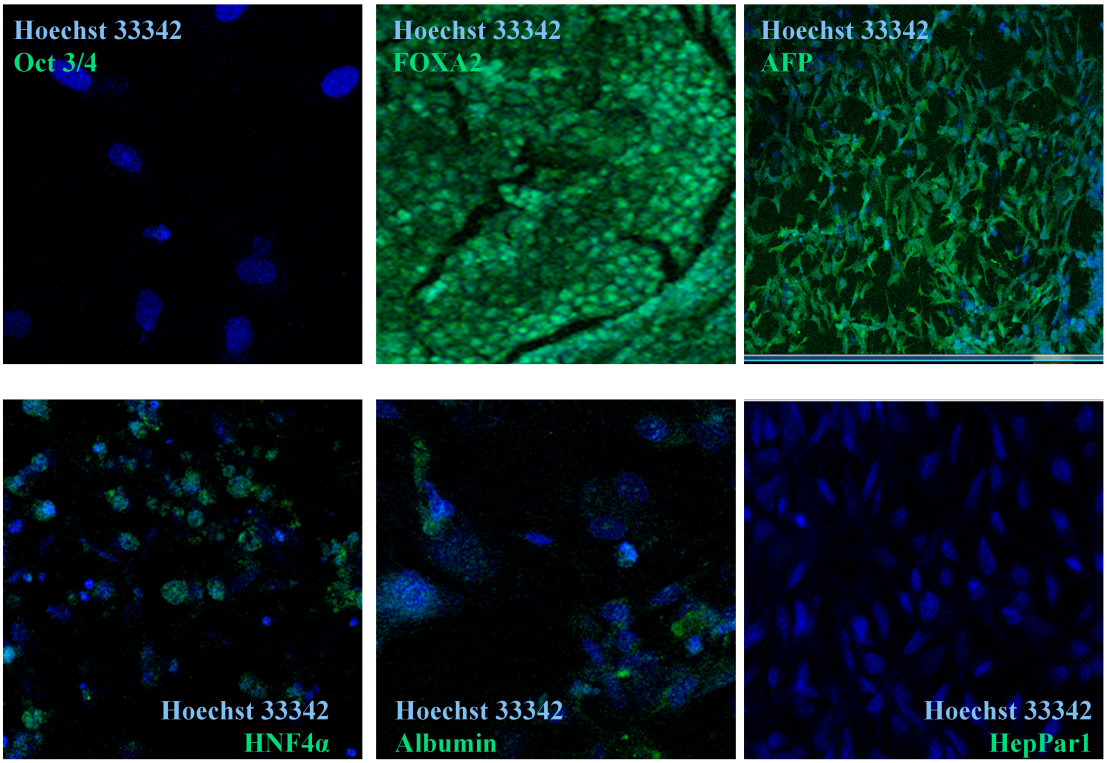

Figure 5.5. Expression of hepatic markers during differentiation of H9 cells detected by immunocytochemistry.

HepG2 cells are hepatocellular carcinoma cells, and are widely used as a model to study human hepatocytes (Pinti et al. 2003). Expression of hepatocyte-associated markers was tested in HepG2 cells in order to establish the baseline level of expression in mature hepatocytes (**Figure 5.6**). The expression of Oct3/4 was not detected, confirming that HepG2 cells are not pluripotent. The expression level of FOXA2 was relatively high, although the expression of AFP was low. HNF4α was upregulated and it colocalized with the nucleus, confirming its transcription factor origin. Albumin was widely expressed in HepG2 cells. When we compared the expression of hepatic markers in differentiated H9 cells and HepG2 cells, we concluded that H9 cells differentiated into early hepatocytes since expression of the mature hepatocytes markers HNF4α and albumin, was low compared to HepG2 cells. This conclusion was also supported by the

observation that both FOXA2 and AFP (premature hepatocyte markers) were highly expressed in differentiated H9 cells, whereas their expression was low in HepG2 cells.

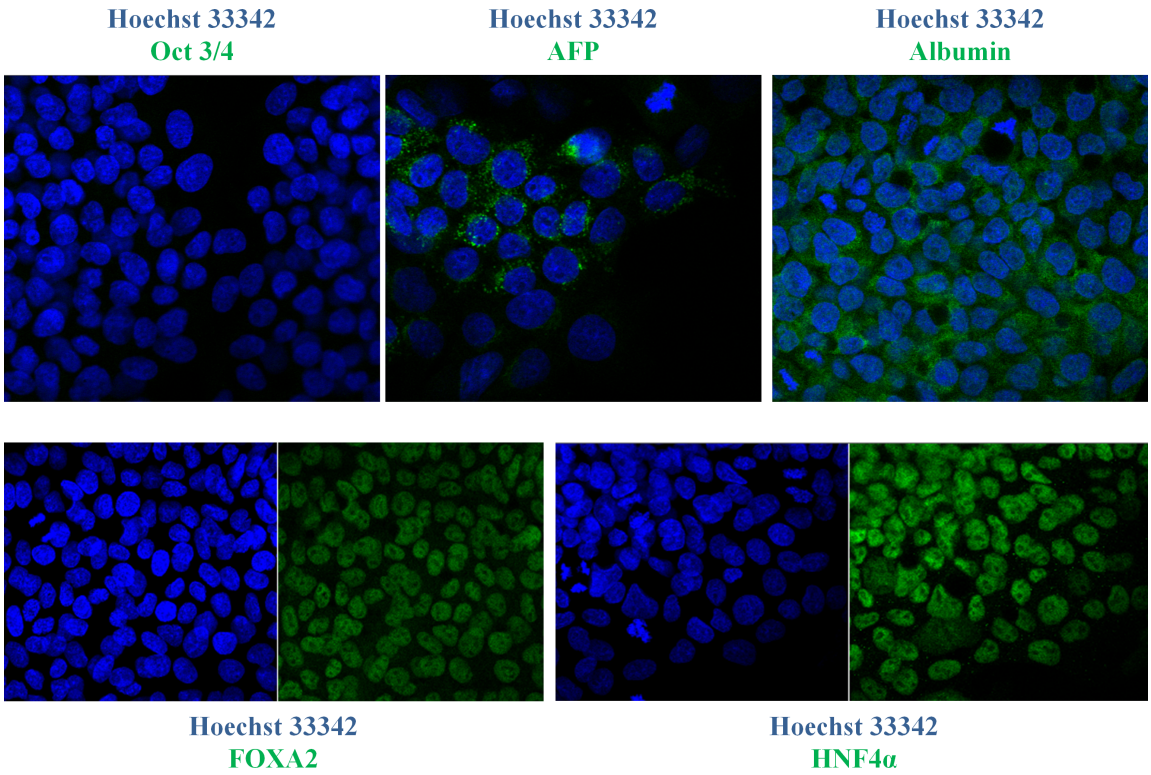

Figure 5.6. HepG2 cells expressing markers of mature hepatocytes.

5.2.4 Expression of GAG core proteins in Isl-1 cells

GAGs are synthesized on core proteins, which can carry keratan sulfate (KS), CS/DS and HS/HP. The primary function of the core proteins has been associated with which GAG chain they carry (Esko, Kimata, and Lindahl 2009). With this in mind, we assessed the expression level of GAG core proteins by qRT-PCR in H9 cells and Isl-1 cells. We were unable to analyze H9 cells differentiated towards hepatocytes. The most striking change was observed in transcript levels of lumican, decorin, serglycin and glypican-5. The expression of lumican transcript increased >100,000-fold in Isl-1 cells compared to H9 cells. Decorin and glypican-5 transcript expression was elevated in Isl-1 cells 682-fold and 238-fold, respectively. However serglycin transcript expression dropped 21-fold in Isl-1 cells. Other core proteins had modest changes in their

expression of transcript. Fibromodulin transcript expression increased about 14-fold, whereas thrombomodulin was elevated ~ 6-fold. Procollagen 1Xa2, biglycan, epican (CD44), syndecan-3, syndecan-4, glypican-1 and glypican-3 all displayed increased transcript levels in Isl-1 cells under 5-fold. The expression of both versican and glypican-4 transcript decreased ~ 5-fold. On the other hand, aggrecan, NG2, neuroglycan, bamacan, brevican, CD74, agrin, syndecan-1, glypican-2, and glypican-4 each exhibited a decrease in transcript level under 5-fold in Isl-1 cells compared to H9 cells. Finally, there was no change detected in the transcript levels of neurocan, perlecan, syndecan-2, and glypican-6 (**Figure 5.7**).

Expression of lumican, decorin, serglycin, and glypican-5 was examined by immunoblotting to assess their variation in Isl-1 cells. Our results showed that Isl-1 cells primarily express the sulfated form of lumican, whereas pluripotent H9 cells express the non-sulfated form (~ 39 kDa). In Isl-1 cells, expression of the non-sulfated form of lumican was low, whereas the sulfated form was highly expressed. The size of sulfated lumican ranged from ~ 50 kDa to ~ 80 kDa. No changes were detected in the levels of decorin or glypican-5 in H9 and Isl-1 cells. Serglycin signal also was not detected in either H9 or Isl-1 cells (**Figure 5.8**).

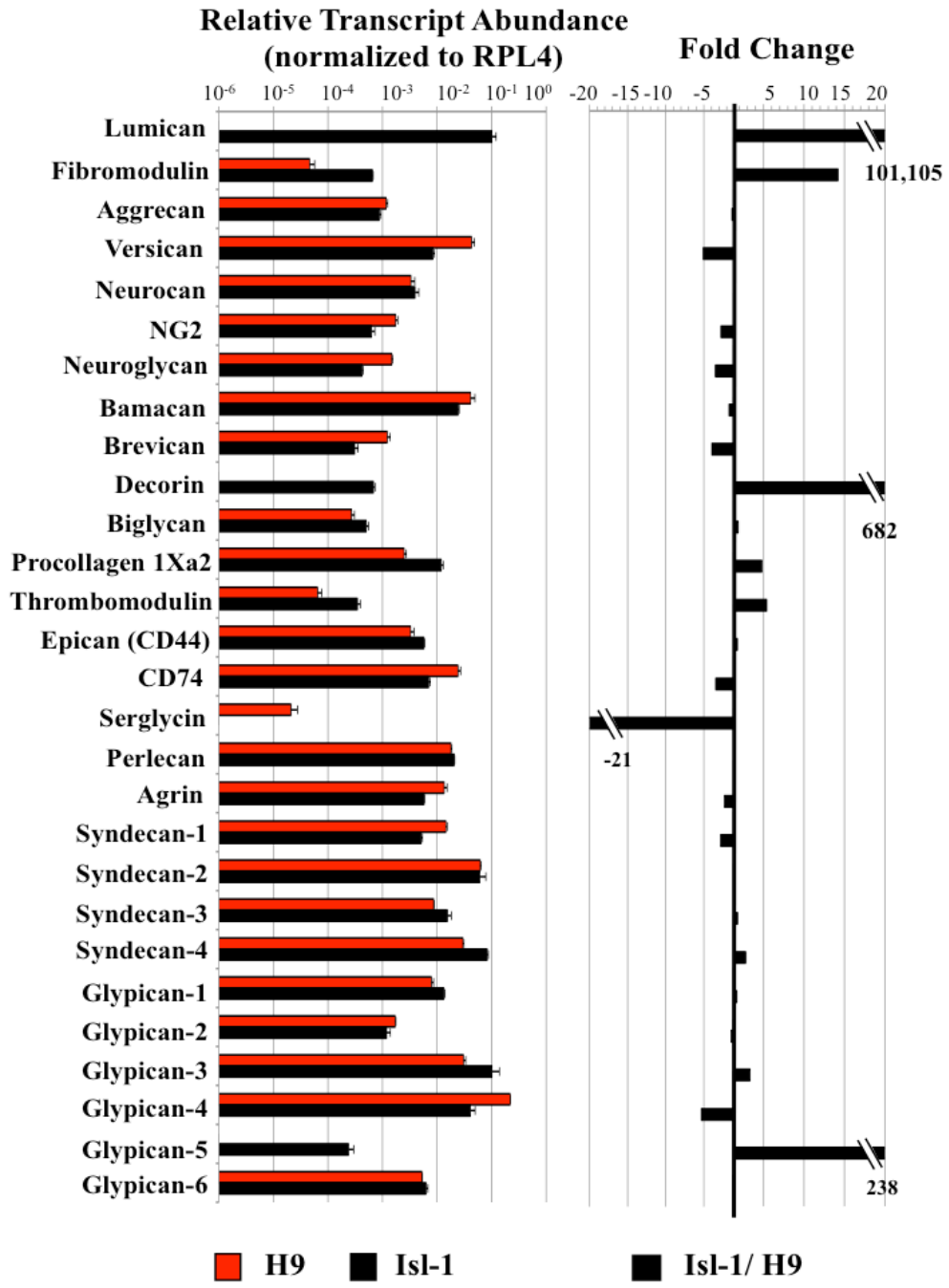

Figure 5.7. Expression of GAG core proteins in H9 and Isl-1 cells detected by qRT-PCR. Fold change (top) and the relative transcript abundance (bottom) of CS/DS and HS/HP core proteins as normalized to RPL4. Relative transcript abundance for H9 pluripotent cells and Isl-1 cells plotted on a log10 scale for each gene assayed. qRT-PCR data has been provided by Dr. A. Nairn, UGA, Complex Carbohydrate Research Center, Athens, GA.

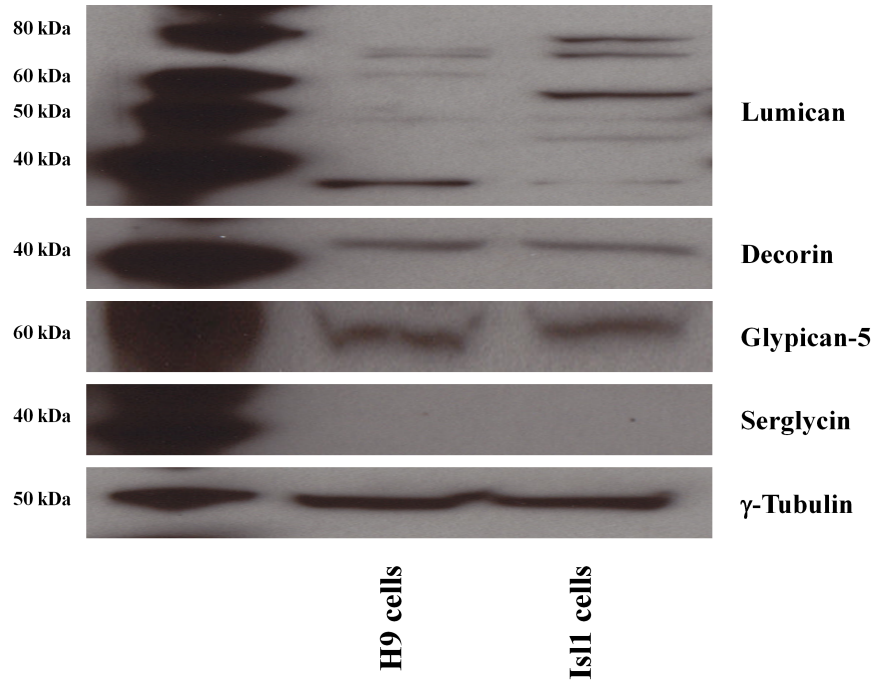

Figure 5.8. Change in expression level of lumican, decorin, glypican-5 and serglyin in hESC line H9 and Isl-1 cells by Western blotting.

5.2.5 Change in the expression of HS/HP chain initiation, elongation and modification enzymes in Isl-1 cells compared to H9 cells.

HS/HP chains are synthesized on a core of carrier proteins, where the initial tetrasaccharide is attached. This reaction is facilitated by the action of several enzymes such as xylosyl transferases (XYLT1 and XYLT2), β4-galactosyltransferase (β4GALT7), β3-galactosyltransferase (β3GALT6), and β3-glucuronosyltransferase (β3GAT3). Further elongation of the HS/HP chain is carried out by α-N-acetylglucosaminyltransferases (EXTL2, EXTL3) and α-*N*-acetylglucosaminyl-β-glucuronosyl transferases (EXT1, EXT2) (**Figure 5.9 A**). For all enzymes involved in chain initiation and elongation steps of HS/HP biosynthesis, we observed modest changes (under ~ 5-fold) in transcript levels. We observed upregulation in transcript levels for β3GALT6, β3GAT3, and EXT1, whereas we saw decreased levels for XYLT1, XYLT2, β4GALT7, EXTL1, EXTL2, EXTL3, and EXT2 in Isl-1 cells compared to H9 cells (**Figure 5.9 B, C**).

Nascent HS/HP chains go through a series of modifications, including sulfonation at multiple positions. These reactions are catalyzed by *N*-deacetylase-*N*-sulfotransferases (NDSTs), C5-epimerase (GLCE), 2-*O*-sulfotransferase (HS2ST1), 6-*O*-sulfotransferases (HS6STs) and 3-*O*-sulfotransferases (HS3STs) (**Figure 5.10 A**). These enzymes also have isozymes, which have spatial and temporal distribution (Sugahara and Kitagawa 2002). Transcripts for NDST1, NDST2, NDST3, GLCE, HS6ST2, HS6ST3, HS3ST1, HS3ST3A1, and HS3ST3B1 are slightly elevated (<5-fold) in Isl-1 cells compared to H9 cells. The maximum difference was discovered in the transcript level of HS3ST1, which was elevated ~ 9-fold in Isl-1 cells compared to H9 cells. NDST4 transcript was not detected in Isl-1 cells, whereas it was in fact observed in H9 cells. We noted only a minor decrease in transcript levels for HS2ST1, HS3ST4, HS3ST5 and HS3ST6 in Isl-1 cells as compared to H9 cells. The HS3ST2 transcript displayed the most substantial change, as those levels were reduced ~ 29 fold in Isl-1 cells. No change was observed in the transcript level of HS6ST1 upon differentiation of H9 cells into Isl-1 cells (**Figure 5.10 B, C**).

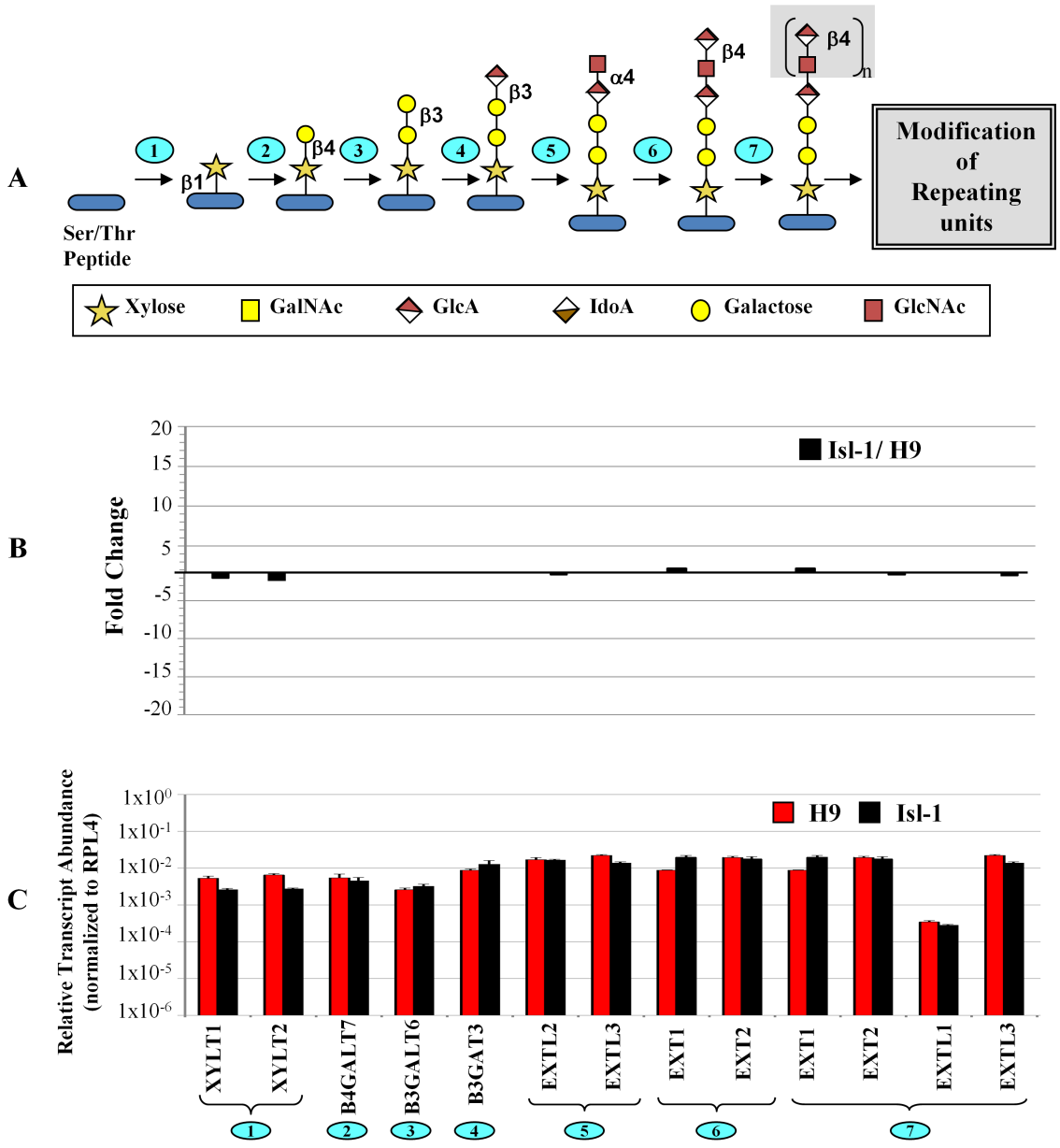

Figure 5.9. Change in expression of HS/HP biosynthetic enzymes. A. Graphic diagram of GAG core tetrasaccharide biosynthesis and HS chain polymerization. The Ser/Thr-containing polypeptide core protein is glycosylated and modified through ten enzymatic reactions occurring in the endoplasmic reticulum and Golgi. Numbered steps correspond to the reactions catalyzed by enzymes coded by (1): XYLT1, XYLT2, (2): B4GALT7, (3): B3GALT6, (4): B3GALT3, (5): EXTL2, EXTL3, (6): EXT1, EXT2, (7): EXT1, EXT2, EXTL1, EXTL3. **B.** Fold change of HS/HP biosynthetic enzymes in Isl-1 cells compared to H9 cells. **C.** Relative transcript levels for genes coding CS/DS and HS/HP chain initiation and elongation enzymes. Plotted as described for Figure 5.6. qRT-PCR data has been provided by Dr. A. Nairn, UGA, Complex Carbohydrate Research Center, Athens, GA.

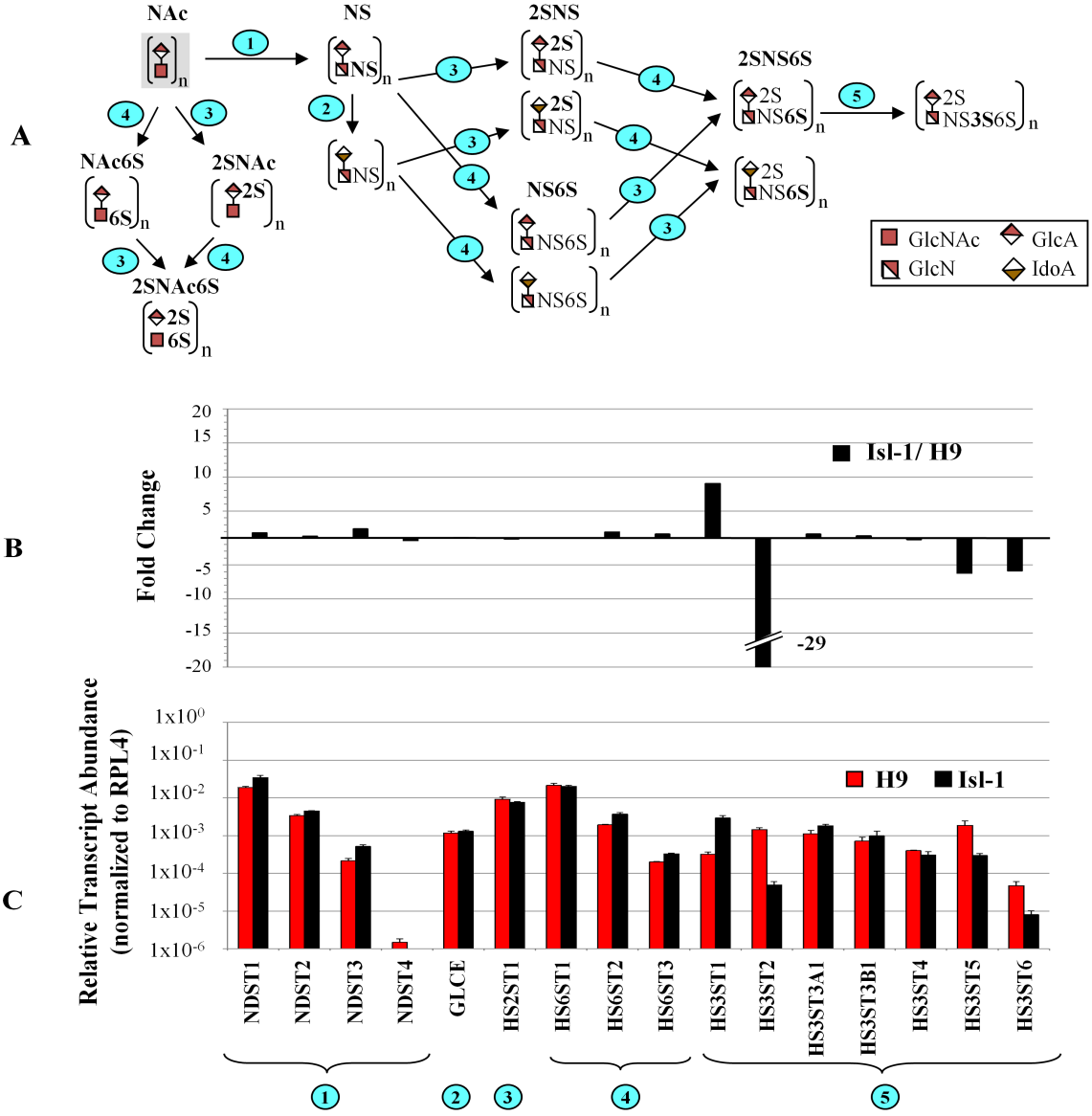

Figure 5.10. Change in expression of HS/HP chain modification enzymes upon differentiation of H9 cells into Isl-1 cells. **A**. Graphic diagram of the modification of the repeating units in the HS/HP chain. Numbers on steps correspond to the reactions catalyzed by enzymes encoded by (1): NDST1, NDST2, NDST3, NDST4, (2): GLCE, (3): HST2T1, (4): HS6ST1, HS6ST2, HS6ST3, and (5): HS3ST1, HS3ST2, HS3ST3A1, HS3ST3B1, HS3ST4, HS3ST5, HS3ST6. **B.** Fold change in transcript level of HS/HP biosynthetic enzymes in Isl-1 cells compared to H9 cells. **C.** Relative transcript abundance for genes involved in HS/HP chain modifications for Isl-1 cells and H9 cells. Plotted as described for **Figure 5.7**. qRT-PCR data has been provided by Dr. A. Nairn, UGA, Complex Carbohydrate Research Center, Athens, GA.

5.2.6 Structural changes in HS/HP GAGs in H9 cells differentiated into Isl-1 cells and early hepatocytes.

HS/HP chain structure was investigated in pluripotent H9 cells, Isl-1 cells and early hepatocytes. In pluripotent H9 cells, the majority of cell-associated disaccharides were non-sulfated 0S disaccharides (73.1%). NS, 6S, NS2S and TriS disaccharides were also detected in H9 cells, but in far lower quantity (7.8%, 6.2%, 7.7%, and 5.2%, respectively). 2S, NS6S and 2S6S disaccharides were not detected in H9 cells (**Figure 5.11** and **Table 5.1**). In Isl-1 cells, NS (39%), and 0S (31.9%) comprised the most substantial fraction of disaccharides. 6S (7.4%), NS6S (7.2%), NS2S (7.0%), and TriS (7.5%) disaccharides were also found in Isl-1 cells, whereas 2S and 2S6S structured disaccharides were not detected. In early hepatocytes, the majority of disaccharides were comprised of 0S (49.1%), followed by NS6S (27.9%), NS (16.5%), 6S (6%), and 2S (0.4%). NS2S, 6S2S and TriS were not detected in early hepatocytes.

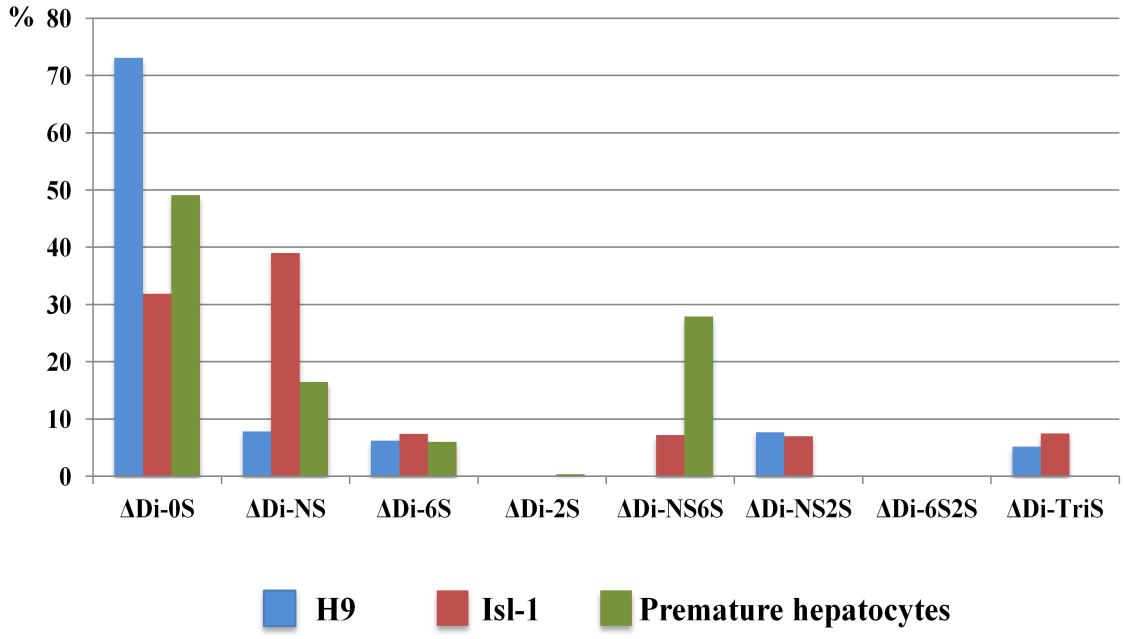

Figure 5.11. Heparan sulfate/heparin disaccharide composition of H9 and Isl-1 cells, and premature hepatocytes. LC-MS data has been provided by Dr. B. Yang, RPI, Center of Biotechnology and Interdisciplinary Studies, Troy, NY.

Table 5.1. Distribution of heparan sulfate/heparin disaccharides in differentiated H9 cells. LC-MS data has been provided by Dr. B. Yang, RPI, Center of Biotechnology and Interdisciplinary Studies, Troy, NY.

Sample	HS/HP disaccharide composition							
	0S	**NS**	**6S**	**2S**	**NS6S**	**NS2S**	**6S2S**	**TriS**
H9 cells	73.1	7.8	6.2	0	0	7.7	0	4.9
Isl-1 cells	31.9	39.0	7.4	0	7.2	7.0	0	7.5
Premature hepatocytes	49.1	16.5	6.0	0.4	27.9	0	0	0

5.3 Discussion

Stem cells possess the potential to influence and advance a vast range of important disciplines, but this prospective value is blunted by the necessity to define and harness advanced methods for control of the stem cell differentiation process. This challenge requires a thorough comprehension of the orchestra of intrinsic and extrinsic signals that regulate stem cell fate. Although intrinsic components have garnered a lion's share of the attention, study of the extrinsic side of the signaling story remains in its infancy. Extrinsic signals from the stem cell niche are essential in the direction of cell state. PGs are primarily associated with the extracellular environment and are indispensable components of the niche. Therefore, it is imperative to establish the role they play in the setting of stem cell mode. We used the hESC line H9 differentiated into Isl-1 cells and hepatocytes to establish glycomic modifications in accompanying cell differentiation processes. Proper differentiation seems to be a somewhat challenging proposition, as additional cell types apart from the type of interest is usually observed within the differentiating culture. We experienced that very process firsthand during our differentiation of H9 cells into a hepatic lineage. Among the culture of cells, we noted cells of dissimilar morphology were obtained in addition to cells that morphologically resembled hepatocytes. Immunostaining of the cell population and HepG2 cells with markers for hepatic lineages suggested that our H9 cells differentiated into premature

hepatocytes with a selected fraction of mature hepatocytes. We used these cells along with Isl-1 cells to accomplish our glycomic analyses.

The heparan sulfate biosynthetic pathway has been extensively characterized and the enzymes involved are well established. Since HS biosynthetic enzymes are responsible for initiation, polymerization and modification of HS chains, and core proteins carry those chains, the expression levels of those enzymes and core proteins were inspected. The most significant change was observed in the transcript levels of lumican, decorin, serglycin and glypican-5. Lumican and decorin are small leucine-rich proteoglycans that can carry CS, DS and KS chains. The molecular weight of lumican is known to be heterogeneous, and is initially translated as a precursor protein of ~ 50 kDa. However in adult cells, it is observed to be ~ 37 kDa, and this corresponds to the non-glycosylated form of lumican. Since it does have glycosylation sites, it is also observed with a ladder of higher molecular weights (Dolhnikoff et al. 1998), and this has been previously reported to occur during corneal development where it begins as a non-glycosylated protein and as development progresses, it is observed in the glycosylated form (Cornuet, Blochberger, and Hassell 1994). This is consistent with results observed from lumican expression upon differentiation of pluripotent stem cells towards Isl-1 cells. H9 cells predominantly utilize the non-glycosylated form of lumican, whereas in Isl-1 cells, the principal portion is glycosylated lumican. Since KS is a major GAG that lumican carries, we could speculate that KS is required for differentiation towards Isl-1 cells. Unfortunately, there is a dearth of information available on the role of KS in developmental processes save those implicating its role in embryo implantation (Graham et al. 1994) and its inhibitory effect on neurite growth (Olsson et al. 1996). The increase in transcription level of lumican observed by qRT-PCR correlated well at the level of translation, which was assessed by immunoblotting. Decorin was shown to be important in the homeostasis regulation of satellite cells, which are committed muscle cell progenitors, through competition with TGF-β for TGFβ receptors (Droguett et al. 2006). Decorin expression was discovered to increase upon differentiation of the teratocarcinoma cell line NCCIT towards a neural lineage when treated with retinoic acid (Gasimli et al. 2012). Glypicans are cell surface associated PGs and are connected to the external side of the membrane through the GPI anchor. The role of glypicans in

important processes such as development and morphogenesis has been defined. They are known to play a role in the regulation of FGF, Hedgehog, Wnt, and BMP signaling primarily through their HS chains (Filmus, Capurro, and Rast 2008). Although we did not detect a change in the protein expression level of decorin and glypican-5 in cell based samples, that does not preclude the possibility of observing such a change in cell culture media. This stands to reason because both decorin and glypican-5 are extracellular PGs that can be shed into the media, and this possibility was not directly explored to this point. Serglycin is a PG that carries heparin chains and is found in connective tissue mast cells (Abrink, Grujic, and Pejler 2004). It has been proposed that serglycin might be involved in neurogenesis (Schick et al. 2003). Even though we observed a change in serglycin transcript level, we could not correlate this change in protein level by Western blot. This contradiction could be explained by the fact that base line expression of serglycin is too low to detect, and so a further drop in expression would remain undetectable.

Modification of HS/HP chains by biosynthetic enzymes is important for creating domains along the chains that are required for interaction with various signaling molecules. Although there were not sizeable changes in transcript levels of HS/HP chain initiation and elongation enzymes upon differentiation of H9 cells into Isl-1 cells, the expression of HS/HP chain modification enzymes was affected. The most prevalent change was observed in level of HS3STs. There are seven isozymes of HS3ST, which have unique spatial and temporal distribution. The transcript of HS3ST1 increased, whereas the transcript level of HS3ST2 decreased in Isl-1 cells compared to H9 cells. HS3ST1 is found in kidney, brain and heart, whereas HS3ST2 was reported only in brain. These enzymes are responsible for creating the 3-*O*-sulfonation modification in the HS/HP chain, which is important for interaction with molecules such as antithrombin (Sugahara and Kitagawa 2002) and also for differentiation of mouse ESCs via Fas signaling (Hirano et al. 2012). Due to the absence of enzymes that can cut the HS/HP chain yielding 3-*O*-sulfonated disaccharides, we could not use LC-MS to verify whether or not a change in expression of HS3STs leads to a change in HS/HP structure. NDST1 is ubiquitously expressed while NDST3 is found in brain, kidney and liver (Sugahara and Kitagawa 2002). While not as dramatic as H3ST1, we observed increases in

expression for NDST1, NDST3, HS6ST1 and HS6ST3 transcripts. This result is echoed by the increase of NS and NS6S disaccharides detected by LC-MS.

We observed that the structure of HS/HP chains was modified upon differentiation towards different lineages. The most prominent change was the drop in the level of non-sulfated disaccharides and increase in *N*-sulfo group containing structures in both Isl-1 and early hepatic cells compared to H9 cells. Another significant change was the appearance of NS6S sulfated disaccharides upon loss of pluripotency, as that structure was observed only in differentiated cells and not in H9 cells. When compared to one another, Isl-1 cells more closely resemble H9 cells in disaccharide composition, although the ratio of different disaccharides is distinctive in both cell types. Disaccharide composition and the ratio of different disaccharides have the greatest differential in early hepatocytes compared to H9 and Isl-1 lines. NS2S and TriS disaccharide were not found in early hepatocytes, but two additional disaccharide structures, 2S and NS6S, appeared in early hepatocytes. This finding assigns early hepatocytes a unique HS/HP disaccharide composition pattern. Taken together, we can surmise that H9 cells principally utilize non-sulfated HS/HP, and as development progresses, the HS/HP structure gets gains complexity via sulfonation at various positions. The greater similarity of Isl-1 cells to H9 cells than early hepatocytes to H9 cells can be explained by the fact that Isl-1 cells are mesendodermal cells, which possess the ability to differentiate into either endodermal or mesodermal lineages, and appear earlier in development than early hepatic cells. As cells progress towards more committed cells types such as early hepatocytes, HS structure changes become more prominent. This is exactly what we have observed experimentally.

5.4 Conclusions and Future Work

Knowledge gained from a greater understanding of the processes leading to differentiation towards hepatocytes and Isl-1 cells is not limited to advancement of the treatment of damaged tissues, but can also be useful in drug discovery applications. The ability of hepatocytes to detoxify numerous compounds makes them invaluable for homeostatic upkeep of organisms. This feature of hepatocytes can be harnessed *in vitro*

for drug toxicology studies. Direction of stem cell fate, coupled with high throughput platforms (Fernandes et al. 2010) can open the door for screening copious compounds simultaneously for their toxicological effect on hepatocytes. Understanding the processes that lead to differentiation towards Isl-1 cells, and further towards pancreatic cells or cardiac progenitor cells, can give hope to many people who have heart issues or those that face advanced disease states such as diabetes that lack effective treatment options. We have established a perspective on changes in HS/HP biosynthetic enzymes and the resultant structural modifications of HS/HP during differentiation of H9 cells towards the hepatic lineage and Isl-1 cells. Future work will be directed towards defining the underlying mechanisms by which the various GAG structures influence differentiation pathway decision making of stem cell fate.

5.5 Materials and Methods

5.5.1 hESC H9 cell culture

hESC line H9 (WiCell Research Institute, Inc, Madison, WI) was maintained on Matrigel coated cell culture dishes in complete mTeSR-1 media (Stem Cell Technologies, Vancouver, Canada) supplemented with 100 U/mL penicillin and streptomycin (Life Technologies, Grand Island, NY) and cultured at 37°C in a humidified atmosphere with 5% CO_2. Cells were passaged every 5-6 days using collagenase IV (Life Technologies) to release cells from Matrigel.

5.5.2 hESC H9 differentiation

5.5.2.1 H9 differentiation toward Isl-1 cell fate

Dr. S. Dalton's Lab at University of Georgia at Athens, Athens, GA, provided H9 cells differentiated into Isl-1 cells.

5.5.2.2 H9 differentiation toward hepatocyte cell fate

H9 differentiation towards hepatocytes was performed as described in (Medine et al. 2011). Briefly, H9 cells were primed towards definitive endoderm in RPMI 1640 (ATCC, Manassas, VA) media supplemented with B27, Activin and Wnt3a for 3 days. Hepatic differentiation was induced in DMEM-KO (ATCC) media supplemented with DMSO and Serum replacer (Life Technologies) for 5 days. Hepatic maturation was continued for 9 days in L-15 (ATCC) media containing hepatic growth factor (R&D Inc., Minneapolis, MN), oncostatin M (R&D Inc.) and 10% FBS (Life technologies).

5.5.3 Total RNA isolation, cDNA synthesis and qRT-PCR reactions

Four biological replicates of untreated and RA-differentiated NCCIT cell samples were harvested after 9 and 20 days growth, flash frozen in liquid nitrogen and stored at -80˚C until use. For measurement of PG-related gene expression levels, RNA was isolated from cell lysates on day 20 of differentiation using the RNeasy Plus kit (Qiagen, Valencia, CA) and cDNA synthesis was performed using Superscript III First Strand Synthesis (Life Technologies) as previously described (Li et al. 2011). The qRT-PCR reactions, done in triplicate for each gene analyzed, cycling conditions and analysis of amplimer products were performed as described. Briefly, reactions contained 1.25 µl of diluted cDNA template (1:10), 1.25 µL of primer pair mix (125 µM final concentration) and 2.5 µl iQ SYBR Green Supermix (BioRad, Hercules, CA) added to 96-well microtiter plates. Primers for the control gene, β-actin (NM 001101), were included on each plate to control for run variation and to normalize individual gene expression. Primer pairs for GAG-related genes were designed within a single exon (Nairn et al. 2007; Nairn et al. 2008) and primer design validated previously using the standard curve method (Nairn et al. 2007; Pfaffl 2001).

5.5.4 Calculation of relative gene expression levels and statistical analysis

An average of the triplicate Ct values for each gene was determined and the standard deviation calculated. Samples were re-run if the standard deviation value was >0.5 Ct

units. The logarithmic average Ct value for the control gene and each tested gene was converted to a linear value by the equation 2^{-Ct}. Converted values were normalized to β-actin by dividing individual gene value by control gene value. Normalized values were scaled so that genes below the level of detection were given a value of 1×10^{-6}, and this value was used as the lower limit on histograms. A non-parametric Mann-Whitney test (GraphPad InStat3, v3.1) was used to determine statistically significant changes ($p<0.05$) in transcript abundance between undifferentiated and RA-treated samples. Fold change was calculated by dividing normalized values of tested genes in RA-treated cells by those in untreated control cells.

5.5.5 Protein isolation, quantification and immunoblotting

For total protein extraction, cells were lysed in Nonidet-P40 lysis buffer (Boston Bioproducts, Ashland, MA) on ice for 30 min in the presence of a cocktail of protease and phosphatase inhibitors (Thermo Fisher Scientific) which included AEBSF, aprotinin, bestatin, E-64, leupeptin, and pepstatin A. Protein concentration was determined using the BCA assay (23227, Pierce). Approximately 40 μg of total protein was loaded and separated on a precast 4-20% gradient polyacrylamide gel. After transfer to a PVDF membrane, proteins of interest were detected using relevant primary and HRP-conjugated secondary antibodies followed by chemiluminescent (Pierce, Super Signal West Pico ECL substrate) exposure on high performance chemiluminescence film (GE Healthcare, Little Chalfont, UK, Amersham Hyperfilm ECL). Primary antibodies used were anti-γ-tubulin (T3320, Sigma Aldrich), anti-decorin (H00001634-B01P, Abnova, Walnut, CA), anti-lumican (H00004060-D01P, Abnova), anti-serglycin (Abnova, H00005552-M03), anti-glypican 5 (sc-84278, Santa Cruz Biotechnology, Santa Cruz, CA), anti-Oct3/4 (611202, BD Biosciences, Franklin Lakes, NJ) and anti-nestin (611658, BD Biosciences).

5.5.6 Immunofluorescence

Cells were grown in Lab-Tek chamber slides. Media from cells was washed off and cells were fixed with 4% paraformaldehyde. Cells were blocked with DPBS-Triton 100-X solution supplemented with 5% Bovine Serum Albumin (BSA). They were incubated overnight at 4°C with primary antibody diluted in DPBS-Triton X-100 solution supplemented with 1% BSA. The following day, after several washes with DPBS, cells were incubated with secondary antibody (goat anti-mouse Alexa Fluor 488, goat anti-rabbit Alexa Fluor 647, A11001, A21244, Life Technologies) diluted in DPBS-Triton X-100 solution supplemented with 1% BSA at room temperature for 1 h. After several washes with DPBS, cells were stained with Hoechst 33342 for 5 min at room temperature. After several washes, slides were detached from chambers and incubated overnight with ProLong Gold antifade reagent and covered with a cover slip. The following day slides were sealed and analyzed with a Zeiss 510 Meta multiphoton confocal microscope. Primary antibodies used were anti-Oct3/4 (611202, BD Biosciences, Franklin Lakes, NJ), anti-Isl (AF1837, R&D Systems, Minneapolis, MN), anti-AFP (WH0000174M1-100g, Sigma-Aldrich), anti-albumin (sc-271605, Santa Cruz Biotechnology), anti-SSEA4 (MAB4304, Millipore, Billerica, MA), anti-HNF4α (sc-6556, Santa Cruz Biotechnology), anti-FOXA2 (AF2400, R&D Systems), and anti-HepPar1 (IR624, DAKO, Carpinteria, CA). Alexa Fluor 488 conjugated phalloidin stain was used for actin staining (Life Technologies, A12379).

5.5.7 Isolation and purification of total and cell surface associated GAGs

For total GAG recovery, H9, Isl-1 and early hepatocyte cells were harvested, washed in PBS three times, and centrifuged to pellet cells. Isolation and purification of GAGs was performed as previously described with some modifications (Li et al. 2011; Zhang et al. 2006). Specifically, cell pellets were resuspended in 1 ml water and subjected to proteolysis at 55°C in 2 mg/ml actinase E (Kaken Biochemicals, Tokyo, Japan) for 20 hours. After proteolysis, particulates were removed by using a 0.22 μm syringe-top filter. Peptides were removed from the samples using Microcon Centrifugal Filter Units YM-10 (10 k MWCO, 15 ml, Vivascience, Ridgewood, NJ). Samples were collected

from the top layer of the filtration membrane and lyophilized, then dissolved in 8 M urea containing 2% CHAPS (pH 8.3, Sigma-Aldrich). A Vivapure MINI Q H spin column was equilibratied with 200 µl of 8 M urea containing 2% CHAPS (pH 8.3). To remove any remaining proteins, the clarified, filtered samples were loaded onto and run through the Vivapure MINI Q H spin columns under centrifugal force (700 × g). The columns were then washed with 200 µl of 8 M urea containing 2% CHAPS at pH 8.3, followed by five washes with 200 µl of 200 mM NaCl. GAGs were released from the spin column by washing three times with 100 µl of 16% NaCl. GAGs were desalted with YM-10 spin columns. The GAGs were lyophilized and stored at room temperature for future use

5.5.8 Enzymatic depolymerization of GAGs for HS/HP analysis

Isolated GAG samples were incubated with chondroitin lyase ABC (10 m-units, Seikagaku Corporation, Tokyo, Japan) and chondroitin lyase ACII (5 m-units, Seikagaku Corporation) at 37°C for 10 h and the enzymatic products were recovered by centrifugal filtration as described above, but at 13,000 x g. CS/DS disaccharides that passed through the filter were freeze-dried for future analysis. GAGs remaining in the retentate were collected by reversing the filter and spinning at 13,000 x g, followed by incubation with 10 m-units of heparin lyases I, II, and III at 37°C for 10 h. The products were recovered by centrifugal filtration and the HS/HP disaccharides collected and freeze-dried for LC-MS analysis. Cloning, overexpression in *Escherichia coli*, and purification of the recombinant heparin lyase I (EC 4.2.2.7), heparin lyase II (no EC assigned), and heparin lyase III (EC 4.2.2.8) from *Flavobacterium heparinum* were all performed as previously described (Shaya et al. 2006; Yoshida et al. 2002).

5.5.9 LC-MS disaccharide composition analysis of HS/HP

LC-MS analyses were performed on an Agilent 1200 LC/MS instrument (Agilent Technologies, Inc. Wilmington, DE) equipped with a 6300 ion trap with two separate systems for the CS/DS disaccharide analysis and HS/HP disaccharide analysis. For HS/HP disaccharide analysis, eluent A was water/acetonitrile (85:15) v/v, and eluent B

was water/acetonitrile (35:65) v/v. Both eluents contained 12 mM tributylamine (TrBA) and 38 mM NH_4OAc with pH adjusted to 6.5 with acetic acid. The column temperature was maintained at 45°C. For disaccharide analysis, solution A was used for 10 min, followed by a linear gradient from 10 to 40 min of 0 to 50% (v/v) solution B at the flow rate of 100 μl/min. The electrospray interface was set in negative ionization mode with the skimmer potential and capillary exit of -40.0 V, with a temperature of 350°C to obtain maximum abundance of the ions in a full-scan spectra (350–1500 Da, 10 full scans/s). Nitrogen was used as a drying gas (8 l/min) and nebulizing gas (40 psi) (Yang et al. 2011).

Quantification analysis of HS/HP disaccharides was performed using calibration curves constructed by separation of increasing amounts of unsaturated HS/HP disaccharide standards (2, 5, 10, 15, 20, 30, 50, and 100 ng per disaccharide). Unsaturated disaccharide standards of HS/HP (0S: ΔUA-GlcNAc, NS: ΔUA-GlcNS, 6S: ΔUA-GlcNAc6S, 2S: ΔUA2S-GlcNAc, NS2S: ΔUA2S-GlcNS, NS6S: ΔUA-GlcNS6S, 2S6S: ΔUA2S-GlcNAc6S, TriS: ΔUA2S-GlcNS6S) were obtained from Iduron (Manchester, UK). Linearity was assessed based on the amount of disaccharide and peak intensity in MS. All analyses were performed in triplicate.

6. REFERENCES

Abdollahi, A., P. Hahnfeldt, C. Maercker, H. J. Grone, J. Debus, W. Ansorge, J. Folkman, L. Hlatky, and P. E. Huber. 2004. Endostatin's antiangiogenic signaling network. *Mol. Cell* 13 (5):649-63.

Abrink, M., M. Grujic, and G. Pejler. 2004. Serglycin is essential for maturation of mast cell secretory granule. *J. Biol. Chem.* 279 (39):40897-905.

Aguirre, A., and V. Gallo. 2004. Postnatal neurogenesis and gliogenesis in the olfactory bulb from NG2-expressing progenitors of the subventricular zone. *J. Neurosci.* 24 (46):10530-41.

Ahn, W. S., and M. R. Antoniewicz. 2011. Metabolic flux analysis of CHO cells at growth and non-growth phases using isotopic tracers and mass spectrometry. *Metab. Eng.* 13 (5):598-609.

Ahsan, A., W. Jeske, D. Hoppensteadt, J. C. Lormeau, H. Wolf, and J. Fareed. 1995. Molecular profiling and weight determination of heparins and depolymerized heparins. *J. Pharm. Sci.* 84 (6):724-7.

Aikawa, J., and J. D. Esko. 1999. Molecular cloning and expression of a third member of the heparan sulfate/heparin GlcNAc N-deacetylase/ N-sulfotransferase family. *J. Biol. Chem.* 274 (5):2690-5.

Aikawa, J., K. Grobe, M. Tsujimoto, and J. D. Esko. 2001. Multiple isozymes of heparan sulfate/heparin GlcNAc N-deacetylase/GlcN N-sulfotransferase. Structure and activity of the fourth member, NDST4. *J. Biol. Chem.* 276 (8):5876-82.

Alarcon, C., A. I. Zaromytidou, Q. Xi, S. Gao, J. Yu, S. Fujisawa, A. Barlas, A. N. Miller, K. Manova-Todorova, M. J. Macias, G. Sapkota, D. Pan, and J. Massague. 2009. Nuclear CDKs drive Smad transcriptional activation and turnover in BMP and TGF-beta pathways. *Cell* 139 (4):757-69.

Aldor, I. S., and J. D. Keasling. 2003. Process design for microbial plastic factories: metabolic engineering of polyhydroxyalkanoates. *Curr. Opin. Biotechnol.* 14 (5):475-83.

Alper, H., C. Fischer, E. Nevoigt, and G. Stephanopoulos. 2005. Tuning genetic control through promoter engineering. *Proc. Natl. Acad. Sci. USA* 102 (36):12678-83.

Amit, M., M. K. Carpenter, M. S. Inokuma, C. P. Chiu, C. P. Harris, M. A. Waknitz, J. Itskovitz-Eldor, and J. A. Thomson. 2000. Clonally derived human embryonic stem cell lines maintain pluripotency and proliferative potential for prolonged periods of culture. *Dev. Biol.* 227 (2):271-8.

Anderson, D. J. 1997. Cellular and molecular biology of neural crest cell lineage determination. *Trends Genet.* 13 (7):276-80.

Andrews, P. W., M. M. Matin, A. R. Bahrami, I. Damjanov, P. Gokhale, and J. S. Draper. 2005. Embryonic stem (ES) cells and embryonal carcinoma (EC) cells: opposite sides of the same coin. *Biochem. Soc. Trans.* 33 (Pt 6):1526-30.

Angelastro, J. M., T. N. Ignatova, V. G. Kukekov, D. A. Steindler, G. B. Stengren, C. Mendelsohn, and L. A. Greene. 2003. Regulated expression of ATF5 is required for the progression of neural progenitor cells to neurons. *J. Neurosci.* 23 (11):4590-600.

Angelastro, J. M., J. L. Mason, T. N. Ignatova, V. G. Kukekov, G. B. Stengren, J. E. Goldman, and L. A. Greene. 2005. Downregulation of activating transcription factor 5 is required for differentiation of neural progenitor cells into astrocytes. *J. Neurosci.* 25 (15):3889-99.

Arai, F., A. Hirao, M. Ohmura, H. Sato, S. Matsuoka, K. Takubo, K. Ito, G. Y. Koh, and T. Suda. 2004. Tie2/angiopoietin-1 signaling regulates hematopoietic stem cell quiescence in the bone marrow niche. *Cell* 118 (2):149-61.

Avilion, A. A., S. K. Nicolis, L. H. Pevny, L. Perez, N. Vivian, and R. Lovell-Badge. 2003. Multipotent cell lineages in early mouse development depend on SOX2 function. *Genes Dev.* 17 (1):126-40.

Bai, X., and J. D. Esko. 1996. An animal cell mutant defective in heparan sulfate hexuronic acid 2-O-sulfation. *J. Biol. Chem.* 271 (30):17711-7.

Bai, X., G. Wei, A. Sinha, and J. D. Esko. 1999. Chinese hamster ovary cell mutants defective in glycosaminoglycan assembly and glucuronosyltransferase I. *J. Biol. Chem.* 274 (19):13017-24.

Baik, J. Y., L. Gasimli, B. Yang, P. Datta, F. Zhang, C. A. Glass, J. D. Esko, R. J. Linhardt, and S. T. Sharfstein. 2012. Metabolic engineering of Chinese hamster ovary cells: towards a bioengineered heparin. *Metab. Eng.*14 (2):81-90.

Balch, W. E., W. G. Dunphy, W. A. Braell, and J. E. Rothman. 1984. Reconstitution of the transport of protein between successive compartments of the Golgi measured by the coupled incorporation of N-acetylglucosamine. *Cell* 39 (2 Pt 1):405-16.

Baldwin, R. J., G. B. ten Dam, T. H. van Kuppevelt, G. Lacaud, J. T. Gallagher, V. Kouskoff, and C. L. Merry. 2008. A developmentally regulated heparan sulfate epitope defines a subpopulation with increased blood potential during mesodermal differentiation. *Stem Cells* 26 (12):3108-18.

Bame, K. J., and J. D. Esko. 1989. Undersulfated heparan sulfate in a Chinese hamster ovary cell mutant defective in heparan sulfate N-sulfotransferase. *J. Biol. Chem.* 264 (14):8059-65.

Bartlett, A. H., K. Hayashida, and P. W. Park. 2007. Molecular and cellular mechanisms of syndecans in tissue injury and inflammation. *Mol. Cells* 24 (2):153-66.

Beattie, G. M., A. D. Lopez, N. Bucay, A. Hinton, M. T. Firpo, C. C. King, and A. Hayek. 2005. Activin A maintains pluripotency of human embryonic stem cells in the absence of feeder layers. *Stem Cells* 23 (4):489-95.

Belachew, S., R. Chittajallu, A. A. Aguirre, X. Yuan, M. Kirby, S. Anderson, and V. Gallo. 2003. Postnatal NG2 proteoglycan-expressing progenitor cells are intrinsically multipotent and generate functional neurons. *J. Cell Biol.* 161 (1):169-86.

Bernabeu, C., J. M. Lopez-Novoa, and M. Quintanilla. 2009. The emerging role of TGF-beta superfamily coreceptors in cancer. *Biochim. Biophys. Acta* 1792 (10):954-73.

Bernfield, M., M. Gotte, P. W. Park, O. Reizes, M. L. Fitzgerald, J. Lincecum, and M. Zako. 1999. Functions of cell surface heparan sulfate proteoglycans. *Annu. Rev. Biochem.* 68:729-77.

Bezakova, G., and M. A. Ruegg. 2003. New insights into the roles of agrin. *Nat. Rev. Mol. Cell Biol.* 4 (4):295-308.

Bi, Y., C. H. Stuelten, T. Kilts, S. Wadhwa, R. V. Iozzo, P. G. Robey, X. D. Chen, and M. F. Young. 2005. Extracellular matrix proteoglycans control the fate of bone marrow stromal cells. *J. Biol. Chem.* 280 (34):30481-9.

Billett, H. H., B. A. Scorziello, E. R. Giannattasio, and H. W. Cohen. 2010. Low molecular weight heparin bridging for atrial fibrillation: is VTE thromboprophylaxis the major benefit? *J. Thromb. Thrombolys* 30 (4):479-85.

Bishop, J. R., M. Schuksz, and J. D. Esko. 2007. Heparan sulphate proteoglycans fine-tune mammalian physiology. *Nature* 446 (7139):1030-7.

Boyer, L. A., T. I. Lee, M. F. Cole, S. E. Johnstone, S. S. Levine, J. P. Zucker, M. G. Guenther, R. M. Kumar, H. L. Murray, R. G. Jenner, D. K. Gifford, D. A. Melton, R. Jaenisch, and R. A. Young. 2005. Core transcriptional regulatory circuitry in human embryonic stem cells. *Cell* 122 (6):947-56.

Brickman, Y. G., M. D. Ford, D. H. Small, P. F. Bartlett, and V. Nurcombe. 1995. Heparan sulfates mediate the binding of basic fibroblast growth factor to a specific receptor on neural precursor cells. *J. Biol. Chem.* 270 (42):24941-8.

Bronner-Fraser, M. 1987. Perturbation of cranial neural crest migration by the HNK-1 antibody. *Dev. Biol.* 123 (2):321-31.

Brown, J. J., and V. E. Papaioannou. 1993. Ontogeny of hyaluronan secretion during early mouse development. *Development* 117 (2):483-92.

Brown, S., A. Teo, S. Pauklin, N. Hannan, C. H. Cho, B. Lim, L. Vardy, N. R. Dunn, M. Trotter, R. Pedersen, and L. Vallier. 2011. Activin/Nodal signaling controls divergent transcriptional networks in human embryonic stem cells and in endoderm progenitors. *Stem Cells* 29 (8):1176-85.

Brunetti, A., and I. D. Goldfine. 1990. Role of myogenin in myoblast differentiation and its regulation by fibroblast growth factor. *J. Biol. Chem.* 265 (11):5960-3.

Bu, L., X. Jiang, S. Martin-Puig, L. Caron, S. Zhu, Y. Shao, D. J. Roberts, P. L. Huang, I. J. Domian, and K. R. Chien. 2009. Human ISL1 heart progenitors generate diverse multipotent cardiovascular cell lineages. *Nature* 460 (7251):113-7.

Capela, A., and S. Temple. 2006. LeX is expressed by principle progenitor cells in the embryonic nervous system, is secreted into their environment and binds Wnt-1. *Dev. Biol.* 291 (2):300-13.

Capila, I., and R. J. Linhardt. 2002. Heparin-protein interactions. *Angew. Chem. Int. Ed. Engl.* 41 (3):391-412.

Capurro, M. I., W. Shi, S. Sandal, and J. Filmus. 2005. Processing by convertases is not required for glypican-3-induced stimulation of hepatocellular carcinoma growth. *J. Biol. Chem.* 280 (50):41201-6.

Capurro, M. I., Y. Y. Xiang, C. Lobe, and J. Filmus. 2005. Glypican-3 promotes the growth of hepatocellular carcinoma by stimulating canonical Wnt signaling. *Cancer Res.* 65 (14):6245-54.

Capurro, M. I., P. Xu, W. Shi, F. Li, A. Jia, and J. Filmus. 2008. Glypican-3 inhibits Hedgehog signaling during development by competing with patched for Hedgehog binding. *Dev. Cell* 14 (5):700-11.

Carlsson, P., and L. Kjellen. 2012. Heparin biosynthesis. *Handb. Exp. Pharmacol.* (207):23-41.

Cartwright, P., C. McLean, A. Sheppard, D. Rivett, K. Jones, and S. Dalton. 2005. LIF/STAT3 controls ES cell self-renewal and pluripotency by a Myc-dependent mechanism. *Development* 132 (5):885-96.

Casu, B. 1985. Structure and biological activity of heparin. *Adv. Carbohydr. Chem. Biochem.* 43:51-134.

Chen, J., F. Y. Avci, E. M. Munoz, L. M. McDowell, M. Chen, L. C. Pedersen, L. Zhang, R. J. Linhardt, and J. Liu. 2005. Enzymatic redesigning of biologically active heparan sulfate. *J. Biol. Chem.* 280 (52):42817-25.

Chen, X., V. B. Vega, and H. H. Ng. 2008. Transcriptional regulatory networks in embryonic stem cells. *Cold Spring Harb. Symp. Quant. Biol.* 73:203-9.

Chen, X., H. Xu, P. Yuan, F. Fang, M. Huss, V. B. Vega, E. Wong, Y. L. Orlov, W. Zhang, J. Jiang, Y. H. Loh, H. C. Yeo, Z. X. Yeo, V. Narang, K. R. Govindarajan, B. Leong, A. Shahab, Y. Ruan, G. Bourque, W. K. Sung, N. D. Clarke, C. L. Wei, and H. H. Ng. 2008. Integration of external signaling pathways with the core transcriptional network in embryonic stem cells. *Cell* 133 (6):1106-17.

Choi, S., E. Lee, S. Kwon, H. Park, J. Y. Yi, S. Kim, I. O. Han, Y. Yun, and E. S. Oh. 2005. Transmembrane domain-induced oligomerization is crucial for the functions of syndecan-2 and syndecan-4. *J. Biol. Chem.* 280 (52):42573-9.

Cole, M. F., S. E. Johnstone, J. J. Newman, M. H. Kagey, and R. A. Young. 2008. Tcf3 is an integral component of the core regulatory circuitry of embryonic stem cells. *Genes Dev.* 22 (6):746-55.

Cornelison, D. D., S. A. Wilcox-Adelman, P. F. Goetinck, H. Rauvala, A. C. Rapraeger, and B. B. Olwin. 2004. Essential and separable roles for Syndecan-3 and Syndecan-4 in skeletal muscle development and regeneration. *Genes Dev.* 18 (18):2231-6.

Cornuet, P. K., T. C. Blochberger, and J. R. Hassell. 1994. Molecular polymorphism of lumican during corneal development. *Invest. Ophthalmol Visual Sci.* 35 (3):870-7.

Couchman, J. R. 2010. Transmembrane signaling proteoglycans. *Annu. Rev. Cell Dev. Biol.* 26:89-114.

Dahlstrand, J., L. B. Zimmerman, R. D. McKay, and U. Lendahl. 1992. Characterization of the human nestin gene reveals a close evolutionary relationship to neurofilaments. *J. Cell Sci.* 103 (Pt 2):589-97.

Damjanov, I. 1990. Teratocarcinoma stem cells. *Cancer Surv.* 9 (2):303-19.

Damjanov, I., B. Horvat, and Z. Gibas. 1993. Retinoic acid-induced differentiation of the developmentally pluripotent human germ cell tumor-derived cell line, NCCIT. *Lab. Invest.* 68 (2):220-32.

Danielsson, A., E. Raub, U. Lindahl, and I. Bjork. 1986. Role of ternary complexes, in which heparin binds both antithrombin and proteinase, in the acceleration of the reactions between antithrombin and thrombin or factor Xa. *J. Biol. Chem.* 261 (33):15467-73.

Davies, J. A., C. E. Fisher, and M. W. Barnett. 2001. Glycosaminoglycans in the study of mammalian organ development. *Biochem. Soc. Trans.* 29 (Pt 2):166-71.

Deakin, J. A., and M. Lyon. 1999. Differential regulation of hepatocyte growth factor/scatter factor by cell surface proteoglycans and free glycosaminoglycan chains. *J. Cell Sci.* 112 (Pt 12):1999-2009.

Dejosez, M., S. S. Levine, G. M. Frampton, W. A. Whyte, S. A. Stratton, M. C. Barton, P. H. Gunaratne, R. A. Young, and T. P. Zwaka. 2010. Ronin/Hcf-1 binds to a hyperconserved enhancer element and regulates genes involved in the growth of embryonic stem cells. *Genes Dev.* 24 (14):1479-84.

Dews, I. C., and K. R. Mackenzie. 2007. Transmembrane domains of the syndecan family of growth factor coreceptors display a hierarchy of homotypic and heterotypic interactions. *Proc. Natl. Acad. Sci. USA* 104 (52):20782-7.

Dolhnikoff, M., J. Morin, P. J. Roughley, and M. S. Ludwig. 1998. Expression of lumican in human lungs. *Am. J. Respir. Cell Mol. Biol.* 19 (4):582-7.

Domowicz, M., H. Li, A. Hennig, J. Henry, B. M. Vertel, and N. B. Schwartz. 1995. The biochemically and immunologically distinct CSPG of notochord is a product of the aggrecan gene. *Dev. Biol.* 171 (2):655-64.

Doty, D. B., H. W. Knott, J. L. Hoyt, and J. A. Koepke. 1979. Heparin dose for accurate anticoagulation in cardiac surgery. *J. Cardiovasc. Surg.* 20 (6):597-604.

Droguett, R., C. Cabello-Verrugio, C. Riquelme, and E. Brandan. 2006. Extracellular proteoglycans modify TGF-beta bio-availability attenuating its signaling during skeletal muscle differentiation. *Matrix Biol.* 25 (6):332-41.

Duncan, M. B., J. Chen, J. P. Krise, and J. Liu. 2004. The biosynthesis of anticoagulant heparan sulfate by the heparan sulfate 3-O-sulfotransferase isoform 5. *Biochim. Biophys. Acta* 1671 (1-3):34-43.

Dunn, M. P., and A. Di Gregorio. 2009. The evolutionarily conserved leprecan gene: its regulation by Brachyury and its role in the developing Ciona notochord. *Dev. Biol.* 328 (2):561-74.

Eberhardt, M., P. Salmon, M. A. von Mach, J. G. Hengstler, M. Brulport, P. Linscheid, D. Seboek, J. Oberholzer, A. Barbero, I. Martin, B. Muller, D. Trono, and H. Zulewski. 2006. Multipotential nestin and Isl-1 positive mesenchymal stem cells isolated from human pancreatic islets. *Biochem. Biophys. Res. Commun.* 345 (3):1167-76.

Esko, J. D. 1991. Genetic analysis of proteoglycan structure, function and metabolism. *Curr. Opin. Cell Biol.* 3 (5):805-16.

Esko, J. D., K. Kimata, and U. Lindahl. 2009. Proteoglycans and sulfated glycosaminoglycans. In *Essentials of Glycobiology*, 2nd ed., edited by A. Varki, R. D. Cummings, J. D. Esko, H. H. Freeze, P. Stanley, C. R. Bertozzi, G. W. Hart and M. E. Etzler. Cold Spring Harbor (NY):229-48.

Esko, J. D., and S. B. Selleck. 2002. Order out of chaos: assembly of ligand binding sites in heparan sulfate. *Annu. Rev. Biochem.* 71:435-71.

Faissner, A., A. Clement, A. Lochter, A. Streit, C. Mandl, and M. Schachner. 1994. Isolation of a neural chondroitin sulfate proteoglycan with neurite outgrowth promoting properties. *J. Cell Biol.* 126 (3):783-99.

Fan, Z., M. van de Rijn, K. Montgomery, and R. V. Rouse. 2003. Hep par 1 antibody stain for the differential diagnosis of hepatocellular carcinoma: 676 tumors tested using tissue microarrays and conventional tissue sections. *Mod. Pathol.* 16 (2):137-44.

Feldman, N., A. Gerson, J. Fang, E. Li, Y. Zhang, Y. Shinkai, H. Cedar, and Y. Bergman. 2006. G9a-mediated irreversible epigenetic inactivation of Oct-3/4 during early embryogenesis. *Nat. Cell Biol.* 8 (2):188-94.

Fernandes, T. G., S. J. Kwon, S. S. Bale, M. Y. Lee, M. M. Diogo, D. S. Clark, J. M. Cabral, and J. S. Dordick. 2010. Three-dimensional cell culture microarray for high-throughput studies of stem cell fate. *Biotechnol. Bioeng.* 106 (1):106-18.

Feyerabend, T. B., J. P. Li, U. Lindahl, and H. R. Rodewald. 2006. Heparan sulfate C5-epimerase is essential for heparin biosynthesis in mast cells. *Nat. Chem. Bio.* 2 (4):195-6.

Filmus, J. 2001. Glypicans in growth control and cancer. *Glycobiology* 11 (3):19R-23R.

Filmus, J., M. Capurro, and J. Rast. 2008. Glypicans. *Genome Biol.* 9 (5):224.

Ford-Perriss, M., K. Turner, S. Guimond, A. Apedaile, H. D. Haubeck, J. Turnbull, and M. Murphy. 2003. Localisation of specific heparan sulfate proteoglycans during the proliferative phase of brain development. *Dev. Dyn.* 227 (2):170-84.

Forsberg, E., G. Pejler, M. Ringvall, C. Lunderius, B. Tomasini-Johansson, M. Kusche-Gullberg, I. Eriksson, J. Ledin, L. Hellman, and L. Kjellen. 1999. Abnormal mast cells in mice deficient in a heparin-synthesizing enzyme. *Nature* 400 (6746):773-6.

Fransson, L. A. 2003. Glypicans. *Int. J. Biochem. Cell Biol.* 35 (2):125-9.

Fryer, C. J., J. B. White, and K. A. Jones. 2004. Mastermind recruits CycC:CDK8 to phosphorylate the Notch ICD and coordinate activation with turnover. *Mol. Cell* 16 (4):509-20.

Fuchs, E., T. Tumbar, and G. Guasch. 2004. Socializing with the neighbors: stem cells and their niche. *Cell* 116 (6):769-78.

Fuller, M. T., and A. C. Spradling. 2007. Male and female Drosophila germline stem cells: two versions of immortality. *Science* 316 (5823):402-4.

Funderburgh, J. L. 2002. Keratan sulfate biosynthesis. *IUBMB life* 54 (4):187-94.

Funderburgh, J. L., B. Caterson, and G. W. Conrad. 1986. Keratan sulfate proteoglycan during embryonic development of the chicken cornea. *Dev. Biol.* 116 (2):267-77.

Fuster, M. M., and L. Wang. 2010. Endothelial heparan sulfate in angiogenesis. *Prog. Mol. Biol. Transl. Sci.* 93:179-212.

Garcion, E., A. Halilagic, A. Faissner, and C. ffrench-Constant. 2004. Generation of an environmental niche for neural stem cell development by the extracellular matrix molecule tenascin C. *Development* 131 (14):3423-32.

Gasimli, L., R. J. Linhardt, and J. S. Dordick. 2012. Proteoglycans in stem cells. *Biotechnol. Appl. Biochem.* 59 (2):65-76.

Gasimli, L., H. E. Stansfield, A. V. Nairn, H. Liu, J. L. Paluh, B. Yang, J. S. Dordick, K. W. Moremen, and R. J. Linhardt. 2012. Structural remodeling of proteoglycans upon retinoic acid-induced differentiation of NCCIT cells. *Glycoconj. J.* Oct 2.

Godavarti, R., M. Davis, G. Venkataraman, C. Cooney, R. Langer, and R. Sasisekharan. 1996. Heparinase III from Flavobacterium heparinum: cloning and recombinant expression in Escherichia coli. *Biochem. Biophys. Res. Commun.* 225 (3):751-8.

Goh, J. S., P. Zhang, K. F. Chan, M. M. Lee, S. F. Lim, and Z. Song. 2010. RCA-I-resistant CHO mutant cells have dysfunctional GnT I and expression of normal GnT I in these mutants enhances sialylation of recombinant erythropoietin. *Metab. Eng.* 12 (4):360-8.

Gohring, W., T. Sasaki, C. H. Heldin, and R. Timpl. 1998. Mapping of the binding of platelet-derived growth factor to distinct domains of the basement membrane proteins BM-40 and perlecan and distinction from the BM-40 collagen-binding epitope. *Eur. J. Biochem.* 255 (1):60-6.

Goretzki, L., M. A. Burg, K. A. Grako, and W. B. Stallcup. 1999. High-affinity binding of basic fibroblast growth factor and platelet-derived growth factor-AA to the core protein of the NG2 proteoglycan. *J. Biol. Chem.* 274 (24):16831-7.

Graham, R. A., T. C. Li, I. D. Cooke, and J. D. Aplin. 1994. Keratan sulphate as a secretory product of human endometrium: cyclic expression in normal women. *Hum. Reprod.* 9 (5):926-30.

Graham, V., J. Khudyakov, P. Ellis, and L. Pevny. 2003. SOX2 functions to maintain neural progenitor identity. *Neuron* 39 (5):749-65.

Green, E. M. 2011. Fermentative production of butanol--the industrial perspective. *Curr. Opin. Biotechnol.* 22 (3):337-43.

Grobe, K., J. Ledin, M. Ringvall, K. Holmborn, E. Forsberg, J. D. Esko, and L. Kjellen. 2002. Heparan sulfate and development: differential roles of the N-acetylglucosamine N-deacetylase/N-sulfotransferase isozymes. *Biochim. Biophys. Acta* 1573 (3):209-15.

Groffen, A. J., M. A. Ruegg, H. Dijkman, T. J. van de Velden, C. A. Buskens, J. van den Born, K. J. Assmann, L. A. Monnens, J. H. Veerkamp, and L. P. van den Heuvel. 1998. Agrin is a major heparan sulfate proteoglycan in the human glomerular basement membrane. *J. Histochem. Cytochem.* 46 (1):19-27.

Guerrini, M., D. Beccati, Z. Shriver, A. Naggi, K. Viswanathan, A. Bisio, I. Capila, J. C. Lansing, S. Guglieri, B. Fraser, A. Al-Hakim, N. S. Gunay, Z. Zhang, L. Robinson, L. Buhse, M. Nasr, J. Woodcock, R. Langer, G. Venkataraman, R. J. Linhardt, B. Casu, G. Torri, and R. Sasisekharan. 2008. Oversulfated chondroitin sulfate is a contaminant in heparin associated with adverse clinical events. *Nat. Biotechnol.* 26 (6):669-75.

Gustafson, G. T., and E. Pihl. 1967. Staining of mast cell acid glycosaminoglycans in ultrathin sections by ruthenium red. *Nature* 216 (5116):697-8.

Hacker, U., K. Nybakken, and N. Perrimon. 2005. Heparan sulphate proteoglycans: the sweet side of development. *Nat. Rev. Mol. Cell Biol.* 6 (7):530-41.

Hagihara, K., K. Watanabe, J. Chun, and Y. Yamaguchi. 2000. Glypican-4 is an FGF2-binding heparan sulfate proteoglycan expressed in neural precursor cells. *Dev. Dyn.* 219 (3):353-67.

Hanemann, C. O., G. Kuhn, A. Lie, C. Gillen, F. Bosse, P. Spreyer, and H. W. Muller. 1993. Expression of decorin mRNA in the nervous system of rat. *J. Histochem. Cytochem.* 41 (9):1383-91.

Hay, D. C., J. Fletcher, C. Payne, J. D. Terrace, R. C. Gallagher, J. Snoeys, J. R. Black, D. Wojtacha, K. Samuel, Z. Hannoun, A. Pryde, C. Filippi, I. S. Currie, S. J. Forbes, J. A. Ross, P. N. Newsome, and J. P. Iredale. 2008. Highly efficient differentiation of hESCs to functional hepatic endoderm requires ActivinA and Wnt3a signaling. *Proc. Natl. Acad. Sci. USA* 105 (34):12301-6.

Hay, D. C., D. Zhao, J. Fletcher, Z. A. Hewitt, D. McLean, A. Urruticoechea-Uriguen, J. R. Black, C. Elcombe, J. A. Ross, R. Wolf, and W. Cui. 2008. Efficient

differentiation of hepatocytes from human embryonic stem cells exhibiting markers recapitulating liver development in vivo. *Stem Cells* 26 (4):894-902.

Hayhurst, G. P., Y. H. Lee, G. Lambert, J. M. Ward, and F. J. Gonzalez. 2001. Hepatocyte nuclear factor 4alpha (nuclear receptor 2A1) is essential for maintenance of hepatic gene expression and lipid homeostasis. *Mol. Cell Biol.* 21 (4):1393-403.

He, L., J. M. Thomson, M. T. Hemann, E. Hernando-Monge, D. Mu, S. Goodson, S. Powers, C. Cordon-Cardo, S. W. Lowe, G. J. Hannon, and S. M. Hammond. 2005. A microRNA polycistron as a potential human oncogene. *Nature* 435 (7043):828-33.

He, S., D. Nakada, and S. J. Morrison. 2009. Mechanisms of stem cell self-renewal. *Annu. Rev. Cell Dev. Biol.* 25:377-406.

Hermanson, O., K. Jepsen, and M. G. Rosenfeld. 2002. N-CoR controls differentiation of neural stem cells into astrocytes. *Nature* 419 (6910):934-9.

Hirano, K., N. Sasaki, T. Ichimiya, T. Miura, T. H. Van Kuppevelt, and S. Nishihara. 2012. 3-O-sulfated heparan sulfate recognized by the antibody HS4C3 contribute to the differentiation of mouse embryonic stem cells via Fas signaling. *PloS one* 7 (8):e43440.

Hirano, K., T. H. Van Kuppevelt, and S. Nishihara. 2013. The transition of mouse pluripotent stem cells from the naive to the primed state requires Fas signaling through 3-O sulfated heparan sulfate structures recognized by the HS4C3 antibody. *Biochem. Biophys. Res. Commun.* 430 (3):1175-81.

Horowitz, A., M. Murakami, Y. Gao, and M. Simons. 1999. Phosphatidylinositol-4,5-bisphosphate mediates the interaction of syndecan-4 with protein kinase C. *Biochemistry* 38 (48):15871-7.

Humphries, D. E., G. W. Wong, D. S. Friend, M. F. Gurish, W. T. Qiu, C. Huang, A. H. Sharpe, and R. L. Stevens. 1999. Heparin is essential for the storage of specific granule proteases in mast cells. *Nature* 400 (6746):769-72.

Ibrahimi, O. A., F. Zhang, S. C. Hrstka, M. Mohammadi, and R. J. Linhardt. 2004. Kinetic model for FGF, FGFR, and proteoglycan signal transduction complex assembly. *Biochemistry* 43 (16):4724-30.

Ida, M., T. Shuo, K. Hirano, Y. Tokita, K. Nakanishi, F. Matsui, S. Aono, H. Fujita, Y. Fujiwara, T. Kaji, and A. Oohira. 2006. Identification and functions of chondroitin sulfate in the milieu of neural stem cells. *J. Biol. Chem.* 281 (9):5982-91.

Inatani, M., F. Irie, A. S. Plump, M. Tessier-Lavigne, and Y. Yamaguchi. 2003. Mammalian brain morphogenesis and midline axon guidance require heparan sulfate. *Science* 302 (5647):1044-6.

Iozzo, R. V. 1998. Matrix proteoglycans: from molecular design to cellular function. *Annu. Rev. Biochem.* 67:609-52.

Repeated Author. 2005. Basement membrane proteoglycans: from cellar to ceiling. *Nat. Rev. Mol. Cell Biol.* 6 (8):646-56.

Iozzo, R. V., and J. D. San Antonio. 2001. Heparan sulfate proteoglycans: heavy hitters in the angiogenesis arena. *J. Clin. Invest.* 108 (3):349-55.

Jackson, M., A. Krassowska, N. Gilbert, T. Chevassut, L. Forrester, J. Ansell, and B. Ramsahoye. 2004. Severe global DNA hypomethylation blocks differentiation

and induces histone hyperacetylation in embryonic stem cells. *Mol. Cell Biol.* 24 (20):8862-71.

James, D., A. J. Levine, D. Besser, and A. Hemmati-Brivanlou. 2005. TGFbeta/activin/nodal signaling is necessary for the maintenance of pluripotency in human embryonic stem cells. *Development* 132 (6):1273-82.

Johnson, C. E., B. E. Crawford, M. Stavridis, G. Ten Dam, A. L. Wat, G. Rushton, C. M. Ward, V. Wilson, T. H. van Kuppevelt, J. D. Esko, A. Smith, J. T. Gallagher, and C. L. Merry. 2007. Essential alterations of heparan sulfate during the differentiation of embryonic stem cells to Sox1-enhanced green fluorescent protein-expressing neural progenitor cells. *Stem Cells* 25 (8):1913-23.

Jones, J. M., and J. A. Thomson. 2000. Human embryonic stem cell technology. *Semin. Reprod. Med.* 18 (2):219-23.

Kabos, P., H. Matundan, M. Zandian, C. Bertolotto, M. L. Robinson, B. E. Davy, J. S. Yu, and R. C. Krueger, Jr. 2004. Neural precursors express multiple chondroitin sulfate proteoglycans, including the lectican family. *Biochem. Biophys. Res. Commun.* 318 (4):955-63.

Kadoya, K., J. Fukushi, Y. Matsumoto, Y. Yamaguchi, and W. B. Stallcup. 2008. NG2 proteoglycan expression in mouse skin: altered postnatal skin development in the NG2 null mouse. *J. Histochem. Cytochem.* 56 (3):295-303.

Kagey, M. H., J. J. Newman, S. Bilodeau, Y. Zhan, D. A. Orlando, N. L. van Berkum, C. C. Ebmeier, J. Goossens, P. B. Rahl, S. S. Levine, D. J. Taatjes, J. Dekker, and R. A. Young. 2010. Mediator and cohesin connect gene expression and chromatin architecture. *Nature* 467 (7314):430-5.

Kanhere, A., K. Viiri, C. C. Araujo, J. Rasaiyaah, R. D. Bouwman, W. A. Whyte, C. F. Pereira, E. Brookes, K. Walker, G. W. Bell, A. Pombo, A. G. Fisher, R. A. Young, and R. G. Jenner. 2010. Short RNAs are transcribed from repressed polycomb target genes and interact with polycomb repressive complex-2. *Mol. Cell* 38 (5):675-88.

Kehat, I., D. Kenyagin-Karsenti, M. Snir, H. Segev, M. Amit, A. Gepstein, E. Livne, O. Binah, J. Itskovitz-Eldor, and L. Gepstein. 2001. Human embryonic stem cells can differentiate into myocytes with structural and functional properties of cardiomyocytes. *J. Clin. Invest.* 108 (3):407-14.

Kiel, M. J., and S. J. Morrison. 2008. Uncertainty in the niches that maintain haematopoietic stem cells. *Nat. Rev. Immunol.* 8 (4):290-301.

Kiger, A. A., D. L. Jones, C. Schulz, M. B. Rogers, and M. T. Fuller. 2001. Stem cell self-renewal specified by JAK-STAT activation in response to a support cell cue. *Science* 294 (5551):2542-5.

Kim, J., J. Chu, X. Shen, J. Wang, and S. H. Orkin. 2008. An extended transcriptional network for pluripotency of embryonic stem cells. *Cell* 132 (6):1049-61.

Kimble, J., and S. L. Crittenden. 2007. Controls of germline stem cells, entry into meiosis, and the sperm/oocyte decision in Caenorhabditis elegans. *Annu. Rev. Cell Dev. Biol.* 23:405-33.

Kitagawa, H., A. Kinoshita, and K. Sugahara. 1995. Microanalysis of glycosaminoglycan-derived disaccharides labeled with the fluorophore 2-aminoacridone by capillary electrophoresis and high-performance liquid chromatography. *Anal. Biochem.* 232 (1):114-21.

Kjellen, L., and U. Lindahl. 1991. Proteoglycans: structures and interactions. *Annu. Rev. Biochem.* 60:443-75.

Klausner, R. D., J. G. Donaldson, and J. Lippincott-Schwartz. 1992. Brefeldin A: insights into the control of membrane traffic and organelle structure. *J. Cell Biol.* 116 (5):1071-80.

Klein, G., S. Beck, and C. A. Muller. 1993. Tenascin is a cytoadhesive extracellular matrix component of the human hematopoietic microenvironment. *J. Cell Biol.* 123 (4):1027-35.

Knox, S., C. Merry, S. Stringer, J. Melrose, and J. Whitelock. 2002. Not all perlecans are created equal: interactions with fibroblast growth factor (FGF) 2 and FGF receptors. *J. Biol. Chem.* 277 (17):14657-65.

Kobayashi, S., K. Morimoto, T. Shimizu, M. Takahashi, H. Kurosawa, and T. Shirasawa. 2000. Association of EXT1 and EXT2, hereditary multiple exostoses gene products, in Golgi apparatus. *Biochem. Biophys. Res. Commun.* 268 (3):860-7.

Kollet, O., A. Dar, S. Shivtiel, A. Kalinkovich, K. Lapid, Y. Sztainberg, M. Tesio, R. M. Samstein, P. Goichberg, A. Spiegel, A. Elson, and T. Lapidot. 2006. Osteoclasts degrade endosteal components and promote mobilization of hematopoietic progenitor cells. *Nat. Med.* 12 (6):657-64.

Kolset, S. O., K. Prydz, and G. Pejler. 2004. Intracellular proteoglycans. *Biochem. J* 379 (Pt 2):217-27.

Korbling, M., and Z. Estrov. 2003. Adult stem cells for tissue repair-a new therapeutic concept. *N. Engl. J. Med.* 349:570-82.

Kraushaar, D. C., Y. Yamaguchi, and L. Wang. 2010. Heparan sulfate is required for embryonic stem cells to exit from self-renewal. *J. Biol. Chem.* 285 (8):5907-16.

Kuberan, B., M. Z. Lech, D. L. Beeler, Z. L. Wu, and R. D. Rosenberg. 2003. Enzymatic synthesis of antithrombin III-binding heparan sulfate pentasaccharide. *Nat. Biotechnol.* 21 (11):1343-6.

Kumar, S., and G. Duester. 2010. Retinoic acid signaling in perioptic mesenchyme represses Wnt signaling via induction of Pitx2 and Dkk2. *Dev. Biol.* 340 (1):67-74.

Kunath, T., M. K. Saba-El-Leil, M. Almousailleakh, J. Wray, S. Meloche, and A. Smith. 2007. FGF stimulation of the Erk1/2 signalling cascade triggers transition of pluripotent embryonic stem cells from self-renewal to lineage commitment. *Development* 134 (16):2895-902.

Kuriyama, S., and R. Mayor. 2009. A role for Syndecan-4 in neural induction involving ERK- and PKC-dependent pathways. *Development* 136 (4):575-84.

Kusche-Gullberg, M., and L. Kjellen. 2003. Sulfotransferases in glycosaminoglycan biosynthesis. *Curr Opin. Struct. Biol.* 13 (5):605-11.

Lagasse E, Connors H, Al-Dhalimy M, Reitsma M, Dohse M, Osborne L, Wang X, Finegold M, Weissman IL, Grompe M. Purified hematopoietic stem cells can differentiate into hepatocytes in vivo. *Nat. Med. 2000* 6 (11):1229-34.

Lai, J. P., D. S. Sandhu, C. Yu, T. Han, C. D. Moser, K. K. Jackson, R. B. Guerrero, I. Aderca, H. Isomoto, M. M. Garrity-Park, H. Zou, A. M. Shire, D. M. Nagorney, S. O. Sanderson, A. A. Adjei, J. S. Lee, S. S. Thorgeirsson, and L. R. Roberts. 2008. Sulfatase 2 up-regulates glypican 3, promotes fibroblast growth factor

signaling, and decreases survival in hepatocellular carcinoma. *Hepatology* 47 (4):1211-22.

Lanctot, P. M., F. H. Gage, and A. P. Varki. 2007. The glycans of stem cells. *Curr Opin. Chem. Biol.* 11 (4):373-80.

Landeira, D., S. Sauer, R. Poot, M. Dvorkina, L. Mazzarella, H. F. Jorgensen, C. F. Pereira, M. Leleu, F. M. Piccolo, M. Spivakov, E. Brookes, A. Pombo, C. Fisher, W. C. Skarnes, T. Snoek, K. Bezstarosti, J. Demmers, R. J. Klose, M. Casanova, L. Tavares, N. Brockdorff, M. Merkenschlager, and A. G. Fisher. 2010. Jarid2 is a PRC2 component in embryonic stem cells required for multi-lineage differentiation and recruitment of PRC1 and RNA Polymerase II to developmental regulators. *Nat. Cell Biol.* 12 (6):618-24.

Lander, A. D., and S. B. Selleck. 2000. The elusive functions of proteoglycans: in vivo veritas. *J. Cell Biol.* 148 (2):227-32.

Langenecker, S. A., M. Felfernig, A. Werba, C. M. Mueller, A. Chiari, and M. Zimpfer. 1994. Anticoagulation with prostacyclin and heparin during continuous venovenous hemofiltration. *Crit. Care Med.* 22 (11):1774-81.

Lee, D. C., K. W. Chan, and S. Y. Chan. 2002. RET receptor tyrosine kinase isoforms in kidney function and disease. *Oncogene* 21 (36):5582-92.

Lemons, M. L., S. Barua, M. L. Abanto, W. Halfter, and M. L. Condic. 2005. Adaptation of sensory neurons to hyalectin and decorin proteoglycans. *J. Neurosci.* 25 (20):4964-73.

Li, B., H. Liu, Z. Zhang, H. E. Stansfield, J. S. Dordick, and R. J. Linhardt. 2011. Analysis of glycosaminoglycans in stem cell glycomics. *Methods Mol. Biol.* 690:285-300.

Lichner, Z., E. Pall, A. Kerekes, E. Pallinger, P. Maraghechi, Z. Bosze, and E. Gocza. 2011. The miR-290-295 cluster promotes pluripotency maintenance by regulating cell cycle phase distribution in mouse embryonic stem cells. *Differentiation* 81 (1):11-24.

Lidholt, K., I. Eriksson, and L. Kjellen. 1995. Heparin proteoglycans synthesized by mouse mastocytoma contain chondroitin sulphate. *Biochem. J.* 311 (Pt 1):233-8.

Ligon, K. L., S. Kesari, M. Kitada, T. Sun, H. A. Arnett, J. A. Alberta, D. J. Anderson, C. D. Stiles, and D. H. Rowitch. 2006. Development of NG2 neural progenitor cells requires Olig gene function. *Proc. Natl. Acad. Sci. USA* 103 (20):7853-8.

Linhardt, R. J. 2003. Heparin: structure and activity. *J. Med Chem.* 46 (13):2551-64.

Linhardt, R. J., J. S. Dordick, P. L. Deangelis, and J. Liu. 2007. Enzymatic synthesis of glycosaminoglycan heparin. *Semin. Thromb. Hemost.* 33 (5):453-65.

Linhardt, R. J., and T. Toida. 2004. Role of glycosaminoglycans in cellular communication. *Acc. Chem. Res.* 37 (7):431-8.

Loh, Y. H., W. Zhang, X. Chen, J. George, and H. H. Ng. 2007. Jmjd1a and Jmjd2c histone H3 Lys 9 demethylases regulate self-renewal in embryonic stem cells. *Genes. Dev.* 21 (20):2545-57.

Ly, M., T. N. Laremore, and R. J. Linhardt. 2010. Proteoglycomics: recent progress and future challenges. *OMICS* 14 (4):389-99.

Marcum, J. A., and R. D. Rosenberg. 1987. Anticoagulantly active heparan sulfate proteoglycan and the vascular endothelium. *Semin. Thromb. Hemost.* 13 (4):464-74.

Marson, A., S. S. Levine, M. F. Cole, G. M. Frampton, T. Brambrink, S. Johnstone, M. G. Guenther, W. K. Johnston, M. Wernig, J. Newman, J. M. Calabrese, L. M. Dennis, T. L. Volkert, S. Gupta, J. Love, N. Hannett, P. A. Sharp, D. P. Bartel, R. Jaenisch, and R. A. Young. 2008. Connecting microRNA genes to the core transcriptional regulatory circuitry of embryonic stem cells. *Cell* 134 (3):521-33.

Martin, J. G., M. Gupta, Y. Xu, S. Akella, J. Liu, J. S. Dordick, and R. J. Linhardt. 2009. Toward an artificial Golgi: redesigning the biological activities of heparan sulfate on a digital microfluidic chip. *J. Am. Chem. Soc.* 131 (31):11041-8.

Martin, V. J., D. J. Pitera, S. T. Withers, J. D. Newman, and J. D. Keasling. 2003. Engineering a mevalonate pathway in Escherichia coli for production of terpenoids. *Nat. Biotechnol.* 21 (7):796-802.

Martynova, M. G., O. A. Bystrova, O. M. Moiseeva, A. L. Evdonin, K. A. Kondratov, and N. D. Medvedeva. 2005. The presence of ANP in rat peritoneal mast cells. *Cell Res.* 15 (10):811-6.

Medine, C. N., B. Lucendo-Villarin, W. Zhou, C. C. West, and D. C. Hay. 2011. Robust generation of hepatocyte-like cells from human embryonic stem cell populations. *J. Visualized Exp.* (56):e2969.

Melton, C., R. L. Judson, and R. Blelloch. 2010. Opposing microRNA families regulate self-renewal in mouse embryonic stem cells. *Nature* 463 (7281):621-6.

Mezey, E., K. J. Chandross, G. Harta, R. A. Maki, and S. R. McKercher. 2000. Turning blood into brain: cells bearing neuronal antigens generated in vivo from bone marrow. *Science* 290 (5497):1779-82.

Michalodimitrakis, K., and M. Isalan. 2009. Engineering prokaryotic gene circuits. *FEMS Microbiol. Rev.* 33 (1):27-37.

Minor, K., X. Tang, G. Kahrilas, S. J. Archibald, J. E. Davies, and S. J. Davies. 2008. Decorin promotes robust axon growth on inhibitory CSPGs and myelin via a direct effect on neurons. *Neurobiol. Dis.* 32 (1):88-95.

Misumi, Y., K. Miki, A. Takatsuki, G. Tamura, and Y. Ikehara. 1986. Novel blockade by brefeldin A of intracellular transport of secretory proteins in cultured rat hepatocytes. *J. Biol. Chem.* 261 (24):11398-403.

Montgomery, R. I., K. Lidholt, N. W. Flay, J. Liang, B. Vertel, U. Lindahl, and J. D. Esko. 1992. Stable heparin-producing cell lines derived from the Furth murine mastocytoma. *Proc. Natl. Acad. Sci. USA* 89 (23):11327-31.

Morrison, S. J., and A. C. Spradling. 2008. Stem cells and niches: mechanisms that promote stem cell maintenance throughout life. *Cell* 132 (4):598-611.

Munesue, S., Y. Yoshitomi, Y. Kusano, Y. Koyama, A. Nishiyama, H. Nakanishi, K. Miyazaki, T. Ishimaru, S. Miyaura, M. Okayama, and K. Oguri. 2007. A novel function of syndecan-2, suppression of matrix metalloproteinase-2 activation, which causes suppression of metastasis. *J. Biol. Chem.* 282 (38):28164-74.

Muramatsu, T., and H. Muramatsu. 2004. Carbohydrate antigens expressed on stem cells and early embryonic cells. *Glycoconj. J.* 21 (1-2):41-5.

Muszbek, L., Z. Bereczky, B. Kovacs, and I. Komaromi. 2010. Antithrombin deficiency and its laboratory diagnosis. *Clin. Chem. Lab. Med.* 48 Suppl 1:S67-78.

Nagase, T., Y. Sanai, S. Nakamura, H. Asato, K. Harii, and N. Osumi. 2003. Roles of HNK-1 carbohydrate epitope and its synthetic glucuronyltransferase genes on migration of rat neural crest cells. *J. Anat.* 203 (1):77-88.

Nairn, A. V., A. Kinoshita-Toyoda, H. Toyoda, J. Xie, K. Harris, S. Dalton, M. Kulik, J. M. Pierce, T. Toida, K. W. Moremen, and R. J. Linhardt. 2007. Glycomics of proteoglycan biosynthesis in murine embryonic stem cell differentiation. *J. Proteome Res.* 6 (11):4374-87.

Nairn, A. V., W. S. York, K. Harris, E. M. Hall, J. M. Pierce, and K. W. Moremen. 2008. Regulation of glycan structures in animal tissues: transcript profiling of glycan-related genes. *J. Biol. Chem.* 283 (25):17298-313.

Nemeth, A., and P. Rohlich. 1980. Rapid separation of rat peritoneal mast cells with Percoll. *Eur. J. Cell Biol.* 20 (3):272-5.

Ng, H. H., and M. A. Surani. 2011. The transcriptional and signalling networks of pluripotency. *Nat. Cell Biol.* 13 (5):490-6.

Nishihara, S. 2011. The function of glycan structures for the maintenance and differentiation of embryonic stem cells. In *Embryonic Stem Cells: The Hormonal Regulation of Pluripotency and Embryogenesis*, edited by C. Atwood. InTech. (Rijeka, Croatia):6-124.

Nishiyama, A., K. J. Dahlin, and W. B. Stallcup. 1991. The expression of NG2 proteoglycan in the developing rat limb. *Development* 111 (4):933-44.

Nishiyama, A., Z. Yang, and A. Butt. 2005. Astrocytes and NG2-glia: what's in a name? *J. Anat*. 207 (6):687-93.

Niwa, H., T. Burdon, I. Chambers, and A. Smith. 1998. Self-renewal of pluripotent embryonic stem cells is mediated via activation of STAT3. *Genes Dev.* 12 (13):2048-60.

Nolan, R. P., and K. Lee. 2011. Dynamic model of CHO cell metabolism. *Metab. Eng.* 13 (1):108-24.

Noti, C., and P. H. Seeberger. 2005. Chemical approaches to define the structure-activity relationship of heparin-like glycosaminoglycans. *Chem. Biol.* 12 (7):731-56.

Ogren, S., and U. Lindahl. 1971. Degradation of heparin in mouse mastocytoma tissue. *Biochem. J.* 125 (4):1119-29.

Oh, E. S., A. Woods, S. T. Lim, A. W. Theibert, and J. R. Couchman. 1998. Syndecan-4 proteoglycan cytoplasmic domain and phosphatidylinositol 4,5-bisphosphate coordinately regulate protein kinase C activity. *J. Biol. Chem.* 273 (17):10624-9.

Oh, S. P., Y. Kamagata, Y. Muragaki, S. Timmons, A. Ooshima, and B. R. Olsen. 1994. Isolation and sequencing of cDNAs for proteins with multiple domains of Gly-Xaa-Yaa repeats identify a distinct family of collagenous proteins. *Proc. Natl. Acad. Sci. USA* 91 (10):4229-33.

Okita, K., and S. Yamanaka. 2006. Intracellular signaling pathways regulating pluripotency of embryonic stem cells. *Curr. Stem Cell Res. Ther.* 1 (1):103-11.

Olsson, L., M. Stigson, R. Perris, J. M. Sorrell, and J. Lofberg. 1996. Distribution of keratan sulphate and chondroitin sulphate in wild type and white mutant axolotl embryos during neural crest cell migration. *Pigm. Cell Res.* 9 (1):5-17.

Orkin, S. H., and L. I. Zon. 2008. Hematopoiesis: an evolving paradigm for stem cell biology. *Cell* 132 (4):631-44.

Packer, A. I., K. G. Mailutha, L. A. Ambrozewicz, and D. J. Wolgemuth. 2000. Regulation of the Hoxa4 and Hoxa5 genes in the embryonic mouse lung by retinoic acid and TGFbeta1: implications for lung development and patterning. *Dev. Dyn.* 217 (1):62-74.

Pan, J., Y. Qian, X. Zhou, A. Pazandak, S. B. Frazier, P. Weiser, H. Lu, and L. Zhang. 2010. Oversulfated chondroitin sulfate is not the sole contaminant in heparin. *Nat. Biotechnol.* 28 (3):203-7.

Park, Y., C. Rangel, M. M. Reynolds, M. C. Caldwell, M. Johns, M. Nayak, C. J. Welsh, S. McDermott, and S. Datta. 2003. Drosophila perlecan modulates FGF and hedgehog signals to activate neural stem cell division. *Dev Biol* 253 (2):247-57.

Pasini, D., P. A. Cloos, J. Walfridsson, L. Olsson, J. P. Bukowski, J. V. Johansen, M. Bak, N. Tommerup, J. Rappsilber, and K. Helin. 2010. JARID2 regulates binding of the Polycomb repressive complex 2 to target genes in ES cells. *Nature* 464 (7286):306-10.

Pejler, G., M. Abrink, and S. Wernersson. 2009. Serglycin proteoglycan: regulating the storage and activities of hematopoietic proteases. *Biofactors* 35 (1):61-8.

Pfaffl, M. W. 2001. A new mathematical model for relative quantification in real-time RT-PCR. *Nucleic Acids Res.* 29 (9):e45.

Pfeifer, B. A., S. J. Admiraal, H. Gramajo, D. E. Cane, and C. Khosla. 2001. Biosynthesis of complex polyketides in a metabolically engineered strain of E. coli. *Science* 291 (5509):1790-2.

Pierce, G. B. 1985. Carcinoma is to Embryology as Mutation is to Genetics. *Amer. Zool.* 25 (3):707-712.

Pinhal, M. A., B. Smith, S. Olson, J. Aikawa, K. Kimata, and J. D. Esko. 2001. Enzyme interactions in heparan sulfate biosynthesis: uronosyl 5-epimerase and 2-O-sulfotransferase interact in vivo. *Proc. Natl. Acad. Sci. USA* 98 (23):12984-9.

Pinti, M., L. Troiano, M. Nasi, R. Ferraresi, J. Dobrucki, and A. Cossarizza. 2003. Hepatoma HepG2 cells as a model for in vitro studies on mitochondrial toxicity of antiviral drugs: which correlation with the patient? *J. Biol. Regul. Homeostatic Agents* 17 (2):166-71.

Pisconti, A., D. D. Cornelison, H. C. Olguin, T. L. Antwine, and B. B. Olwin. 2010. Syndecan-3 and Notch cooperate in regulating adult myogenesis. *J. Cell Biol.* 190 (3):427-41.

Pitera, D. J., C. J. Paddon, J. D. Newman, and J. D. Keasling. 2007. Balancing a heterologous mevalonate pathway for improved isoprenoid production in Escherichia coli. *Metab. Eng.* 9 (2):193-207.

Ponta, H., L. Sherman, and P. A. Herrlich. 2003. CD44: from adhesion molecules to signalling regulators. *Nat. Rev. Mol. Cell Biol.* 4 (1):33-45.

Poulsom, R., M. R. Alison, S. J. Forbes, and N. A. Wright. 2002. Adult stem cell plasticity. *J. Pathol.* 197 (4):441-56.

Presto, J., M. Thuveson, P. Carlsson, M. Busse, M. Wilen, I. Eriksson, M. Kusche-Gullberg, and L. Kjellen. 2008. Heparan sulfate biosynthesis enzymes EXT1 and EXT2 affect NDST1 expression and heparan sulfate sulfation. *Proc. Natl. Acad. Sci. USA* 105 (12):4751-6.

Rahl, P. B., C. Y. Lin, A. C. Seila, R. A. Flynn, S. McCuine, C. B. Burge, P. A. Sharp, and R. A. Young. 2010. c-Myc regulates transcriptional pause release. *Cell* 141 (3):432-45.

Rathjen, P. D., J. Lake, L. M. Whyatt, M. D. Bettess, and J. Rathjen. 1998. Properties and uses of embryonic stem cells: prospects for application to human biology and gene therapy. *Reprod. Fertil. Dev.* 10 (1):31-47.

Robinson, H. C., A. A. Horner, M. Hook, S. Ogren, and U. Lindahl. 1978. A proteoglycan form of heparin and its degradation to single-chain molecules. *J. Biol. Chem.* 253 (19):6687-93.

Ryu, H. Y., J. Lee, S. Yang, H. Park, S. Choi, K. C. Jung, S. T. Lee, J. K. Seong, I. O. Han, and E. S. Oh. 2009. Syndecan-2 functions as a docking receptor for pro-matrix metalloproteinase-7 in human colon cancer cells. *J. Biol. Chem.* 284 (51):35692-701.

Sacchetti, B., A. Funari, S. Michienzi, S. Di Cesare, S. Piersanti, I. Saggio, E. Tagliafico, S. Ferrari, P. G. Robey, M. Riminucci, and P. Bianco. 2007. Self-renewing osteoprogenitors in bone marrow sinusoids can organize a hematopoietic microenvironment. *Cell* 131 (2):324-36.

Sato, N., L. Meijer, L. Skaltsounis, P. Greengard, and A. H. Brivanlou. 2004. Maintenance of pluripotency in human and mouse embryonic stem cells through activation of Wnt signaling by a pharmacological GSK-3-specific inhibitor. *Nat. Med.* 10 (1):55-63.

Saunders, S., S. Paine-Saunders, and A. D. Lander. 1997. Expression of the cell surface proteoglycan glypican-5 is developmentally regulated in kidney, limb, and brain. *Dev. Biol.* 190 (1):78-93.

Schaefer, L., and R. V. Iozzo. 2008. Biological functions of the small leucine-rich proteoglycans: from genetics to signal transduction. *J. Biol. Chem.* 283 (31):21305-9.

Schick, B. P., H. C. Ho, K. C. Brodbeck, C. W. Wrigley, and J. Klimas. 2003. Serglycin proteoglycan expression and synthesis in embryonic stem cells. *Biochim. Biophys. Acta* 1593 (2-3):259-67.

Schuldiner, M., R. Eiges, A. Eden, O. Yanuka, J. Itskovitz-Eldor, R. S. Goldstein, and N. Benvenisty. 2001. Induced neuronal differentiation of human embryonic stem cells. *Brain Res.* 913 (2):201-5.

Schwartz, N. B. 1975. Biosynthesis of chondroitin sulfate: immunoprecipitation of interacting xylosyltransferase and galactosyltransferase. *FEBS letters* 49 (3):342-5.

Schwarz, Q., and C. Ruhrberg. 2010. Neuropilin, you gotta let me know: should I stay or should I go? *Cell Adh. Migr.* 4 (1):61-6.

Shah, N. M., A. K. Groves, and D. J. Anderson. 1996. Alternative neural crest cell fates are instructively promoted by TGFbeta superfamily members. *Cell* 85 (3):331-43.

Shah, N. M., M. A. Marchionni, I. Isaacs, P. Stroobant, and D. J. Anderson. 1994. Glial growth factor restricts mammalian neural crest stem cells to a glial fate. *Cell* 77 (3):349-60.

Shaya, D., A. Tocilj, Y. Li, J. Myette, G. Venkataraman, R. Sasisekharan, and M. Cygler. 2006. Crystal structure of heparinase II from Pedobacter heparinus and its complex with a disaccharide product. *J. Biol. Chem.* 281 (22):15525-35.

Shen, X., W. Kim, Y. Fujiwara, M. D. Simon, Y. Liu, M. R. Mysliwiec, G. C. Yuan, Y. Lee, and S. H. Orkin. 2009. Jumonji modulates polycomb activity and self-renewal versus differentiation of stem cells. *Cell* 139 (7):1303-14.

Shi, Y., D. Chichung Lie, P. Taupin, K. Nakashima, J. Ray, R. T. Yu, F. H. Gage, and R. M. Evans. 2004. Expression and function of orphan nuclear receptor TLX in adult neural stem cells. *Nature* 427 (6969):78-83.

Shimo, T., C. Gentili, M. Iwamoto, C. Wu, E. Koyama, and M. Pacifici. 2004. Indian hedgehog and syndecans-3 coregulate chondrocyte proliferation and function during chick limb skeletogenesis. *Dev. Dyn.* 229 (3):607-17.

Shworak, N. W., J. Liu, L. M. Fritze, J. J. Schwartz, L. Zhang, D. Logeart, and R. D. Rosenberg. 1997. Molecular cloning and expression of mouse and human cDNAs encoding heparan sulfate D-glucosaminyl 3-O-sulfotransferase. *J. Biol. Chem.* 272 (44):28008-19.

Sieber-Blum, M. 1989. Commitment of neural crest cells to the sensory neuron lineage. *Science* 243 (4898):1608-11.

Skidmore, M. A., S. E. Guimond, T. R. Rudd, D. G. Fernig, J. E. Turnbull, and E. A. Yates. 2008. The activities of heparan sulfate and its analogue heparin are dictated by biosynthesis, sequence, and conformation. *Connect. Tissue Res.* 49 (3):140-4.

Smith, A. G., J. K. Heath, D. D. Donaldson, G. G. Wong, J. Moreau, M. Stahl, and D. Rogers. 1988. Inhibition of pluripotential embryonic stem cell differentiation by purified polypeptides. *Nature* 336 (6200):688-90.

Solakyildirim, K., Z. Zhang, and R. J. Linhardt. 2010. Ultraperformance liquid chromatography with electrospray ionization ion trap mass spectrometry for chondroitin disaccharide analysis. *Anal. biochem.* 397 (1):24-8.

Song, H. H., W. Shi, and J. Filmus. 1997. OCI-5/rat glypican-3 binds to fibroblast growth factor-2 but not to insulin-like growth factor-2. *J. Biol. Chem.* 272 (12):7574-7.

Spear, P. G., M. T. Shieh, B. C. Herold, D. WuDunn, and T. I. Koshy. 1992. Heparan sulfate glycosaminoglycans as primary cell surface receptors for herpes simplex virus. *Adv. Exp. Med. Biol.* 313:341-53.

Stallcup, W. B., and F. J. Huang. 2008. A role for the NG2 proteoglycan in glioma progression. *Cell Adh. Migr.* 2 (3):192-201.

Sugahara, K., and H. Kitagawa. 2002. Heparin and heparan sulfate biosynthesis. *IUBMB Life* 54 (4):163-75.

Sugiyama, T., H. Kohara, M. Noda, and T. Nagasawa. 2006. Maintenance of the hematopoietic stem cell pool by CXCL12-CXCR4 chemokine signaling in bone marrow stromal cell niches. *Immunity* 25 (6):977-88.

Sung, Y. K., S. Y. Hwang, M. K. Park, M. Farooq, I. S. Han, H. I. Bae, J. C. Kim, and M. Kim. 2003. Glypican-3 is overexpressed in human hepatocellular carcinoma. *Cancer Sci.* 94 (3):259-62.

Taatjes, D. J. 2010. The human mediator complex: a versatile, genome-wide regulator of transcription. *Trends Biochem. Sci.* 35 (6):315-22.

Takizawa, T., K. Nakashima, M. Namihira, W. Ochiai, A. Uemura, M. Yanagisawa, N. Fujita, M. Nakao, and T. Taga. 2001. DNA methylation is a critical cell-intrinsic determinant of astrocyte differentiation in the fetal brain. *Dev. Cell.* 1 (6):749-58.

Tam, P. P., and R. R. Behringer. 1997. Mouse gastrulation: the formation of a mammalian body plan. *Mech. Dev.* 68 (1-2):3-25.

Tam, W. L., C. Y. Lim, J. Han, J. Zhang, Y. S. Ang, H. H. Ng, H. Yang, and B. Lim. 2008. T-cell factor 3 regulates embryonic stem cell pluripotency and self-renewal by the transcriptional control of multiple lineage pathways. *Stem Cells* 26 (8):2019-31.

Tay, Y., J. Zhang, A. M. Thomson, B. Lim, and I. Rigoutsos. 2008. MicroRNAs to Nanog, Oct4 and Sox2 coding regions modulate embryonic stem cell differentiation. *Nature* 455 (7216):1124-8.

Tchougounova, E., and G. Pejler. 2001. Regulation of extravascular coagulation and fibrinolysis by heparin-dependent mast cell chymase. *FASEB J.* 15 (14):2763-5.

Teshima, S., Y. Shimosato, S. Hirohashi, Y. Tome, I. Hayashi, H. Kanazawa, and T. Kakizoe. 1988. Four new human germ cell tumor cell lines. *Lab. Invest.* 59 (3):328-36.

Theise, N. D., M. Nimmakayalu, R. Gardner, P. B. Illei, G. Morgan, L. Teperman, O. Henegariu, and D. S. Krause. 2000. Liver from bone marrow in humans. *Hepatology* 32 (1):11-6.

Theoharides, T. C., and D. E. Cochrane. 2004. Critical role of mast cells in inflammatory diseases and the effect of acute stress. *J. Neuroimmunol.* 146 (1-2):1-12.

Thompson, H. L., E. S. Schulman, and D. D. Metcalfe. 1988. Identification of chondroitin sulfate E in human lung mast cells. *J. Immunol.* 140 (8):2708-13.

Tkachenko, E., J. M. Rhodes, and M. Simons. 2005. Syndecans: new kids on the signaling block. *Circ. Res.* 96 (5):488-500.

Toole, B. P. 2001. Hyaluronan in morphogenesis. *Semin. Cell Dev. Biol.* 12 (2):79-87.

Troup, S., C. Njue, E. V. Kliewer, M. Parisien, C. Roskelley, S. Chakravarti, P. J. Roughley, L. C. Murphy, and P. H. Watson. 2003. Reduced expression of the small leucine-rich proteoglycans, lumican, and decorin is associated with poor outcome in node-negative invasive breast cancer. *Clin. Cancer. Res.* 9 (1):207-14.

Tulina, N., and E. Matunis. 2001. Control of stem cell self-renewal in Drosophila spermatogenesis by JAK-STAT signaling. *Science* 294 (5551):2546-9.

Tumova, S., A. Woods, and J. R. Couchman. 2000. Heparan sulfate proteoglycans on the cell surface: versatile coordinators of cellular functions. *Int. J. Biochem. Cell Biol.* 32 (3):269-88.

Uhlin-Hansen, L., M. Kusche-Gullberg, E. Berg, I. Eriksson, and L. Kjellen. 1997. Mouse mastocytoma cells synthesize undersulfated heparin and chondroitin sulfate in the presence of brefeldin A. *J. Biol. Chem.* 272 (6):3200-6.

Vallier, L., S. Mendjan, S. Brown, Z. Chng, A. Teo, L. E. Smithers, M. W. Trotter, C. H. Cho, A. Martinez, P. Rugg-Gunn, G. Brons, and R. A. Pedersen. 2009. Activin/Nodal signalling maintains pluripotency by controlling Nanog expression. *Development* 136 (8):1339-49.

Voigt, A., R. Pflanz, U. Schafer, and H. Jackle. 2002. Perlecan participates in proliferation activation of quiescent Drosophila neuroblasts. *Dev. Dyn.* 224 (4):403-12.

Wang, L., M. Fuster, P. Sriramarao, and J. D. Esko. 2005. Endothelial heparan sulfate deficiency impairs L-selectin- and chemokine-mediated neutrophil trafficking during inflammatory responses. *Nat. Immunol.* 6 (9):902-10.

Wang, Y., S. Baskerville, A. Shenoy, J. E. Babiarz, L. Baehner, and R. Blelloch. 2008. Embryonic stem cell-specific microRNAs regulate the G1-S transition and promote rapid proliferation. *Nat. Genet.* 40 (12):1478-83.

Wang, Z., M. Ly, F. Zhang, W. Zhong, A. Suen, A. M. Hickey, J. S. Dordick, and R. J. Linhardt. 2010. E. coli K5 fermentation and the preparation of heparosan, a bioengineered heparin precursor. *Biotechnol. Bioeng.* 107 (6):964-73.

Weber, C. K., G. Sommer, P. Michl, H. Fensterer, M. Weimer, F. Gansauge, G. Leder, G. Adler, and T. M. Gress. 2001. Biglycan is overexpressed in pancreatic cancer and induces G1-arrest in pancreatic cancer cell lines. *Gastroenterology* 121 (3):657-67.

Wederell, E. D., M. Bilenky, R. Cullum, N. Thiessen, M. Dagpinar, A. Delaney, R. Varhol, Y. Zhao, T. Zeng, B. Bernier, M. Ingham, M. Hirst, G. Robertson, M. A. Marra, S. Jones, and P. A. Hoodless. 2008. Global analysis of in vivo Foxa2-binding sites in mouse adult liver using massively parallel sequencing. *Nucleic Acids Res.* 36 (14):4549-64.

Williams, R. L., D. J. Hilton, S. Pease, T. A. Willson, C. L. Stewart, D. P. Gearing, E. F. Wagner, D. Metcalf, N. A. Nicola, and N. M. Gough. 1988. Myeloid leukaemia inhibitory factor maintains the developmental potential of embryonic stem cells. *Nature* 336 (6200):684-7.

Williamson, D., J. Selfe, T. Gordon, Y. J. Lu, K. Pritchard-Jones, K. Murai, P. Jones, P. Workman, and J. Shipley. 2007. Role for amplification and expression of glypican-5 in rhabdomyosarcoma. *Cancer Res.* 67 (1):57-65.

Wu, Q., X. Chen, J. Zhang, Y. H. Loh, T. Y. Low, W. Zhang, S. K. Sze, B. Lim, and H. H. Ng. 2006. Sall4 interacts with Nanog and co-occupies Nanog genomic sites in embryonic stem cells. *J. Biol. Chem.* 281 (34):24090-4.

Xiong, B., and J. L. Gerton. 2010. Regulators of the cohesin network. *Annu. Rev. Biochem.* 79:131-53.

Xu, D., A. F. Moon, D. Song, L. C. Pedersen, and J. Liu. 2008. Engineering sulfotransferases to modify heparan sulfate. *Nat. Chem. Biol.* 4 (3):200-2.

Xu, R. H., R. M. Peck, D. S. Li, X. Feng, T. Ludwig, and J. A. Thomson. 2005. Basic FGF and suppression of BMP signaling sustain undifferentiated proliferation of human ES cells. *Nat. Methods* 2 (3):185-90.

Xu, R. H., T. L. Sampsell-Barron, F. Gu, S. Root, R. M. Peck, G. Pan, J. Yu, J. Antosiewicz-Bourget, S. Tian, R. Stewart, and J. A. Thomson. 2008. NANOG is a direct target of TGFbeta/activin-mediated SMAD signaling in human ESCs. *Cell Stem Cell* 3 (2):196-206.

Yamaguchi, Y., M. Inatani, Y. Matsumoto, J. Ogawa, and F. Irie. 2010. Roles of heparan sulfate in mammalian brain development current views based on the findings from Ext1 conditional knockout studies. *Prog. Mol. Biol. Transl. Sci.* 93:133-52.

Yamamoto, S., S. Oka, M. Inoue, M. Shimuta, T. Manabe, H. Takahashi, M. Miyamoto, M. Asano, J. Sakagami, K. Sudo, Y. Iwakura, K. Ono, and T. Kawasaki. 2002. Mice deficient in nervous system-specific carbohydrate epitope HNK-1 exhibit impaired synaptic plasticity and spatial learning. *J. Biol. Chem.* 277 (30):27227-31.

Yanagisawa, M., T. Taga, K. Nakamura, T. Ariga, and R. K. Yu. 2005. Characterization of glycoconjugate antigens in mouse embryonic neural precursor cells. *J. Neurochem.* 95 (5):1311-20.

Yang, B., Y. Chang, A. M. Weyers, E. Sterner, and R. J. Linhardt. 2012. Disaccharide analysis of glycosaminoglycan mixtures by ultra-high-performance liquid chromatography-mass spectrometry. *J. Chromatogr. A* 1225:91-8.

Yang, B., A. Weyers, J. Y. Baik, E. Sterner, S. Sharfstein, S. A. Mousa, F. Zhang, J. S. Dordick, and R. J. Linhardt. 2011. Ultra-performance ion-pairing liquid chromatography with on-line electrospray ion trap mass spectrometry for heparin disaccharide analysis. *Anal. Biochem.* 415 (1):59-66.

Repeated Author. 2011. Ultra-performance ion-pairing liquid chromatography with on-line electrospray ion trap mass spectrometry for heparin disaccharide analysis. *Anal. biochem.* 415 (1):59-66.

Yap, K. L., S. Li, A. M. Munoz-Cabello, S. Raguz, L. Zeng, S. Mujtaba, J. Gil, M. J. Walsh, and M. M. Zhou. 2010. Molecular interplay of the noncoding RNA ANRIL and methylated histone H3 lysine 27 by polycomb CBX7 in transcriptional silencing of INK4a. *Mol. Cell* 38 (5):662-74.

Ye, M., H. Iwasaki, C. V. Laiosa, M. Stadtfeld, H. Xie, S. Heck, B. Clausen, K. Akashi, and T. Graf. 2003. Hematopoietic stem cells expressing the myeloid lysozyme gene retain long-term, multilineage repopulation potential. *Immunity* 19 (5):689-99.

Ying, Q. L., J. Nichols, I. Chambers, and A. Smith. 2003. BMP induction of Id proteins suppresses differentiation and sustains embryonic stem cell self-renewal in collaboration with STAT3. *Cell* 115 (3):281-92.

Yoneda, A., and J. R. Couchman. 2003. Regulation of cytoskeletal organization by syndecan transmembrane proteoglycans. *Matrix Biol.* 22 (1):25-33.

Yoshida, E., S. Arakawa, T. Matsunaga, S. Toriumi, S. Tokuyama, K. Morikawa, and Y. Tahara. 2002. Cloning, sequencing, and expression of the gene from bacillus circulans that codes for a heparinase that degrades both heparin and heparan sulfate. *Biosci. Biotechnol. Biochem.* 66 (9):1873-9.

Young, J. D., C. C. Liu, G. Butler, Z. A. Cohn, and S. J. Galli. 1987. Identification, purification, and characterization of a mast cell-associated cytolytic factor related to tumor necrosis factor. *Proc. Natl. Acad. Sci. USA* 84 (24):9175-9.

Young, R. A. 2011. Control of the embryonic stem cell state. *Cell* 144 (6):940-54.

Yu, W. H., S. Yu, Q. Meng, K. Brew, and J. F. Woessner, Jr. 2000. TIMP-3 binds to sulfated glycosaminoglycans of the extracellular matrix. *J. Biol. Chem.* 275 (40):31226-32.

Yun, C. Y., S. Liu, S. F. Lim, T. Wang, B. Y. Chung, J. Jiat Teo, K. H. Chuan, A. S. Soon, K. S. Goh, and Z. Song. 2007. Specific inhibition of caspase-8 and -9 in CHO cells enhances cell viability in batch and fed-batch cultures. *Metab. Eng.* 9 (5-6):406-18.

Zhang, F., P. Sun, E. Munoz, L. Chi, S. Sakai, T. Toida, H. Zhang, S. Mousa, and R. J. Linhardt. 2006. Microscale isolation and analysis of heparin from plasma using an anion-exchange spin column. *Anal. Biochem.* 353 (2):284-6.

Zhang, J., W. L. Tam, G. Q. Tong, Q. Wu, H. Y. Chan, B. S. Soh, Y. Lou, J. Yang, Y. Ma, L. Chai, H. H. Ng, T. Lufkin, P. Robson, and B. Lim. 2006. Sall4 modulates

embryonic stem cell pluripotency and early embryonic development by the transcriptional regulation of Pou5f1. *Nat. Cell Biol.* 8 (10):1114-23.

Zhang, L., D. L. Beeler, R. Lawrence, M. Lech, J. Liu, J. C. Davis, Z. Shriver, R. Sasisekharan, and R. D. Rosenberg. 2001. 6-O-sulfotransferase-1 represents a critical enzyme in the anticoagulant heparan sulfate biosynthetic pathway. *J. Biol. Chem.* 276 (45):42311-21.

Zhang, L., R. Lawrence, B. A. Frazier, and J. D. Esko. 2006. CHO glycosylation mutants: proteoglycans. *Methods Enzymol.* 416:205-21.

Zhang, L., R. Lawrence, J. J. Schwartz, X. Bai, G. Wei, J. D. Esko, and R. D. Rosenberg. 2001. The effect of precursor structures on the action of glucosaminyl 3-O-sulfotransferase-1 and the biosynthesis of anticoagulant heparan sulfate. *J. Biol. Chem.* 276 (31):28806-13.

Zhang, Z., J. Xie, H. Liu, J. Liu, and R. J. Linhardt. 2009. Quantification of heparan sulfate disaccharides using ion-pairing reversed-phase microflow high-performance liquid chromatography with electrospray ionization trap mass spectrometry. *Anal. Chem.* 81 (11):4349-55.

Zhao, J., T. K. Ohsumi, J. T. Kung, Y. Ogawa, D. J. Grau, K. Sarma, J. J. Song, R. E. Kingston, M. Borowsky, and J. T. Lee. 2010. Genome-wide identification of polycomb-associated RNAs by RIP-seq. *Mol. Cell* 40 (6):939-53.

Zhao, W., M. L. Garron, B. Yang, Z. Xiao, J. D. Esko, M. Cygler, and R. J. Linhardt. 2011. Asparagine 405 of heparin lyase II prevents the cleavage of glycosidic linkages proximate to a 3-O-sulfoglucosamine residue. *FEBS Lett.* 585 (15):2461-6.

APPENDIX

A. Expression of NDST2 and Hs3st1 in Dual NDST2 and Hs3st1 Expressing Clones. (A) Total 40 Dual-transfected clones were screened for successful transfection of *NDST2* and *Hs3st1* by RT-PCT. (B) Clones expressing both genes at a relatively high level were screened by immunoblotting.

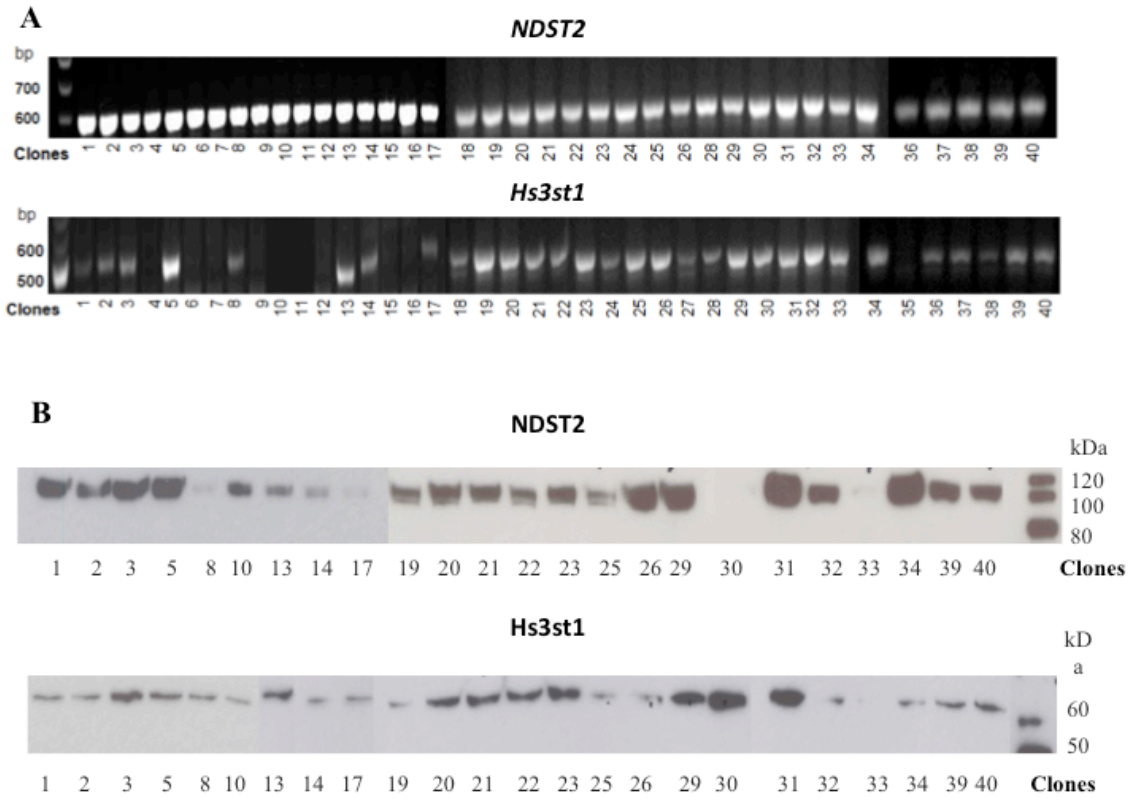

B. Primers Used for RT-PCR Reaction with CHO-S cells, Rat Mast Cells and Dual-expressing Clones.

Cell type	Gene of interest	Forward primer (F) Reverse primer (R)	PCR product size (bp)
CHO-S	*Ext1*	F: 5`-GTTGATTGGGAAACTTGGGTG-3` R: 5`- ACAAAAGGGCGAGACAAGAG -3`	125
	Ext2	F: 5`- TCTGTTTGTCCCCTCCATTG -3` R: 5`- ATTTGTTCCTCGATCCCACC -3`	103
	Ndst1	F: 5`- GCTTCTTCAAGGCCAATGAG -3` R: 5`- AAAGAGGGAAGCCTTTGAGC -3`	60
	Ndst2	F: 5`- TGAAGGTGGCTGATGTTGAG -3` R: 5`- AGGTTGAAGGTGAAGTTGGG -3`	79
	Glce	F: 5`- GAGATCCTTGTATGAGCGTGG -3` R: 5`- AAGTGGCGAAGGTCATAGATG -3`	93
	Hs2st1	F: 5`-CGAGTACTTTCTGGTGGGAGTT-3` R: 5`-GCCTCGAGTAGCATGATGAAG-3`	60
	Hs3st1	F: 5`- CTCTCAACCGCAGTCTGTAC -3` R: 5`- GGATCTCAGGAAAAGGGTCTC -3`	117
	Hs3st5	F: 5`- TTGATCATTGTCAGGGAGCC -3` R: 5`- CTTCCTCTCCTTCCCCTCTAG -3`	75
	Hs6st1	F: 5`- TTAAGTTCATCCGGCCCTTC -3` R: 5`- TCCTTGGCATAGTCATACAGC -3`	130
	Hs6st2	F: 5`- CTCGGTGTATCTGGGTTGTG -3` R: 5`- CCTCCATTCGCTCAAGTACC -3`	126
	Hs6st3	F: 5`- CACAATTCAACATCACTCGGG -3` R: 5`- ATATTCATAGAGCTGCACGTCC -3`	101
Rat	*Ndst1*	F: 5`-AACTATGGAAATGACCGCCTGGGA-3` R: 5`-GCCAATGATGAGCAGCTTTGGGAA-3`	240
	Ndst2	F: 5`-GAAAACCTGTGACCGACTCC-3` R: 5`-AGGAAGAAGTGAATGGCTGTG-3`	78
	Glce	F: 5`-GCTGATAAGTCTAGATCCACCAATG-3` R: 5`-CTGCAAAGACACACCCTCAC-3`	72
	Hs2st1	F: 5`-TCTTGGAGAACCAGATCCAGA-3` R: 5`-ATGTCTTGCAATTGCCCTCT-3`	68

	Hs3st1	F: 5`-AGAAGGTGCAGCCACCAAT-3` R: 5`-ACCCTTGCGTACTCCAATGA-3`	70
	Hs3st5	F: 5`-AGGCGTGTCTGAATGTAGGC-3` R: 5`-CCAGGAGCTTCTGTCTTAGCC-3`	93
	Hs6st1	F: 5`-GTGTTCCCGGTGTGCTAGA-3` R: 5`-CAGCAGGGTGATGTAGTAGAACTTT-3`	77
	Hs6st2	F: 5`-TGATCGTGTTCCTGCACATCCAGA-3` R: 5`-TGGAGAGTTGGCACCTGAGTTGAA-3`	347
	Hs6st3	F: 5`-CACCTGGTGAAGAACATTCG-3` R: 5`-ACTTTTTCTGGCCAGCTTTG-3`	61
	Ext1	F: 5`- AGGAGACAATGATGGGACAGA-3` R: 5`- CTGGGCAAAGTGGTCAGG-3`	65
	Ext2	F: 5`- TCTCCCAGAGAAAGCACCAG-3` R: 5`- CTCTGTACTCAGGGTGGATGG-3`	77
Enginee-red CHO	*NDST2* (*Homo sapiens*)	F: 5`-ATCCCTGTGATGACAAGAGGCACA-3` R: 5`-TTGCCCATCCACAATCAGCAACTG-3`	587
	Hs3st1 (*Mus musculus*)	F: 5`-TAATCAAGAGGGAGCCTTGCTGCT-3` R: 5`-TAATCAAGAGGGAGCCTTGCTGCT-3`	494

C. Primers Used for RT-PCR Reaction with MST and MST-10H cells.

Cell type	Gene of interest	Forward primer (F) Reverse primer (R)	PCR product size (bp)
MST and MST-10H	*Ndst1*	F: 5`- TGCCTTTGGACCGATACATC -3` R: 5`- TGTGCGGAGTTCATTCTGTG -3`	119
	Ndst2	F: 5`-TCCACAAACGGAGCTTTGTA-3` R: 5`-ATGCCTCAGGCTGAAACTTG-3`	117
	Ext1	F: 5`- TTGAAGTCTTTACAGGCGGG -3` R: 5`- TGAGAGCAGGATGAAATAGCG -3`	145
	Ext2	F: 5`- TGGGATCGAGGAACAAATCAC -3` R: 5`- GTAAGTCCAGGTAGAAAAGCCG -3`	129
	Gcle	F: 5`-GCCAGTGTGGCAGACAAGT-3` R: 5`-CAGCTGCAAAGACACACCTT-3`	50
	Hs2st1	F: 5`- TGCTCTTCTTGGAGAACCAGA -3` R: 5`- CCTTGCAATTGCCCTTTCTA -3`	71
	Serglycin	F: 5`-CCTTCGTCCTGGTTTGGG A-3` R: 5`-GTCAAACTGTGGTCCCTTCTC-3`	130
	Hs6st1	F: 5`- GGACCGAACTCACCAACTGT -3` R: 5`- CGCAGCAGGGTGATGTAGTA -3`	97
	Hs6st2	F: 5`- CTTCAAACTTCAACTCAGGCG -3` R: 5`- TCCATTCACTCAAGTACCGTG -3`	129
	Hs6st3	F: 5`-TCATGGAGAAGAAGGATTGTCC-3` R: 5`-CGCAACATCGTGATGTAGTAGAA-3`	70
	Hs3st1	F: 5`-AGTGTGAATTTGCTCCAAAGG-3` R: 5`-GAGTATCTCCAGTTGCCAATTACTG-3`	131
	Hs3st5	F: 5`-CCAGAGTTGGGAGCTTGG-3` R: 5`-CACCACCAAATCGACTTTCA-3`	63
	GAPDH	F: 5`- CTTTGTCAAGCTCATTTCCTGG -3` R: 5`- TCTTGCTCAGTGTCCTTGC -3`	133

LEYLA GASIMLI EHTIBAR **gasimlyl@gmail.com**

238 Pawling ave. ●Troy, NY 12180 ● 518 698 5823

Education

Rensselaer Polytechnic Institute — Troy, NY
Doctor of Philosophy in Biology GPA 3.8 — ***September 2008- current***

Mississippi Valley State University (MVSU) — Itta Bena, MS
Master of Science in Bioinformatics GPA 4.0 — ***May 2007***

Baku State University — Baku, Azerbaijan
Master of Science in Microbiology GPA 4.0 — ***June 2005***

Baku State University — Baku, Azerbaijan
Bachelor of Science in Biology GPA 3.9 — ***June 2003***

Languages

Fluent in **English, Russian, Turkish,** and **Azeri**

Experience

Rensselaer Polytechnic Institute, Biology Department **Troy, NY**
Graduate Assistant *August 2008- May 2010*

- Assist in preparation and development of course materials
- Help organize, direct, and evaluate laboratory activities in general biology, biochemistry and cell biology
- Prepare, administer, and grade examinations

MVSU Student Support Services **Itta Bena, MS**
Tutor *August 2005- May 2007*

- Provide tutoring to students and monitoring their progress in biology area
- Assist in the development of positive study habits and study skills for students

Azecolab, Physical Environment Research Center **Baku, Azerbaijan**
Microbiologist *May 2002- August 2005*

- Established a microbiology laboratory to carry out microbiological analyzes
- Conducted analyses on petroleum-, phenol-oxidizing microorganisms, enterobacteria etc.
- Analyzed different water samples including waste - water, produce water, drinking water, etc.
- Carried out the microbiological analysis of different soil samples
- Assisted in preparation of projects on bioremediation of petroleum contaminated water and soils

Publications

1. **Proteoglycans in stem cells. *L. E. Gasimli***, J. S. Dordick, R. J. Linhardt. *Biotechnology and Applied Biochemistry* (2012), 59 (2), p 65-76
2. **Metabolic engineering of Chinese hamster ovary cells: towards a bioengineered heparin**. ***L. E. Gasimli***, J. Y. Baik, B. Yang, et al. *Metabolic Engineering*.(2012), 14(2), p 81-90
3. **Cell-based microscale isolation of glycosaminoglycans for glycomics study**. X. Zhao, B. Yang, P. Datta, ***L. E. Gasimli,*** et al. *Journal of Carbohydrate Chemistry* (2012), 31, p. 420-435
4. **Analysis of the structural remodeling of glycosaminoglycans upon retinoic acid-induced differentiation of NCCIT cells. *L. E. Gasimli***, H. Stansfield, A. V. Nairn, et al. *Glycobiology*. Submitted
5. **Bioremediation of drill cuttings in processes of chemical fixing. *L. E. Gasimli***, N. A. Ibadov, F. K. Kasumov, N. M. Ismaylov. *International Sci. Journal for Alternative Energy and Ecology* ISJAEE (2005), 4 (24), p. 86 – 90

Presentations

1. **Role of proteoglycans in stem cell fate commitment. *L. E. Gasimli***, A. M. Hickey, A. Nairn, et al. American Chemical Society 244th Annual Meeting, Philadelphia, PA, August 19-23, 2012
2. **Metabolic engineering of CHO cells for production of anti-coagulant heparin**. ***L. E. Gasimli***, J. Baik, P. Datta, et al. American Chemical Society 243th Annual Meeting, San Diego, CA, March 25-29, 2012
3. **Culture and analysis of human embryonic stem cells and embryonal cancinoma cells using three-dimensional microarrays**. ***L. E. Gasimli***, L. Meli, H. E. Stansfield, et al. New York State Stem Cell Science Annual Meeting, New York, NY, May 24-25, 2011
4. **Characterization of heparan sulfate biosynthetic pathways in Chinese Hamster ovary cells**. ***L. E. Gasimli***, J. Baik, P. Datta, et al. American Chemical Society 241th Annual Meeting, Anaheim, CA, March 27-31, 2011
5. **Biosynthesis of Heparin by metabolic engineering of Chinese Hamster Ovary Cells**. ***L. E. Gasimli***, J. Baik, B. Li, et al. American Chemical Society 240th Annual Meeting, Boston, MA, August 22-26, 2010

Awards/Honors

Azerbaijan Republic Honors Diploma, Baku State University, 2003
Azerbaijan Republic Honors Master's Diploma, Baku State University, 2005
Best First -Year Graduate Student, Mississippi Valley State University, Department of Natural Sciences and Envir. Health/ Bioinformatics, 2006
Outstanding Bioinformatics Scholar, Mississippi Valley State University, Department of Natural Sciences and Envir. Health/ Bioinformatics, 2007